Exploring the use of Carbon Monoxide-Releasing Molecules as Antimicrobials Against *Pseudomonas aeruginosa*

Thomas C. P. Reed

MSc by Research

University of York

Biology

December 2019

Abstract

Antimicrobial resistance is a major public health risk that currently contributes to hundreds of thousands of deaths every year and is predicted to continue rising if the issue is not addressed. One method of addressing this problem is through the development of new antimicrobials. Carbon monoxide-releasing molecules (CORMs) have emerged as a potential new class of antimicrobial that have shown to be effective at reducing the growth of bacterial pathogens and have synergistic effects with some currently used antibiotics. This study explored the use of two novel CORMs, namely the photo-activated Trypto-CORM and the water-triggered Ebor-CORM, against *Pseudomonas aeruginosa* strain PAO1. This study demonstrates that the time at which photoirradiation of Trypto-CORM occurs, relative to the bacterial growth phase, can significantly alter its antimicrobial effects. Photoirradiation of Trypto-CORM during the mid-exponential growth phase resulted in the greatest reduction in bacterial densities. While Ebor-CORM was shown to effectively reduce densities of PAO1 alone and in combination with sub-inhibitory concentrations of colistin, in the presence of 4 μg/ml colistin, Ebor-CORM provided a cytoprotective effect and facilitated growth. Additionally, Ebor-CORM was shown to be effective against a colistin-resistant mutant of *P. aeruginosa* with no cytoprotective effects being observed. Interestingly, both CORMs were less effective against PAO1 growing under oxygen limiting conditions. This is hypothesised to result from the expression of cytochromes with a lower affinity for carbon monoxide. Finally, both CORMs significantly altered the virulence of PAO1 and increased production of pyocyanin, however, opposing effects were observed for biofilm and pyoverdine production with Ebor-CORM significantly reducing the production of these virulence factors. It is hypothesised that the CORMs are interacting with different pathways that regulate virulence. Together these results suggest that CORMs could be effective antimicrobials, however, their interactions with bacterial pathways are complex and the mechanisms by which they induce cell death remain unknown.

Table of Contents

List of Figures

Acknowledgments

I would like to thank my supervisor's Dr Ville Friman and Dr Jason Lynam for their support and guidance through the project. I also want to thank the Friman lab group for their support during the project. I also want to thank Anders Hammerback and Johnathan Eastwood for synthesising the CORMs for me to use. I wish to thank Dr Karen Hogg for all her assistance in setting up and conducting the flow cytometry experiments. Finally, I would like to thank the University of York for providing me with the funding and resources to conduct this research.

Authors Declaration

I declare that this thesis is a presentation of original work and I am the sole author. This work has not previously been presented for an award at this, or any other, University. All sources are acknowledged as References.

1.0 Background

1.1 Introduction

Antibiotic resistance is a growing issue that currently contributes to hundreds of thousands of deaths every year (O'Neill, 2014). This total is predicted to increase to 10 million by 2050, and cost over 70 trillion GBP, if the issue is not addressed (O'Neill, 2014). Antibiotic resistant bacteria account for over 50% of infections acquired in hospitals (Mauldin et al., 2009). These infections increase the number of unsuccessful treatments and in turn, the risk of mortality and the cost of treating bacterial infections increases (Mauldin et al., 2009; Händel et al., 2015). The emergence of multi-drug resistant bacteria has only amplified current issues as there are fewer treatment options for these infections (Magiorakos et al., 2012; Xu, Qin and Liu, 2014). Infections caused by multi-drug bacteria including *Klebsiella pneumoniae* and *Acinetobacter* spp. could be resistant to all contemporary antibiotics (Magiorakos et al., 2012). This creates a significant need for new antibiotics to treat the infections caused by multi-drug resistant bacteria and to try to reduce the current levels of antibiotic resistance (Xu, Qin and Liu, 2014).

1.2 Mechanisms of action of Conventional Antibiotics

Antibiotics can induce the death of bacteria in a variety of ways with most targeting features that are unique to prokaryotic cells (Kohanski, Dwyer and Collins, 2010). Several classes of antimicrobials disrupt the integrity of the bacterial cells by targeting the bacterial cell wall (Tenover, 2006). β-Lactam antibiotics are one of the most commonly used antibiotics that bind to and inhibit penicillin binding proteins (PBPs), which are required to form cross links between peptidoglycan strands within the cell wall (Cho, Uehara and Bernhardt, 2014; Fishovitz et al., 2014). Bacterial cell wall synthesis is also the target of moenomycin which binds to an alternative active site of the PBP's to prevent the development of peptidoglycan strands (Huang et al., 2012). Finally, vancomycin and the newly discovered teixobactin, bind to lipid II which is a key building block of the peptidoglycan and prevent its incorporation into the cell wall (Chiorean et al., 2019; Cui et al., 2006).

In addition to inhibiting cell wall synthesis, several classes of antibiotics are taken up by bacterial cells and disrupt cellular functions (Tenover, 2006). For example, tetracyclines

and chloramphenicol bind to the 30s and 50s ribosome subunits respectively to prevent the translation of RNA and inhibit protein synthesis (Kohanski, Dwyer and Collins, 2010). Additionally, DNA synthesis and transcription can also be targeted by rifampicin and fluoroquinolones (Feklistov et al., 2008; Tenover, 2006). Rifampicin binds to RNA polymerase and prevents the transcription of DNA, while fluoroquinolones bind to DNA gyrase to prevent DNA uncoiling and replicating (Feklistov et al., 2008; Blondeau, 2004).

1.3 Resistance Development

1.3.1 Contributing Factors

The development of antibiotic resistance is being driven largely by the overuse and abuse of antibiotics (Monroe and Polk, 2000; Hecker et al., 2003). Antibiotics are the second most prescribed drug in the US and the use of around 50% of these has been classified as inappropriate (Dellit et al., 2007; Monroe and Polk, 2000). This is largely due to incorrect antibiotics being prescribed and longer than necessary treatment periods (Fridkin et al., 2014). Additionally, the use of 30 % of these antibiotics has been deemed unnecessary (Hecker et al., 2003). This is because antibiotics are prescribed for non-bacterial infections or in combination with another antibiotic resulting in redundant coverage (Hecker et al., 2003; Glowacki et al., 2003). All of these inappropriate uses of antibiotics are increasing environmental levels of antibiotics because 50% of antibiotics are excreted unaltered and enter the environment (Lundborg and Tamhankar, 2017).

Over- and mis-prescription of antibiotic is not the only issue as self-medication with antibiotics occurs globally. Self -medication is most prevalent in developing countries with 40% to over 70% of antibiotics being source without prescriptions (Zarb and Goossens, 2012). In developed countries measures, such as antibiotic stewardship, are being implemented to decrease resistance to antibiotics and prolong their effectiveness (Nice.org.uk, 2015; Mulvey and Simor, 2009). This is achieved through optimising treatments, reducing the number of unnecessary treatments and controlling the distribution of antibiotics (Fridkin et al., 2014; Dellit et al., 2007). These programs are more difficult to implement in developing countries due to lack of funding (Zarb and Goossens, 2012). However, even with sufficient funds the usage and acquisition of

antibiotics is a part of daily life and culture and people would likely resist change (Radyowijati and Haak, 2003).

Although the improper consumption of antibiotics by humans is a contributing factor to antibiotic resistance it is matched, if not overshadowed, by the contribution of agriculture (Goldman, 2004). Roughly 50% of antibiotics are produced for human treatments the majority of the remainders are used in agriculture (Stöhr and Wegener, 2000). Antibiotics used in agriculture are mainly non-therapeutic and most are incorporated in feed as growth promotors to prevent the spread of diseases and increase productivity (Krishnasamy, Otte and Silbergeld, 2015; Goldman, 2004). Consequently, low concentrations of intact antibiotics or residues of antibiotics are excreted by the animals and pollute the environment in the same way as with humans (Lundborg and Tamhankar, 2017). This practice has been banned in the EU and US in efforts to reduce the unnecessary use of antibiotics, however, it is still common in less developed countries (Morris, Helliwell and Raman, 2016; Agga, Schmidt and Arthur, 2016; Krishnasamy, Otte and Silbergeld, 2015).

1.3.2 Development of Resistance

Antibiotics act as a selective pressure on bacteria resulting in increased levels of resistance (Lundborg and Tamhankar, 2017; Tello, Austin and Telfer, 2012). Levels of resistant bacteria increase through different means depending on the concentration of antibiotic the bacteria are exposed to (Gullberg et al., 2011). For example, at therapeutic doses, the increased levels of resistance can be caused by the dissemination of an already resistant species or strain. This is because the concentration of antibiotic is high enough to kill bacteria within the community that are susceptible to it, however, it may not be high enough to kill bacteria that have resistance (Mulvey and Simor, 2009). Alternatively, the increase in resistance can be due to the emergence of new resistant strains. This is also what happens at low concentrations of antibiotics, like those found in polluted environments (Gullberg et al., 2011). In both cases the resistant bacteria proliferates and become the prevalent species (Lundborg and Tamhankar, 2017).

De novo resistance is attained through the mutation of genes which prevent antimicrobials from binding to their targets (Händel et al., 2014). Exposure to antibiotics such as polymyxins, beta-lactams and fluoroquinolone have been shown to alter

expression of genes encoding stress-induced proteins and stimulate SOS response (Ramos et al., 2016; Maiques et al., 2006; Qin et al., 2015b). Additionally, the altered expression of genes encoding efflux pumps and ribosomes-sensed methylases play a key role in resistance to certain antibiotics and cell survival when no key mutated genes confer resistance (Händel et al., 2014). However, when resistance mutations occur the contribution of expression to resistance is reduced (Händel et al., 2014). To develop resistance mutations bacteria undergo an increased rate of general 'random' mutagenesis upon exposure to antimicrobials (McKenzie and Rosenberg, 2001). Mutations that confer a beneficial advantage, that enable the bacteria to proliferate, are selected for within the population (Gullberg et al., 2011). The increased rate of mutagenesis is proposed to occur via inducible mutators which are error-prone DNA polymerases and increase the number of mutations (Andersson, 2003; McKenzie and Rosenberg, 2001). The SOS response allows the bacteria to tolerate a higher amount of DNA damage and increases DNA repair, therefore, facilitating the increased mutation rate (Qin et al., 2015a; McKenzie et al., 2000).

1.3.3 Antibiotic Resistance Mechanisms and Transfer

There are several mechanisms by which bacteria can become resistant to an antimicrobial. These mechanisms include the alterations to the antibiotic binding sites, inactivation of the antibiotic and reduced accumulation within the cell (Santajit and Indrawattana, 2016). Additionally, biofilms can play a large role in resistance by preventing antibiotics from reaching the cell (Santajit and Indrawattana, 2016).

The alteration of binding sites is a common resistance mechanism that reduces the binding affinity of the antibiotic but still allows the enzyme to function (Fishovitz et al., 2014). This type of resistance mechanism is the result of mutations within the genes encoding the enzymes and results from the SOS response described in section 1.3.2 (Santajit and Indrawattana, 2016; McKenzie et al., 2000). This mechanism is also not limited to the alteration of enzymes and during colistin resistance, modifications to lipopolysaccharide are made to reduce the binding affinity (Bialvaei and Samadi Kafil, 2015).

The inactivation of an antimicrobial is also a common mechanism of resistance by which the bacteria produce enzymes that either cleave the antimicrobial or modify its

structure to prevent its binding (Wilke, Lovering and Strynadka, 2005). The most common example of this is the production of β-lactamases which cleave and inactivate β-lactams and prevent them from binding to PBPs (Wilke, Lovering and Strynadka, 2005).

The final mechanism of resistance prevents the accumulation of the antibiotics within the cell. This mechanism is largely mediated by efflux pumps which, actively transport compounds out of the cytoplasm or periplasmic space, preventing them from accumulating and producing an antimicrobial effect (Santajit and Indrawattana, 2016; Schindler and Kaatz, 2016). Most efflux pumps are non-specific and transport a range of compounds, however, some bacteria can possess drug-specific efflux pumps. These efflux pumps are normally encoded on plasmids rather than in the chromosome and can, therefore, be transferred between bacteria (Schindler and Kaatz, 2016).

Plasmids and other mobile genetic elements, such as transposons, which commonly encode antibiotic resistance genes are readily transferred between bacteria of both the same species and different species via conjugation (Goldman, 2004; Xu, Qin and Liu, 2014). This mechanism utilises cell to cell interaction to transfer genes from one bacterium to another. Additionally, conjugation allows for the rapid spread of resistance genes within bacterial populations (Baharoglu, Bikard and Mazel, 2010). Another mechanism by which antibiotic resistance is thought to be transferred is via transduction. This is where bacteriophage acquire antibiotic resistance genes and transfer them into other bacteria with their DNA during infection, however it is not fully understood how large a role this actually plays in the transfer of resistance. The final mechanism by which bacteria become resistant, and also the simplest, is through transformation. This involves the uptake and incorporation of antibiotic resistance genes from the environment into the genome (Munita and Arias, 2016).

1.4 Carbon Monoxide-Releasing Molecules (CORMs)

1.4.1 Carbon monoxide

Carbon monoxide (CO) is a colourless, odourless gas that is extremely toxic to humans at high concentrations (Heinemann et al., 2014; Wareham et al., 2016). It is produced endogenously through metabolism and exogenously via the incomplete combustion of

fuels and burning of tobacco (Turino, 1981; Gozubuyuk et al., 2017). CO toxicity results from the 200 times greater binding affinity to haemoglobin than oxygen, resulting in reduced O_2 availability and transport (Turino, 1981; Gozubuyuk et al., 2017). CO also binds to cellular haem proteins (cytochrome C-oxidase and myoglobin) which reduces the cellular uptake and transport of Oxygen (Heinemann et al., 2014; Gozubuyuk et al., 2017; Blumenthal, 2001). Binding of CO to cytochrome C induces a state of hypoxia which impedes cellular respiration and generates reactive oxygen species (ROS) (Tafani et al., 2016; Ernst and Zibrak, 1998). ROS have several degradative effects on cells including the peroxidation of unsaturated lipids, which results in altered membrane permeabilities, and the damage and impaired repair of DNA resulting in genetic mutations (Tafani et al., 2016; Blumenthal, 2001). Tissues such as the central nervous system which are sensitive to oxygen deprivation are affected most by CO (Turino, 1981).

Although CO has extremely adverse effects on tissues and cells it is being acknowledged as an important signalling molecule, with similar effects to nitric oxide (NO), at low quantities (Motterlini, 2007; Heinemann et al., 2014). As mentioned CO is produced endogenously through the degradation of haem by haem oxygenase enzymes (Motterlini and Otterbein, 2010; Kim, Ryter and Choi, 2006). The CO produced plays key roles in vasodilation, smooth muscle proliferation and both platelet aggregation and anticoagulation (Ryter et al., 2002; Olas, 2015). Additionally, it is associated with cytoprotection, neuronal signalling and the reduction of inflammation (Kim, Ryter and Choi, 2006).

The spectrum of action of CO and NO overlap as shown by the increased endogenous production of CO to compensate for decreased NO levels (Motterlini and Otterbein, 2010; Olas, 2015). NO is currently used therapeutically to treat neonatal pulmonary hypertension and acute respiratory distress syndrome because it induces vasodilation resulting in decreased arteriole pressure (Clark et al., 2000; Benzing et al., 1996). CO could provide a more favourable treatment as it acts specifically on metalloproteins, unlike NO which acts randomly within the cell. The greater stability of CO could also provide longer-lasting effects than NO (Motterlini and Otterbein, 2010; Kim, Ryter and Choi, 2006).

1.4.2 CORMs

Carbon monoxide releasing molecules (CORMs) are metal-carbonyl complexes that deliver controlled release of CO (Ward et al., 2012; Rana et al., 2017). CORMs were originally developed to deliver CO therapeutically to achieve its anti-inflammatory, vasodilatory and antiapoptotic effects (Nobre et al., 2007; Rana et al., 2017). However, due to the inhibitory effects of CO on respiration substantial research has investigated the antimicrobial effects CORMs (Flanagan et al., 2018; Nobre et al., 2007; Ward et al., 2014).

Ruthenium based CORMs, CORM-2 and CORM-3 (Figure 1), have both shown to be effective at reducing the viability of *Escherichia coli* and S*taphylococcus aureus*, with the greatest effects being observed at anaerobic or near anaerobic conditions (Nobre et al., 2007). It was therefore concluded that CO must be acting at additional sites other than respiration (Nobre et al., 2009). This is also confirmed by Wilson et al. (2015) who showed that CORM-3 is effective against haem deficient bacteria. Transcriptomic analysis has revealed that CORMs-2 and -3 alter the expression of genes involved with biofilm formation and envelope stress to a greater extent than that of CO (Nobre et al., 2009; Davidge et al., 2009). Although CORMs alter expression to a greater extent than CO it is still thought that the observed antimicrobial effects of CORMs-2 and -3 are elicited by CO. This is because little to no antimicrobial effect is observed when cultures treated with CORMs were co-inoculated with haemoglobin (a molecule with high affinity for CO) (Nobre et al., 2007). Subsequent research has also revealed that although inactive CORM-3 (iCORM-3) does not significantly inhibit bacterial growth, it can produce toxic effects and significantly alter gene expression under anaerobic conditions (McLean et al., 2013; Wareham, Poole and Tinajero-Trejo, 2015). These effects are predicted to be due to the accumulation of ruthenium within the cell because it is a non-native ion and several ruthenium complexes have been reported to have antimicrobial activity (Davidge et al., 2009; Li, Collins and Keene, 2015; Wareham et al., 2018).

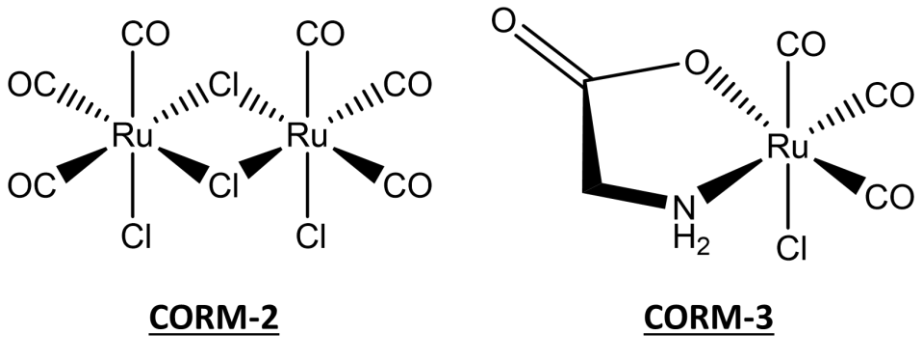

CORM-2 **CORM-3**

Figure 1: Ruthenium-based CORMs – Structures of the ruthenium based CORMs, CORM-2 and CORM-3.

Research into alternative metal ions has been conducted due to the potential contribution of ruthenium to the toxicity of CORMs against bacteria (Zhang et al., 2009; Rana et al., 2017). Photo-CORM is a manganese-based complex that releases CO in response to photochemical activation and is effective against *Escherichia coli* (Rana et al., 2017) (Figure 2). In addition to photo-CORMS there are triggered-CORMs (like CORMs-2 and -3 which release CO when exposed to a certain chemical or protein) and thermo-CORMs (which are thermally unstable and release CO at a specific temperature) (Ward et al., 2012). Although effective at reducing bacterial viability, Photo-CORM has shown to be less effective than classical ruthenium-based CORMs (Nagel et al., 2014). However, the advantages of photo-CORMs are significant, for example the release of CO can be more tightly controlled as it is not released until exposed to light (Rana et al., 2017). The advances in photoactivated chemotherapy have also made it possible for the activation of photo-CORMs after therapeutic administration (Farrer, Salassa and Sadler, 2009). Photo-CORM has also shown to enhance the effects doxycycline, polymyxins and tetracycline, while CORM-401 (another manganese based CORM) has shown to enhances other antibiotics (Figure 2) (Rana et al., 2017; Wareham et al., 2018). The synergy observed between photo-CORM and polymyxins is predicted to result from and increased uptake of Photo-CORM facilitated by the membrane disruption caused by the polymyxins (Rana et al., 2017). While the Iron chelating effects of the products of PhotoCORM are predicted to contribute to the synergies with tetracycline and doxycycline. This effect mimics a function of tetracycline and doxycycline is more effective in iron-limited conditions (Rana et al., 2017).

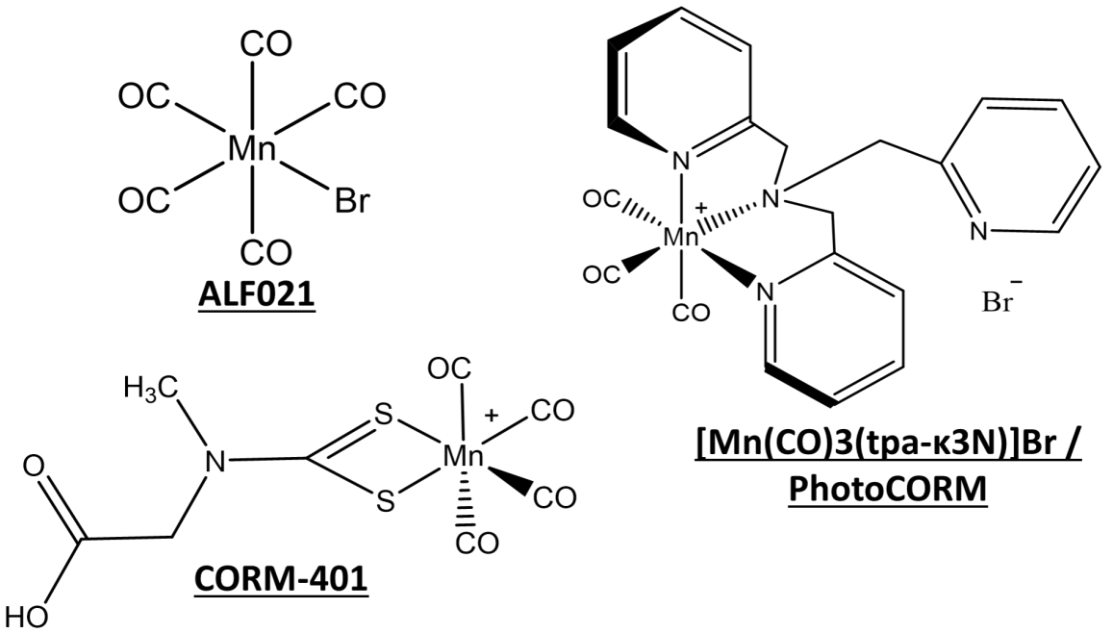

Figure 2: Manganese-based CORMs – Structures of ALF021, CORM-401 and [Mn(CO)3(tpa-κ3N)]Br (sometimes referred to as PhotoCORM)

1.5 Cystic Fibrosis and *Pseudomonal* Infections

Cystic fibrosis (CF) is a genetic condition that affects roughly 1 in 2000-3000 Caucasians with European heritage (Coutinho et al., 2008; O'Sullivan and Freedman, 2009). The condition is caused by mutations in the CF transmembrane conductance regulator (CFTR) (Zemanick and Hoffman, 2016). The protein normally regulates vesicle transport, chloride channels and ATP channels, and inhibits sodium channels and calcium-activated chloride channels (O'Sullivan and Freedman, 2009). However, defective proteins result in the retention of sodium and water and the loss of chloride resulting in the dehydration of the airways (O'Sullivan and Freedman, 2009) The reduced water results in thicker mucus and the loss of the periciliary layer (which prevents mucus from sticking to the cell surface) (Boucher, 2007). This results in the build-up of thick mucus that cannot be removed and provides a unique niche that can be inhabited by bacteria (O'Sullivan and Freedman, 2009). During early life of a CF patient the main bacterial pathogens that infect the lung are *Staphylococcus aureus* and *Hemophilus influenzae*, however, as patients age *Pseudomonas aeruginosa* becomes the dominant pathogen (Zemanick and Hoffman, 2016; Coutinho et al., 2008).

P. aeruginosa is not only a concern for CF patients, as it is the most prevalent pathogen associated with nosocomial infections (Bassetti et al., 2018). This opportunistic pathogen is the most common pathogen associated with the infection of burn wounds and surgical sights with 75% of deaths predicted to result from infection (Altoparlak et al., 2004). Additionally, *P. aeruginosa* is the leading cause of sepsis within patients suffering burns and sepsis is predicted to be the cause 75% of deaths in sever burn cases (Church et al., 2006). The bacterium utilises a range of cellular and extracellular components to infect and colonise these wounds (Pavlovskis' and Wretlind2, 1979; Sato, Okinaga and Saito, 1988). Additionally, *P. aeruginosa* readily produces biofilms that integrate with the wound tissues in as little as 10 to 72 hours and these infections can extend the hospital stay of patients by 15 days (Altoparlak et al., 2004; Church et al., 2006; Coetzee, Rode and Kahn, 2013) This pathogen is also intrinsically resistant to multiple antibiotics due to the expression of active efflux pumps (Rampioni et al., 2017). Additionally, *P. aeruginosa* can have multiple mobile resistance genes allowing this pathogen to rapidly acquire resistance to antibiotics (Bassetti et al., 2018). The multiple resistance methods make treating *P. aeruginosa* infections difficult and are the reason that this pathogen can cause serious acute and chronic infections (Kang et al., 2019; Bassetti et al., 2018).

Chronic infections are the largest contributing factor to mortality in CF patients as the infections cause significant damage to epithelial tissues and result in severely impaired pulmonary function (Lyczak et al., 2002; Rogers et al., 2003). For example, *P. aeruginosa* secretes a range of virulence factors including pyoverdine which sequesters iron from host ferroproteins causing disruption of the normal function of these cells (Kang et al., 2018). Additionally, the pyoverdine activates a signalling cascade resulting in the expression and secretion of additional toxins such as endotoxin A (Kang et al., 2019). Endotoxin A stimulates over secretion of mucus and host inflammation along with several proteases which activate inflammation through the cleavage of host receptors (Muhlebach and Noah, 2002; Kida et al., 2008). This is one of the mechanisms utilised by P. aeruginosa when establishing infections. Once infections are established *P. aeruginosa* produces a different range virulence factors including elastases and phospholipases which degrade elastin and cellular membranes to access cellular

nutrients. Additionally protease IV is produced to cleave host surfactant proteins which function in innate immunity (Ballok and O'Toole, 2013). These factors play a crucial role in CF infection, result in the decline of lung function and increase the longevity and severity of the both CF and burn wound infections.

CF patients regularly take antibiotics and repeatedly undergo eradication therapy which uses high doses of antibiotics in an attempt to clear the infections (Coutinho et al., 2008). However, there are concerns that repeated exposure to the antibiotics may result in increased levels of resistance (Williams et al., 2016; Zemanick and Hoffman, 2016; Coutinho et al., 2008). Resistance to these antibiotics used to clear *Pseudomonas* infections results in reduced treatment options and the use of 'last resort' antibiotics which often come with side effects for patients (Spapen et al., 2011; Jansen et al., 2016). The necessity to use last resort antibiotics generates a significant need for new antimicrobials, this is where CORMs could be crucial and implemented as a treatment. However, the mechanism of CORM activation must be taken into account when treating an infection. Photo-CORMs require photo stimulation and would be difficult to activate within the body, therefore, they may be more applicable for the treatment of burns and dermal infections where they can be easily irradiated. Soluble triggered- and thermo-CORMs however, could be used within the body and to treating CF associated infections. Although the release of CO may be a concern in the lungs, preliminary studies show that CORMs can be effective antimicrobials at concentrations lower than ones that damage mammalian cells (Ward et al., 2014).

1.6 Project Aims

The major aims of the project are to 1. determine whether Trypto-CORM is an effective antimicrobial treatment for *Pseudomonas aeruginosa*. and 2. determine if the antimicrobial effects of Ebor-CORM-1 against P. aeruginosa can be improved. To explore this, a range of varying factors were investigated for each compound.

2.0 Materials and Methods

2.1 Bacterial Strain Preparation

The bacterial strains used in these experiments were *Pseudomonas aeruginosa* (PAO1) and a colistin resistant mutant of *P. aeruginosa* (Col16b). Bacterial cultures were inoculated into LB broth (Formulation) from Cryo-preserved stocks. Cultures were grown overnight at 37^{o}C with shaking at 180 rpm. Overnight cultures were diluted to an optical density 600 nm of approximately 0.05 before inoculation in experiments.

2.2 Carbon Monoxide-Releasing Molecule Preparation

Stock solutions of CORMs were prepared fresh when starting an experiment.

Trypto-CORM solution was prepared by dissolving 6 mg of Trypto-CORM in 250 µl of 100% Dimethyl sulphoxide (DMSO). This was then diluted with LB broth to a total volume of 5 ml. Working concentrations were prepared by further diluting the stock solution in LB broth with 5% DMSO.

Ebor-CORM stock solution was prepared by dissolving 16.5 mg CORM powder in 360 µl of 100% DMSO. This solution was made up to 18 ml using LB broth. Working solutions of EBOR corm were prepared by diluting the stock with LB broth supplemented with 2% DMSO.

2.3 Photo-irradiation System

A new irradiation system has been developed to maximise the number of samples that can be irradiated at any time (Figure S1). A UV LED blacklight bar is supported by pipette tip boxes at either side of a Grant-bio PMS-1000i microplate shaker allowing the LED bar to span the shaker and irradiate up to 4x 96 well plates. The blacklight Bar consists of 6x 3W LED's, that emit 395-400 nm wavelength light, encased in reflective units to provide a 120-degree beam angle (Figure S2). As the LED bar is not permanently fixed the distance between the LED's and the microplate shaker can be altered to change the intensity of the light. The blacklight bar is also connected to a Timeguard Tg77 electrical timer plug that has up to 20 programmable on/off allowing for accurate control of exposure times (Figure S3). The setup is all located within an incubator set to 37^{o}C.

2.4 Monitoring CO Release using Myoglobin Assays

The myoglobin assay was used to assess the release of carbon monoxide from the CO-releasing molecules as described by Zhang et al. (2009). By monitoring the Q-bands of the myoglobin spectrum the conversion from deoxy-myoglobin to carboxy-myoglobin can be observed and thus the release of CO from the CO-releasing molecules can be evaluated.

The myoglobin solution was prepared by dissolving 13.2g of myoglobin from equine heart (Sigma-Aldrich) into 12ml of phosphate-buffered saline (PBS) (0.01M, pH 7.4). To ensure the myoglobin fully dissolved, the solution was sonicated for 5 minutes in an Ultrawave sonicating water bath. Optical impurities were removed from the solution by filtering it through a ball of cotton wool. 1 mg of sodium dithionite (Acros Organics) was added per ml of the myoglobin solution to convert this to deoxy- myoglobin. 195 µl of the solution was pipetted into wells of a flat-bottom 96-well microplate. A stock solution of CORM was prepared by dissolving the CORM in 50% DMSO. From this stock, 2.4, 1.6, 1.2, 0.8 and 0.4 mM solutions were prepared with dH_2O. 5 µl of these solutions were added to the myoglobin in the microplates to achieve; 60, 40, 30, 20 and 10 µM concentrations. 5 µl of dH_2O was added to myoglobin as a negative control. To limit gaseous exchange and the re-oxidation of myoglobin a 60 µl layer of light mineral oil/ paraffin oil (Alfa Aesar) was added to the top of the well. The absorption spectrum between 500 and 600 nm (1 nm intervals) was recorded every 6 minutes using a SPECTROstar Nano plate reader.

2.5 Assaying Virulence

2.5.1 Pyoverdine and Pyocyanin assay

Bacterial cultures of *Pseudomonas aeruginosa* grown on microplates were first aerated to ensure oxidation of the pyocyanin. This was conducted at room temperature by shaking the microplates (without lids) at 500 rpm on a Grant-bio PMS-1000i microplate shaker for 10 minutes. Following oxidation, cultures were transferred to round-bottom microplates and centrifuged at 4000 rpm for 15 minutes at 4^{o}C to pellet the bacteria. The supernatant was then removed, transferred into a flat bottom microplate and the absorbance at 691nm was measured using a Tecan Infinite M-200 microplate reader to

quantify pyocyanin. Additionally, fluorescence was measured using the same Tecan microplate reader (400nm $_{ex}\lambda$, 460nm $_{em}\lambda$) to quantify Pyoverdine.

2.5.2 Biofilm Assay

To quantify biofilm production, crystal violet was added to microplate cultures equal to 10% of the volume in the well. Plates were left to stain for 15 minutes after which they were submerged in deionised water and well contents were removed three times. Plates were allowed to dry at room temperature for 24 hours. 100% ethanol was added to wells to dissolve the crystal violet that had stained the biofilm and the absorbance at 600nm was recorded as a measure of biofilm using a Tecan Infinite M-200 microplate reader.

3.0 Trypto-CORM

3.1 Introduction

Photo-CORMs are compounds which release carbon monoxide upon exposure to specific wavelengths of light which is usually around the UV region of the spectrum (Ward et al., 2012). In recent years, photo-CORMs have gained significant attention and have been studied by several groups (Ward et al., 2017; Tinajero-Trejo et al., 2016; Wareham et al., 2016). The thermal stability of photo-CORMs and their stability in solution makes them appealing as this provides tighter temporal and spatial regulation of CO release meaning that CO will not be released until irradiated (Ward et al., 2017; Tinajero-Trejo et al., 2016).

In addition to the development of photo-CORMs, several groups have focused on the incorporation of biological compounds into these CORMs to utilise the compounds chemical properties and to make them more appealing. For example, Zobi et al. (2012) have developed several CORMs that are based on vitamin B_{12}, while Mohr et al. (2012) utilised histidine for their photo-CORM.

Trypto-CORM is a tryptophan based, manganese-carbonyl complex developed by Ward et al, (2014) that releases CO upon exposure to photo-irradiation of 465 or 400 nm light (Figure 3). However, more moles of CO are released per molecule following irradiation with 400 nm light than with 465 nm (Ward et al., 2014). Treatment of 100 µM Trypto-CORM has been shown to effectively reduce the viability of aged cultures of *E. coli and S. aureus* following irradiation (Ward et al., 2014, 2017). Interestingly, in the absence of photo-irradiation, Trypto-CORM significantly reduces the growth of *Neisseria gonorrhoeae*. Additionally, *N. gonorrhoeae* is also susceptible to irradiated Trypto-CORM in the presence of leg-haemoglobin, a molecule with a high CO

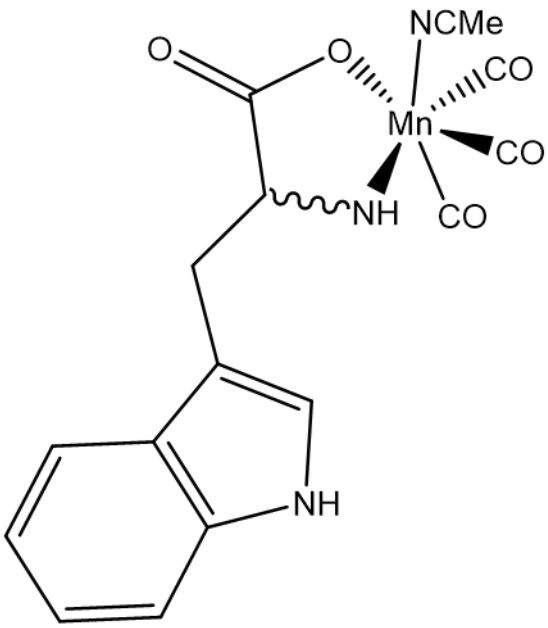

Figure 3: Structure of Trypto-CORM

affinity (Ward et al., 2017). These results suggest that *N. gonorrhoeae* is very sensitive to CO and could be a potential target for CORMs. However, it is not stated as to whether the inactive Trypto-CORM can exert antimicrobial effects. Additionally, it is not yet clear how broad activity Trypto-CORM has against different bacterial pathogens and how its efficiency is affected by light-activation cycles.

3.1.1 Aims and Objectives

The main aim of this series of experiments is to determine if Trypto-CORM is an effective antimicrobial treatment for *P. aeruginosa* and how this activity is affected by oxygen availability and different light activation regimes. A new photoirradiation experiment was designed, (described in section 2.3) to allow for a higher throughput of screening.

To investigate whether Trypto-CORM is effective against *P. aeruginosa* using the new photoactivation set up, it first had to be determined if CO was released when exposed to the light from the LED bar in the new set up. Following this, the length of photoirradiation time and Trypto-CORM concentration were varied to test the hypothesis that increasing both Trypto-CORM concentration and photoirradiation exposure would result in a greater amount of CO being released and have greater antimicrobial effects.

Secondly, a study conducted by Nobre et al., (2007) found that the CORMs they tested (ALF 021, CORM-2 and CORM-3) (Figures 1 & 2) exhibited their greatest antimicrobial effects at near anaerobic to anaerobic conditions. Therefore, exploration into how limiting oxygen availability during treatment with Trypto-CORM affected the growth of *P. aeruginosa* was conducted to test the hypothesis that the antimicrobial effects of Trypto-CORM would be greater at near anaerobic conditions.

Thirdly, interaction of CO from CORMs with ferrous proteins within the respiratory chain is proposed to be the major contributing factor to CORMs antimicrobial effects. This led to the hypothesis that Trypto-CORM would be more effective if activated during the bacterial growth phase than the lag phase as more cells would be utilising cytochrome oxidase enzymes.

Finally, how Trypto-CORM treatment affected the production of biofilms and virulence factors by *P. aeruginosa* was explored. The virulence factors produced by *P. aeruginosa*

play a key role during infections by interacting with host cellular function and resulting in damage to host cells (Ballok and O'Toole, 2013). Therefore, we need to ensure that treating an infection with CORMs is not likely to increase bacterial virulence and result in additional damage to patients.

3.2 Methods

3.2.1 Assessing CO Release under different levels of photoirradiation

Myoglobin assays were conducted as described in section 2.4 to assess the release of CO from Trypto-CORM under different photoirradiation conditions. The LED bar was cycled through 17 on/off states of varying lengths of time to achieve different levels of photoirradiation. The LEDs were on for 1, 2 or 4 minutes in every 6 minutes to provide total exposure times of 17, 34 and 68 minutes respectively. The photoirradiation cycles occurred between spectrum reads.

3.2.2 Treatment of bacterial cultures with Trypto-CORM

Overnight cultures of *P. aeruginosa* strain PAO1 were diluted to an optical density 600 nm of 0.05 using LB broth. The diluted cultures were inoculated in a 96-well microplate with 1600, 800, 400 and 0 µM Trypto-CORM (prepared as described in section 2.2). Cultures not treated with Trypto-CORM were inoculated with LB broth containing 5% DMSO, to achieve a final concentration of 2.5% like the treated cultures. The cultures were incubated at 37^{o}C, 200 rpm for 24 hours and optical density measurements at 600nm were taken hourly. Trypto-CORM was activated using the set up described in section 2.3. Additionally, controls were prepared and placed in a thin card box to prevent light exposure and these samples were not photoirradiated. The box was placed on a second microplate shaker within the same 37^{o}C incubator.

3.2.3 Effects of varying Photoirradiation

To determine how changing the photoirradiation that Trypto-CORM was exposed to effected bacterial growth, activation cycles similar to those described in section 3.2.1 were used. Cultures treated with Trypto-CORM (as described in 3.2.2) were prepared were exposed to photoirradiation cycles of 1, 3 and 4 minutes on in every 5 minutes starting 1-hour post-inoculation.

When determining how changing the time of Trypto-CORM activation affected bacterial growth the activation cycle was maintained at 2-min-on-3-min-off on in every 5 minutes. However, activation occurred at 1-, 3-, 4- or 5-hours post-inoculation. Bacterial cultures treated with Trypto-CORM were prepared as described in 3.2.2 with the exception of each different Trypto-CORM condition being inoculated on separate microplates.

3.2.4 Limiting Oxygen Availability

To determine if Trypto-CORM was more effective against PAO1 under aerobic or near anaerobic conditions bacterial cultures were prepared, as described above, and with the addition of a 60 µl layer of paraffin oil added to the top of the wells to limit gaseous exchange.

3.2.5 Assessing the effect of Trypto-CORM on neighbouring cultures.

Because the activation of Trypto-CORM results in the release of CO, it is plausible that the CO may be released from the media and be able to affect bacteria growing in neighbouring wells of 96-well microplate. To determine if this occurs during photoirradiation, cultures of PAO1 were inoculated in LB media at increasing distances (different columns on 96-well plates) from a 1600 µM Trypto-CORM solution. Photoirradiation of 2-min-on-3-min-off cycled 17 times was used 5-hours post-inoculation. The optical density at 600 nm was recorded hourly, for 11 hours except during photoirradiation, using a Tecan Sunrise microplate reader to assess bacterial growth.

3.2.6 Assessing the effect of Trypto-CORM on Virulence

When assessing the effect of Trypto-CORM on the production of pyocyanin, pyoverdine and biofilms, cultures were prepared as described in 3.2.2, however, each different Trypto-CORM condition was inoculated on separate microplates and optical density reads were not taken every hour. Photoirradiation occurred for 2 minutes in every 5 minutes cycled 17 times, providing a total exposure time 34 minutes. Photoactivation started either 1 or 5 hours post-inoculation. The virulence assays were performed as described in section 2.5.

3.3 Results and Discussion

3.3.1 Release of CO from Trypto-CORM

Myoglobin assays were carried out to determine if CO was released from Trypto-CORM when exposed to photoirradiation under the new activation conditions. Additionally, the effects of Trypto-CORM concentration and total photoirradiation exposure on CO release were explored by monitoring the rate of deoxy-myoglobin to carboxy-myoglobin conversion. Before the raw data can be used to explore the release of CO it must first be corrected to account for any drifts in the spectra. The drift observed in the spectrum of (Figure 4a) could potentially be due to the precipitation of Trypto-CORM as it is only partially soluble in PBS. Additionally, the error in the spectrum could be as a result of condensation on the lid of the 96-well plate.

The Q band spectrum of Myoglobin contains 4 isosbestic points that can be used to correct spectral drift. These points at wavelengths 510, 550, 570 and 585 nm should retain the same absorbance value in both the deoxy-myoglobin and carboxy-myoglobin states (Atkin et al., 2011). The method initially corrects the data by calculating the difference between in the reference spectrum (in this case the time = 0 spectrum) and the measured spectrum. The value is then subtracted from every wavelength so that all spectra align at 510 nm (Figure 4b). Although this correction accounts for most of the difference in the spectra it does not fully align them. The spectrum can be aligned by the remaining three isosbestic points by calculating the difference between them and the reference and plotting this against the wavelength to obtain a non-linear regression. The non-linear regression can then be applied to all wavelengths to align the spectrum. However, as seen in Figure 4c this correction has further skewed these spectra. I believe that the error in this final correction is the result of the calculated equation not fitting the data well. The model fitted a quadratic equation (Figure 5 dotted line), however, due to the positioning of the points a cubic model may fit the data better as suggested in (Figure 5 solid line). Due to the number of replicates and tested conditions, it would not be feasible to plot each individually to establish the equation. Additionally, a model fitting only cubic equations may fit other sets of the data worse than a quadratic. For these reasons it was decided to only correct the data by the 510 nm isosbestic point,

which only moves the spectrum up or down but corrects for the majority of the drift and leaves only a little skewness in the data.

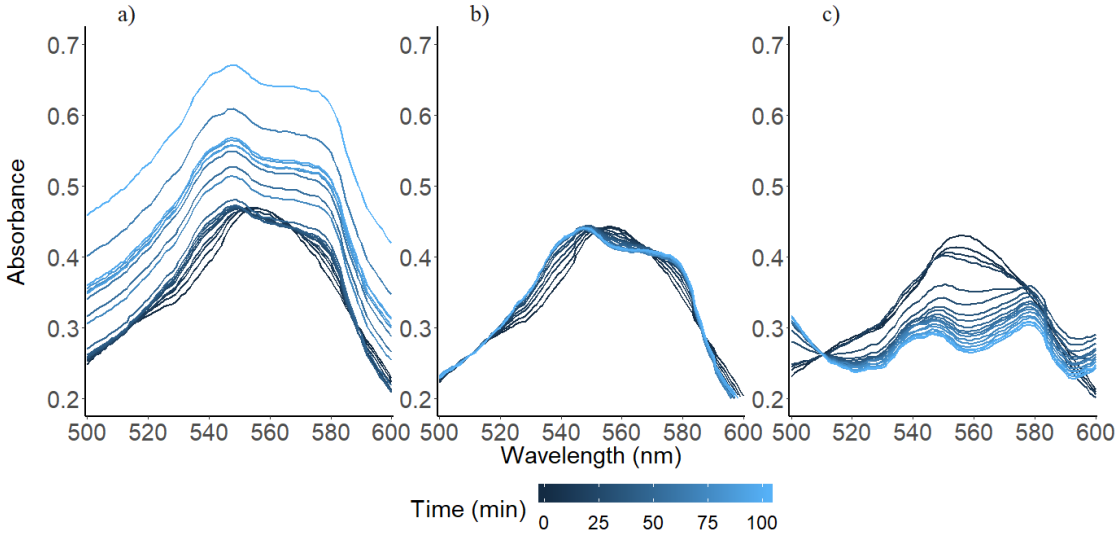

Figure 4: Correction of myoglobin spectra – correction of myoglobin assays is required to account for precipitation with a sample which result in increases in absorbance a). Initial correction utilises the differences in the isosbestic point of 510 nm of a sample and the reference to shift the spectrum up or down b). Final correction utilises the remaining isosbestic points to fully align the spectrum by calculating the difference between them and the reference and plotting this against the wavelength to obtain a non-linear regression which is then applied to each point of the spectrum c). The non-linear regression model used in this case was not a good fit for the data and results increased error in the spectrum.

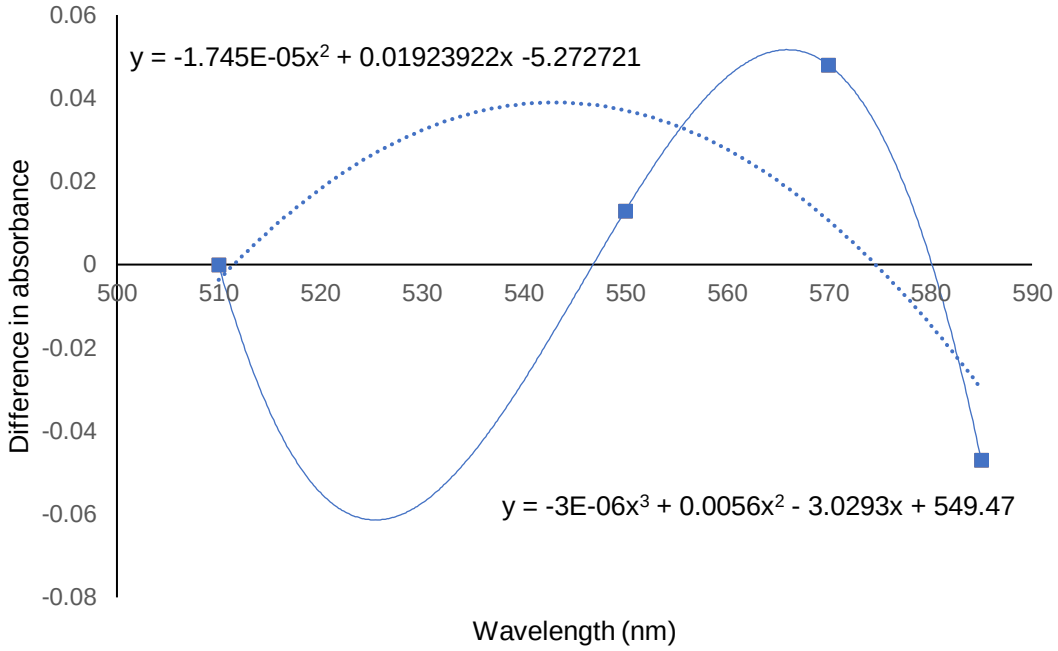

Figure 5: Myoglobin spectra correction model – A quadratic model was used to correct the myoglobin spectrum by the isosbestic points 550, 570 and 585 nm (dotted line). This model does not fit the data well and utilisation of cubic model would have resulted in a better fit (solid line).

With the data corrected to account for precipitation, it can be used to determine if CO is being released from Trypto-CORM under the new activation set up and to determine how changing Trypto-CORM concentration and the total length of light exposure affects the release of CO from Trypto-CORM. The data in Figure 6 shows the increase in the absorption at 540 nm which is indicative of conversion from deoxy-myoglobin to carboxy-myoglobin as when treated with no Trypto-CORM there is no increase in the absorbance at 540 nm (Figure 6a). Thus, it can be established the CO is being released from Trypto-CORM under the new activation set up and that photoirradiation alone has no effect on the myoglobin.

Figure 6 show the data from myoglobin assays using 0, 10, 30, 40 and 60 µM concentrations of Trypto-CORM that were exposed to photoirradiation from the LED bar previously described that emits 395-400 nm light with either an activation cycle of one-minute-on-four-minutes-off (a), two-minute-on-three-minutes-off (b) or four-minutes-on-one-minute-off (c). All on/ off timings were cycled 17 times to provide total exposure times of 17, 34 and 68 minutes respectively. As predicted, increasing the concentration

of Trypto-CORM increases the total amount of CO released. This can be seen clearly in Figure 6 as irradiation of 10 µM Trypto-CORM results in an absorption increase which plateaus at approx. 0.05 higher than the time 0 spectrum, whereas, treatments of 30-60 µM plateau at an absorption of approx. 0.12 higher than the time 0 spectrum. The plateau of the 10 µM treatment is due to all the CO being released from Trypto-CORM thus it cannot reach the same absorbance at 540 nm as higher concentrations. The reason for there being little to no difference between the 30-60 µM absorbance increase is likely that at these concentrations the myoglobin is saturated and therefore, further CO release cannot be observed. The slight decrease observed in the plateaus of Figure 6 is most likely due to the degradation of the myoglobin as this compound has only a short lifespan in solution. Exact concentrations of myoglobin could not be calculated in these experiments due to the unavailability of pure carbon monoxide gas. To calculate the concentration of myoglobin in the solution, CO gas would have been bubbled through the myoglobin solution to saturate the myoglobin. The absorbance of the saturated myoglobin at 540 nm and the extinction co-efficient of myoglobin-CO would then have been used to calculate the myoglobin concentration.

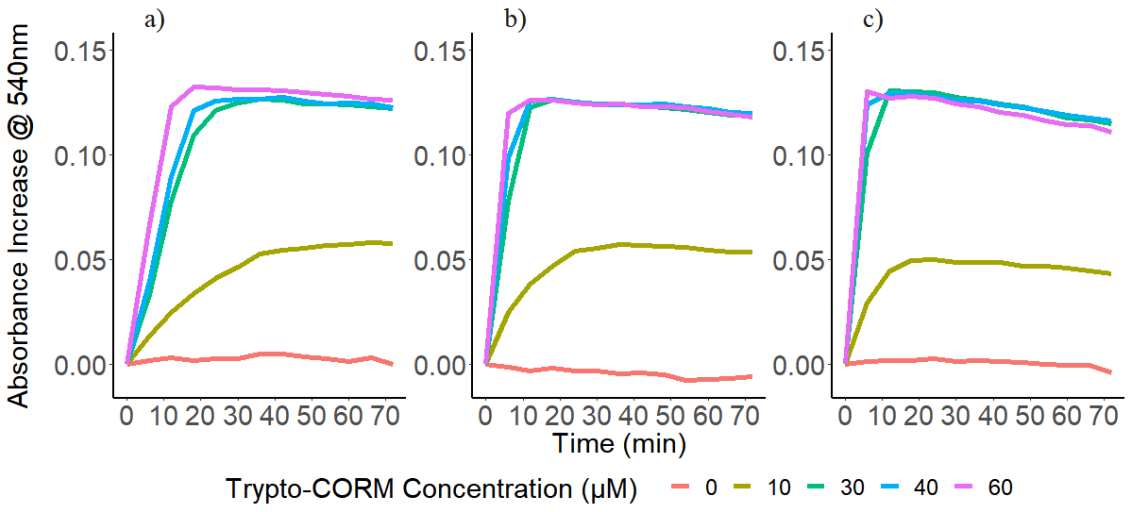

Figure 6: Carbon monoxide release from Trypto-CORM exposed to varying photoirradiation – the increase in absorbance at 540 nm indicates the conversion of deoxy-myoglobin to carboxy-myoglobin. Increase in the absorbacne at 540 nm resulting from the irradiation of 0 (red), 10 (yellow), 30 (green), 40 (blue) and 60 µM (purple) Trypto-CORM for a) one-minute-on-five-minutes-off cycled 17 times, b) two-minutes-on-four-minutes-off cycled 17 times or c) four-minutes-on-two-miutes-off cycled 17 times. The data shown is the mean of six replicates.

The data in Figure 6 also show how changing the total length of time the light is on (and thus the amount of light the solution is exposed to) effects the release of CO. When comparing the 10 µM treatments across the three different activation cycles used there is a clear decrease in the number of activation cycles required for the absorbance increase to plateau as the length of exposure increases. Thus, fewer activation cycles are required to release all the CO from the Trypto-CORM if each activation cycle is longer. This is also as predicted because the longer the light is on, the more photon there will be to interact with the Trypto-CORM per activation cycle. Myoglobin assays were not conducted in the absence of photo-irradiation as it has been concluded by a previous study (Ward, 2014) that in the absence of photochemical stimulation there is a slow release of CO from Trypto-CORM that can be detected by the assay. However, it was established that this release accounted for only a small fraction of the CO that could be released when exposed to photoirradiation.

3.3.2 Effect of Total Irradiation Time on the Growth of *P. aeruginosa* PAO1

Knowing that CO is being released from Trypto-CORM while using the new activation conditions, allows for the effects of Trypto-CORM on bacterial cultures of *P. aeruginosa* PAO1 strain to be evaluated. Again, it is necessary to investigate the effects of altering the length of light exposure, concentration of Trypto-CORM and the role they would play on the growth of PAO1. Changing these factors directly links to amount of CO that is released in a given time. PAO1 was grown in LB media, treated with Trypto-CORM and irradiated one-hour post-inoculation. Figure 7 shows the growth of PAO1 following Trypto-CORM treatment (a) and photoirradiation for one minute (b), three minutes (c) or four minutes (d) in every five minutes cycled seventeen times.

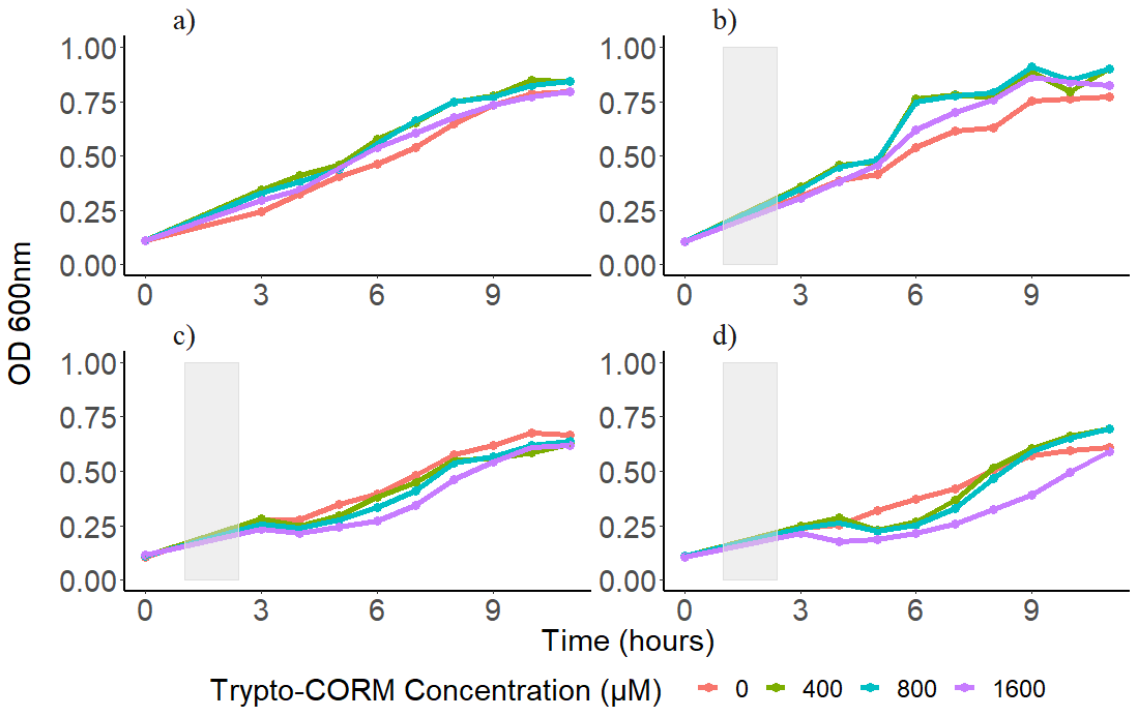

Figure 7: Growth of *P. aeruginosa* treated with Trypto-CORM exposed to varying Photoirradiation – Growth of PAO1 following treatment of 0 (red), 400 (green), 800 (blue) and 1600 (purple) µM Trypto-CORM in the absence of photoirradiation a). b) exposed to photoirradiation of one-minute-on-four-minutes-off cycled seventeen times. c) photoirradiation of three-minutes-on-two-minutes-off cycled seventeen times. d) photoirradiation of four-minutes-on-one-minute-off cycled seventeen times. All photoactivation occurred one-hour after inoculation and is indicated by grey bars. The data shown represents the mean of four replicates.

Interestingly, in the absence of photoirradiation cultures treated with Trypto-CORM grew faster than untreated cultures over the first 8 hours of growth (Figure 7). This was also observed with cultures irradiated for one-minute-on-four-minutes-off in every five minutes (Figure 7b). However, when activation time increases to three-minutes-on-two-minutes-off (Figure 7c) or four-minutes-on-one-minute-off in every five minutes (Figure 7d) a decrease in growth can be observed following photo-irradiation of treated cultures. This suggests that the levels of CO released through irradiated for one minute or less in every five were insufficient and activation for longer than this is required to have any inhibitory effect on the growth of PAO1.

From Figure 7c-d it can be seen that increasing the concentration of Trypto-CORM results in a lower density of cells and reduced bacterial growth. The data in Figure 8 highlight the difference in bacterial densities after 6 hours of growth, following Trypto-

CORM treatment activated by different activation cycles. This data can be used to determine if Trypto-CORM is significantly reducing the growth of PAO1 and if changing the length of activation has an effect.

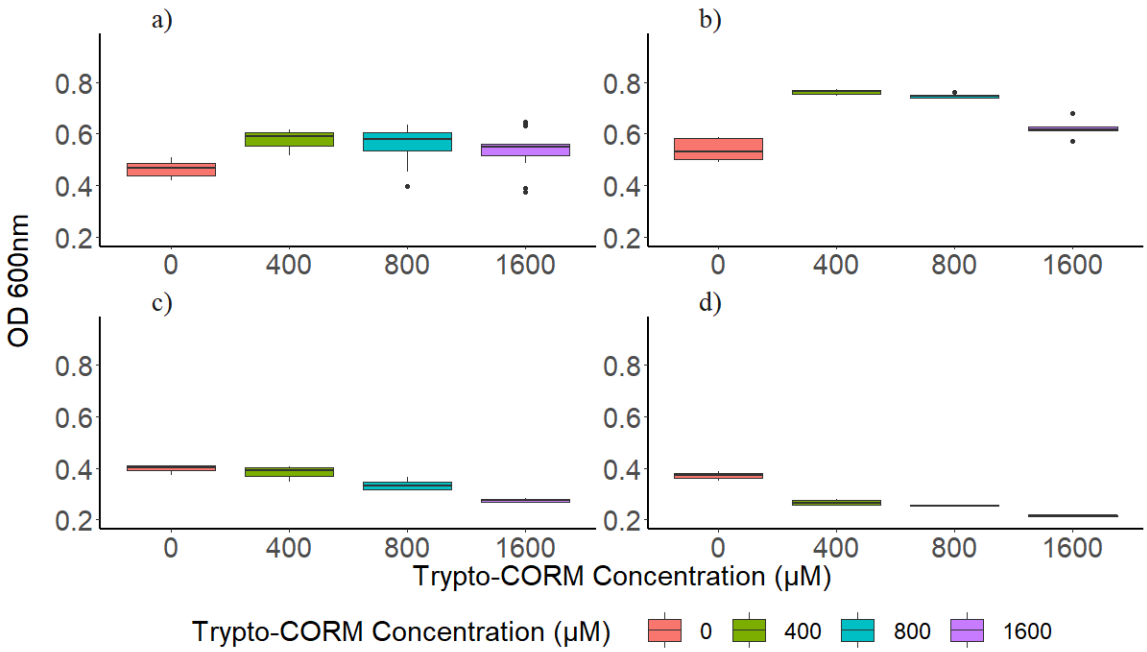

Figure 8: Effect of varying photoirradiation time on the density of *P. aeruginosa* following Trypto-CORM treatment - a) Density of PAO1 following six hours of growth at 37°C and treatment of 0 (red), 400 (green), 800 (blue) and 1600 (purple) µM Trypto-CORM in the absence of photoirradiation. b) photoirradiation of one-minute-on-four-minutes-off cycled seventeen times. c) photoirradiation of three-minutes-on-two-minutes-off cycled seventeen times. d) photoirradiation for four-minutes-on-one-minute-off cycled seventeen times. Boxes represents the range between the 25th quartile and the 75th quartile of the data with the black line in within the box representing the median. Whiskers represent the smallest and largest values within 1.5 times the interquartile range where n = 4.

Kruskal-Wallis tests were conducted on each different activation cycle to determine if Trypto-CORM concentration significantly altered bacterial densities. Trypto-CORM treatment increased the growth of PAO1 in the absence of photo-irradiation (chi-squared = 20.043, p-value < 0.005, DF = 3) with all concentrations having higher densities than untreated cultures (Wilcoxon pairwise p-values <0.01). Photo-activation using the activation cycle one-minute-on-four-minutes-off also resulted in treated cultures having a higher density than untreated ones (chi-squared = 16.577, p-value < 0.005, DF = 3), with 400 and 800 µM treatments stimulating growth more than the 1600 µM treatment (both Wilcoxon pairwise p-value = 0.012). Trypto-CORM significantly lower bacterial densities when exposed to irradiation cycle of three-minutes-on-two-

minutes-off (chi-squared = 12.463, p-value = 0.006, DF = 3). Treatments of 800 and 1600µM Trypto-CORM resulted in significantly lower densities than the control (both Wilcoxon pairwise p-values = 0.043). Photoactivation cycle of four-minutes-on-one-minute-off also resulted in treated cultures having lower densities than untreated ones (all p-values = 0.035).

Photoactivation cycles of greater than one-minute-on-four-minutes-off every five minutes cycled seventeen times resulted in treated cultures having lower bacterial densities than untreated ones. However, analysis of the controls revealed that the densities of the controls exposed to the four-minutes-on-one-minute-off activation cycle were significantly lower than cultures not exposed to photo-irradiation (Kruskal-Wallis - chi-squared = 12.134, p-value < 0.05, DF = 3). This suggests that exposure to the 400nm light for this length of time is having an effect on bacterial growth. Light with a wavelength of 400 nm falls on the edge of the ultraviolet-A spectrum, which is known to have lethal effects on *P. aeruginosa* (Fernández and Pizarro, 1996). UV-A radiation results in DNA damage through the generation of singlet oxygen species, which can also be generated by visible light (Rastogi et al., 2010). This could explain the results obtained by Amin et al. (2016) who found that exposure to 415nm light, which is outside of the UV spectrum, resulted in reduced viability of *P. aeruginosa*. This study suggested that exposure to blue light at a dose of 48 J/cm^2 was sufficient to significantly reduce cell viability. The four-minute-on-one-minute-off activation cycle generates a dose of approximately 166 J/cm^2 which is almost four times higher than the dose stated by Amin et al. (2016). This could explain the difference in bacterial densities observed between the cultures exposed to the four-minute-on-one-minute-off activation cycle and those not exposed to photoirradiation.

Because of the significant difference between the four-minute-on-one-minute-off activation cycle and the control, the near significant value for the three-minutes-on-two-minutes-off activation cycle and the fact that both the three-minute-on-two-minutes-off and four-minute-on-one-minute-off activation cycles produced doses higher than that quoted by Amin et al. (2016) preliminary experiments we conducted utilising a two-minutes-on-three-minutes-off photoirradiation cycle, cycled seventeen

times. Based on these results, this photoirradiation cycle was utilised for the data in 3.3.3 and in turn was used for all future activations.

3.3.3 Trypto-CORM effects on the Growth of *P. aeruginosa* PAO1 Under Oxygen Limiting Conditions.

With confirmation that CO is being released from Trypto-CORM and an established activation cycle, the effects of Trypto-CORM on the growth of PAO1 was explored further under oxygen limited conditions. To test the hypothesis that Trypto-CORM is more effective as an antimicrobial when cultures are growing under near anaerobic conditions, cultures of PAO1 were prepared in LB media. These were then treated with various Trypto-CORM concentrations and covered with a layer of paraffin oil similar to the myoglobin assays (Section 2.4). Figure 9 shows the growth of PAO1 treated with 0, 400, 800 or 1600 µM Trypto-CORM which is exposed to irradiation through the two-minute-on-three-minute-off activation cycle, five hours post-inoculation. Cultures in Figure 9a were covered with a layer of paraffin oil to limit gaseous exchange at the surface of the culture, whereas cultures in Figure 9b did not and gas could freely diffuse into the media.

The addition of paraffin oil to the surface of the bacterial cultures changes the growth dynamics of the bacteria. These cultures grow slower than cultures without the paraffin oil layer and only reach a density approximately equal to half of the cultures lacking paraffin oil (Figure 9).

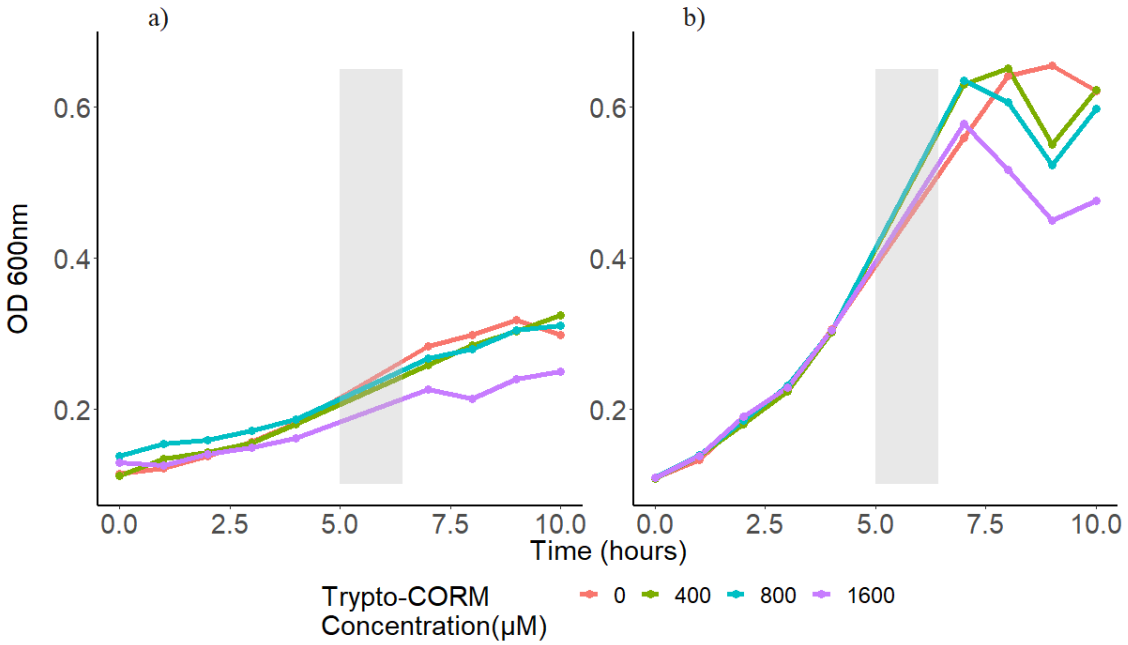

Figure 9: Growth of Trypto-CORM treated *P. aeruginosa* under oxygen limiting conditions - a) Growth of PAO1 under oxygen limiting conditions induced through the addition of a layer of paraffin oil to the top of cultures. Cultures were treated with 0 (red), 400 (green), 800 (blue) and 1600 μM (purple) Trypto-CORM. b) Growth of PAO1 treated with Trypto-CORM, growing under aerobic conditions. Cultures were allowed to grow for eleven hours with optical density 600 nm measurements taken hourly except from when photoirradiation occurred. Grey bars indicate the start time and duration of photoirradiation using a two-minute-on-three-minute-off activation, cycled seventeen times. The data shown represents the mean of four replicates.

P. aeruginosa is capable of growing under anaerobic conditions in the presence of nitrogen electron acceptors or with *L*-arginine, which is present in LB media (Wu et al., 2005). However, growth solely on *L*-arginine is very slow because less energy is produced through its metabolism than through respiration (Arai, 2011). The growth observed in Figure 9a suggests that the paraffin oil is having the desired effects of limiting gaseous exchange but is unlikely to be inducing full anaerobic conditions.

As with the previous experiment Trypto-CORM treatments of 1600 μM appear to be having the greatest effects on the growth of PAO1. Under oxygen-limiting conditions the 1600μM concentration appears to reduce the growth of the bacteria before photoirradiation, however, this could be due to the lack of a time point just prior to irradiation. Overall though the growth of this treatment does appear to be reduced more than other treatments and the culture does not reach the same density as the other treatments after ten hours of growth (Figure 9a).

The growth of all Trypto-CORM treatments in non-oxygen limiting conditions are comparable with variation in densities only occurring after Trypto-CORM activation. Following irradiation, the densities of all treatments decrease with the greatest effect being observed for the 1600µM treatment which does not appear to recover.

The relative growth of the treatments compared to the controls at nine and ten hours were calculated and plotted to allow for the comparison between the cultures covered with paraffin oil and those without it (Figure 10). To determine if the difference on the observed densities at ten hours is significant and if limiting oxygen availability increases Trypto-CORM efficiency, a Two-way ANOVA was conducted.

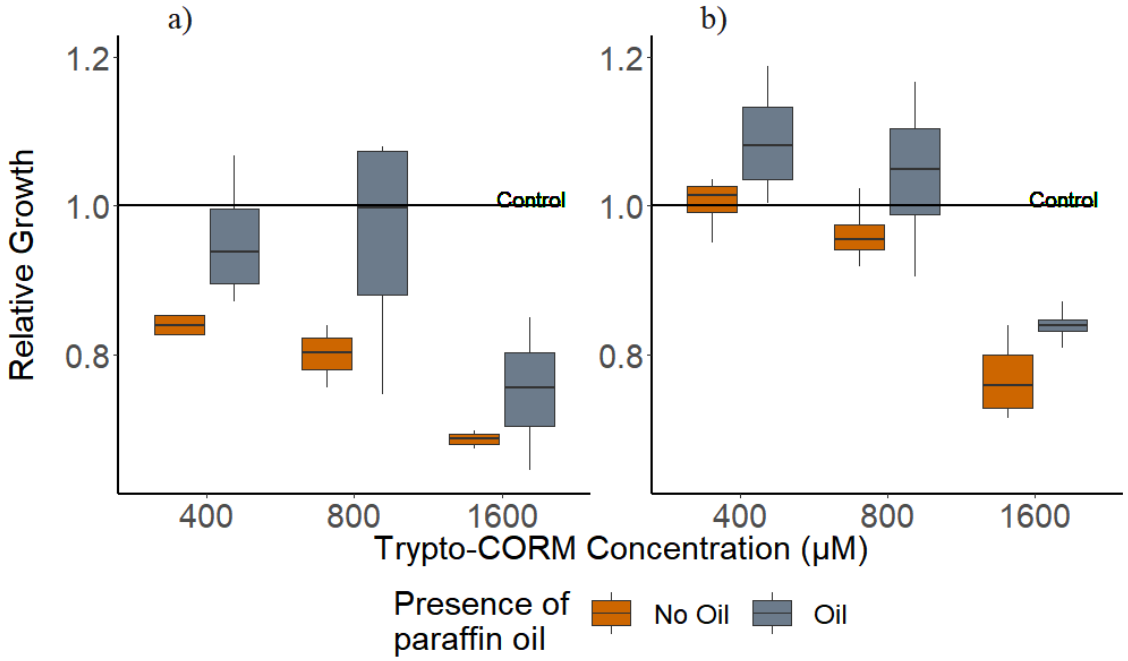

Figure 10: Densities of Trypto-CORM treated *P. aeruginosa* under oxygen limiting conditions – The relative growth of trypto-CORM treated cultures compared to untreated cultures following A) nine hours and b) ten hours of growth at 37°C. Comparision of cultures growing under anerobic condions (orange) and under oxygen limiting cnditions induced through the addition of parrafin oil on the top of cultures (grey). Boxes represents the range between the 25th quartile and the 75th quartile of the data with the black line in within the box representing the median. Whiskers represent the smallest and largest values within 1.5 times the interquartile range where n = 4.

Analysis via two-way ANOVA was conducted for both the relative densities after 9 and 10 hours. Significant effect of Trypto-CORM on relative bacterial densities was noted for both 9 hours ($F_{(2,18)}$ =11.064 , p-value <0.005) and Tukey post-hoc analysis revealed that, after 9 hours growth, Trypto-CORM treatment of 1600 µM, in the absence of

paraffin oil, reduced the density of PAO1 significantly more than the other Trypto-CORM concentrations tested (both p-value <0.005). While 1600 µM Trypto-corm treatment in the presence of paraffin oil did not result in significantly lower densities than 800 and 400µM treatments (p-values = 0.411 & 0.666 respectively). Additionally a significant effect of Trypto-CORM on relative densities was noted after 10 hours ($F_{(2,18)}$ = 30.787, p-value <0.005) with Trypto-CORM treatment of 1600 µM reduced the density of PAO1 significantly more than the other Trypto-CORM concentrations tested independent of the presence of paraffin oil (all p-values <0.005). As described previously this result is presumably due to the increased amount of CO that is released from this treatment. Interestingly, Tukey post-hoc analysis also revealed that the addition of paraffin oil had no significant effect on the relative densities of cultures treated with the same concentration of Trypto-CORM at either nine hours or ten hours (p-values >0.05). No significant interaction was noted between the presence paraffin oil and Trypto-CORM concentration on relative densities after 9 ($F_{(2,18)}$ = 0.586, p-value = 0.567048) or 10 hours ($F_{(2,18)}$ = 0.020, p-value = 0.097984) of growth.

P. aeruginosa, like many bacteria, has several terminal oxidases that have different electron donors and are expressed under differential conditions (Arai, 2011). Under conditions where oxygen is freely available cytochrome *aa3* is expressed as the major cytochrome involved with respiration. This cytochrome has a low affinity for oxygen but is efficient at pumping H^+ to generate high proton gradients required for ATP synthesis (Arai, Jung and Kaplan, 2008). Under limited oxygen conditions its expression of *aa3* is reduced and the expression of cytochromes with a high affinity for oxygen, such as cytochromes *cbb3*-1 and -2, are increased (Comolli and Donohue, 2004). A study conducted by Jesse et al., (2013) found that cytochrome *bd*-I, which is expressed under limited oxygen conditions, is less sensitive to CORM treatment and cells only expressing this cytochrome were inhibited less than cells expressing other cytochromes (Giuffrè et al., 2014; Jesse et al., 2013). This cytochrome shares significant homology to the cyanide-insensitive oxides of *P. aeruginosa* which is also expressed under low oxygen conditions (Cunningham, Pitt and Williams, 1997).

It is plausible that cultures covered with a layer of paraffin oil, thus having limited oxygen availability, have reduced the expression of the CO-sensitive cytochromes and

increased the expression of cytochromes such as *cbb3s*. This would explain why the growth of these cultures is lower than those that are not covered with oil. However, as the addition of paraffin oil has no effect on Trypto-CORM efficiency, it is unlikely that cyanide-insensitive oxides are being expressed. The observed differences in Figure 10 between cultures covered with paraffin oil and those not likely results for the differences in total growth.

3.3.4 Diffusion of Carbon Monoxide and its Effects on Neighbouring PAO1 Cultures

In previous experiments, there were some differences in the growth of cultures that were not treated with Trypto-CORM but were exposed to photoirradiation and the cultures that were not. It was suggested in 3.3.2 that this could be due to the amount of light that the cultures were exposed to. However, the effect was also observed in experiments where cultures were exposed to less light (data not shown). Following this result, it was hypothesised that the Trypto-CORM is able to affect the growth of neighbouring culture wells presumably through the diffusion of CO. To test this hypothesis cultures of PAO1 were inoculated at increasing distances from a solution of 1600 µM Trypto-CORM on a 96-well microplate. The plate was exposed to irradiation for two minutes in every five minutes cycled seventeen times, one hour after inoculation. The data in Figure 11 shows the densities of cultures at different distances from Trypto-CORM following 10 hours of growth.

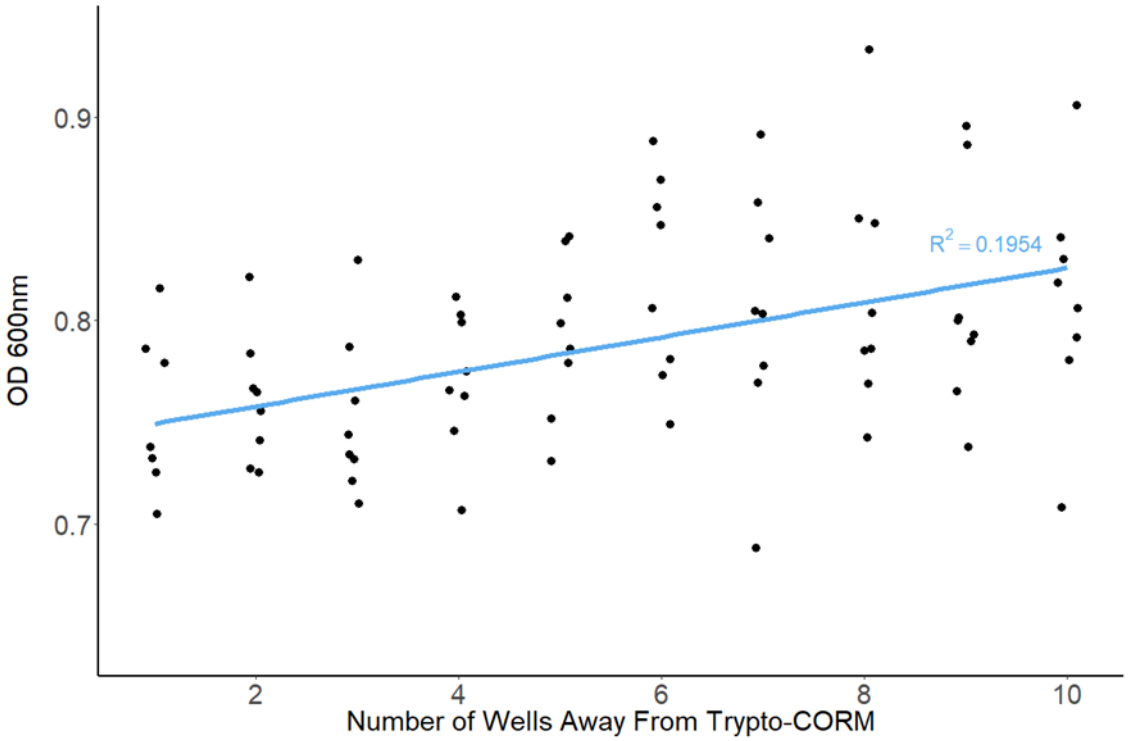

Figure 11: Effects of Trypto-CORM on the growth of neighbouring untreated cultures of *P. aeruginosa* – Densities of PAO1 cultures that were inculated for 11 hours in wells, of a 96-well microplate, at increasing distances from 1600 µM Trypro-CORM. Trypto-CORM was irradiated for two-minutes-on-three-minutes-off cycled 17 times, 1 hour post innoculation.

There was a significant increase in bacterial densities as distance from Trypto-CORM increases (Pearson's correlation r = 0.453402, p-value < 0.005), this suggests that there is some effect of Trypto-CORM on neighbouring cultures on a 96-well plate. In previous experiments, Trypto-CORM was diluted one in two down the length of the 96-well plate and probably resulted in an accumulative effect causing greater reductions in growth for untreated cultures. Because of this finding all following experiments separated cultures by concentration onto separate plates.

3.3.5 Time of Trypto-CORM Activation and its Effects on *P. aeruginosa* PAO1 Growth

To determine if the phase of bacterial growth had any effect on Trypto-CORM treatment cultures of PAO1 were inoculated in varying concentrations of Trypto-CORM and exposed to photoirradiation (two-minutes-on-three-minutes-off, cycled 17 times) one, three, four or five hours after inoculation. This experiment explored the hypothesis that cultures would be more susceptible to Trypto-CORM treatment during the exponential growth phase than the lag phase as more cells in the culture would be actively respiring

and utilising respiratory enzymes, which are thought to be a key target of the CO from CORMs (Nobre et al., 2009). The data in Figure 12 shows the relative densities of Trypto-CORM treated cultures to untreated ones, which were photo irradiated at a) one hour, b) three hours, c) four hours and d) five hours after inoculation.

A two-way ANOVA was conducted on the relative growth resulting from altering the time of activation and concentration of Trypto-CORM. Increasing Trypto-CORM concentration resulted in significantly lower bacterial densities ($F_{(2,48)=}$ = 85.28, p-value < 0.005), with treatments of 1600 µM Trypto-CORM resulted in significantly lower growth than treatments of 400 and 800 µM Trypto-CORM in all activation times (all Tukey p-values < 0.005). Additionally, Tukey analysis revealed that activating Trypto-CORM five hours after inoculation resulted in significantly less growth than activation at four hours (p-value <0.005), three hours (p-value <0.005) and one hour (p-value = 0.0055). However, this effect was dependent on concentration as there was a significant interaction between the concentration of Trypto-CORM and the time of activation on the relative growth of PAO1 ($F_{(6,48)}$ = 3.83, p-value < 0.005). Interestingly, when treatments of 400 and 800 µM Trypto-CORM are activated 4 hours after inoculation there was a significantly higher density of cells than untreated cultures (Figure 12c).

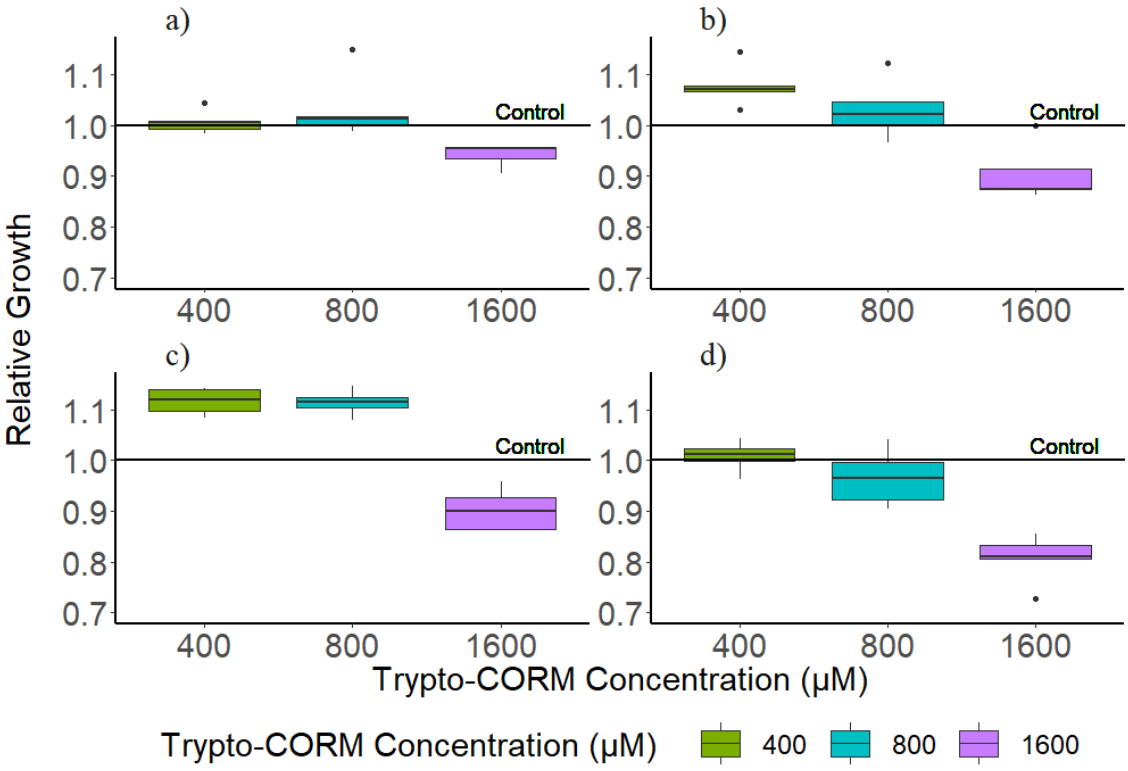

Figure 12: Effect of Trypto-CORM activation time on the density of *P. aeruginosa* – Relative growth of PAO1 treated with 400 (green), 800 (blue) or 1600 µM (purple) Trypto-CORM compared to untreated cultures. Photoirraditaion *via* a two-minutes-on-three-minutes-off activation cycle which cycled 17 times occurred a) one hour, b) three hours, c) four hours or d) five hours post incoulation. Boxes represents the range between the 25th quartile and the 75th quartile of the data with the black line in within the box representing the median. Whiskers represent the smallest and largest values within 1.5 times the interquartile range where n = 4.

A study by Sahlberg Bang et al., (2016) also found that bacteria were more susceptible to CORM treatment during the exponential phase of growth. In this study, they showed that application of CORM-2 during mid-exponential growth of E. coli reduced the colony-forming units (CFU) by 6 log units after 4 hours. However, when applied to cultures that had reached stationary phase the reduction in CFU was not observed until 24 hours after application and was not as large as application during exponential phase. Additionally, when stationary phase cultures where regrown to exponential phase and treated with CORM-2 the decrease in CFU is seen after 4 hours (Sahlberg Bang et al., 2016). This suggests that the growth phase of the bacteria plays a key role in the efficiency of CORM treatments and that cultures are more susceptible to CORM treatment when actively metabolising. As predicted previously this could be due to

more cells expressing cytochrome oxidases during the exponential growth phase than in the lag phase.

3.3.6 Effects of Trypto-CORM on PAO1 Virulence

Pseudomonas aeruginosa produces a range of virulence factors that can result in damage to host cells during infections. When treating infections, it is important to minimise the negative effects this has on patients. Therefore, it is essential to ensure that treatment of *P. aeruginosa* with CORMs does not result in the increased virulence of the pathogen which in turn may increase damage to the host and increase the survival of the pathogen. To determine if Trypto-CORM treatment affected the virulence of *P. aeruginosa*, three key virulence factors (pyocyanin, pyoverdine and biofilm) were measured following Trypto-CORM treatment. Cultures were treated and exposed to irradiation to activate Trypto-CORM one and five hours after inoculation. Figure 13 shows the absorbance at 691 nm which is a key absorbance peak for oxidised pyocyanin and can be used as a proxy to quantify production levels. The data show the levels of pyocyanin when cultures are exposed to a) no irradiation, b) irradiation after 1 hour of growth and c) irradiation after 5 hours of growth. This assay was combined with the pyoverdine assay which utilised the fluorescent properties of pyoverdine and emission values at 460 nm following irradiation at 400nm. Figure 14 shows the emission at 460 nm and is separated as described for Figure 13.

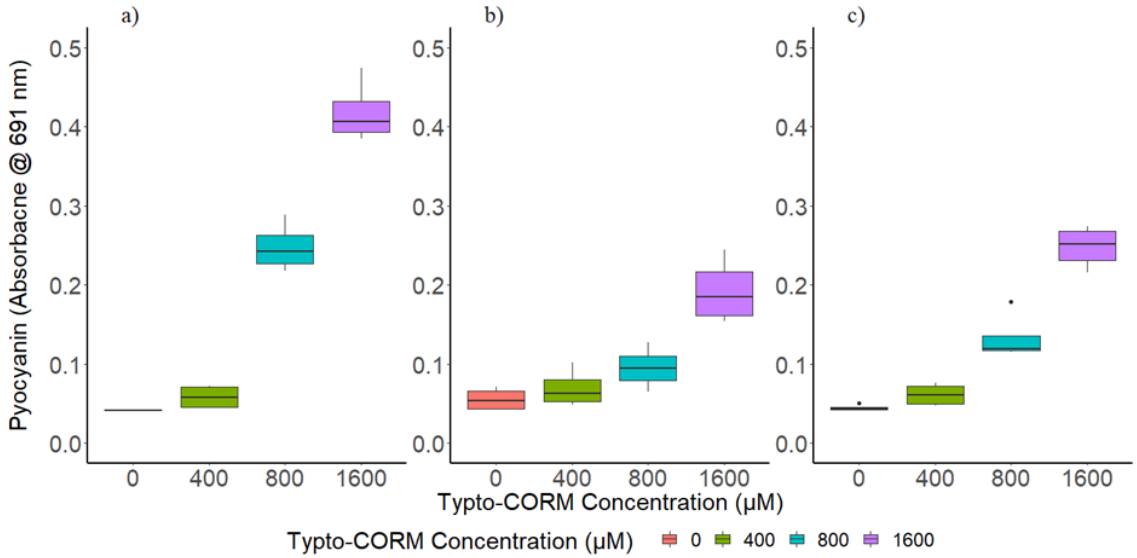

Figure 13: Effects of Trypto-CORM on pyocyanin production – Absorbance at 691 nm representing pyocyanin from *P. aeruginosa* supernatant in the absence of Trypto-CORM treatment (red), treatment of 400 (green), 800 (blue) and 1600 µM (purple) Trypto-CORM. Cultures were incubated for 24 hours at 37°C

in the absence of photoirradiation a), irradiation via two-minutes-on-three-minutes-off cycled 17 times one hour post inoculation b) and five hours after incoulation c). Boxes represents the range between the 25th quartile and the 75th quartile of the data with the black line in within the box representing the median. Whiskers represent the smallest and largest values within 1.5 times the interquartile range where n = 4.

A significant increase in pyocyanin was observed as Trypto-CORM concentration increased (Two-way ANOVA: $F_{(3,36)}$ = 218.25, p-value < 0.005). Treatment of 1600µM Trypto-CORM resulted in significantly higher levels of pyocyanin than other treatments in all three activation conditions. Interestingly, Tukey *post hoc* analysis revealed the greatest increase in the 1600 µM treatment was observed in the absence of photoirradiation, with an OD 0.17 higher than activation after 5 hours of growth and 0.2258 higher than activation after 1 hour of growth. A significant interaction was also observed between the concentration of Trypto-CORM treatment and when photoirradiation occurred on the levels pyocyanin produced ($F_{(6,36)}$ = 23.18, p-value <0.005).

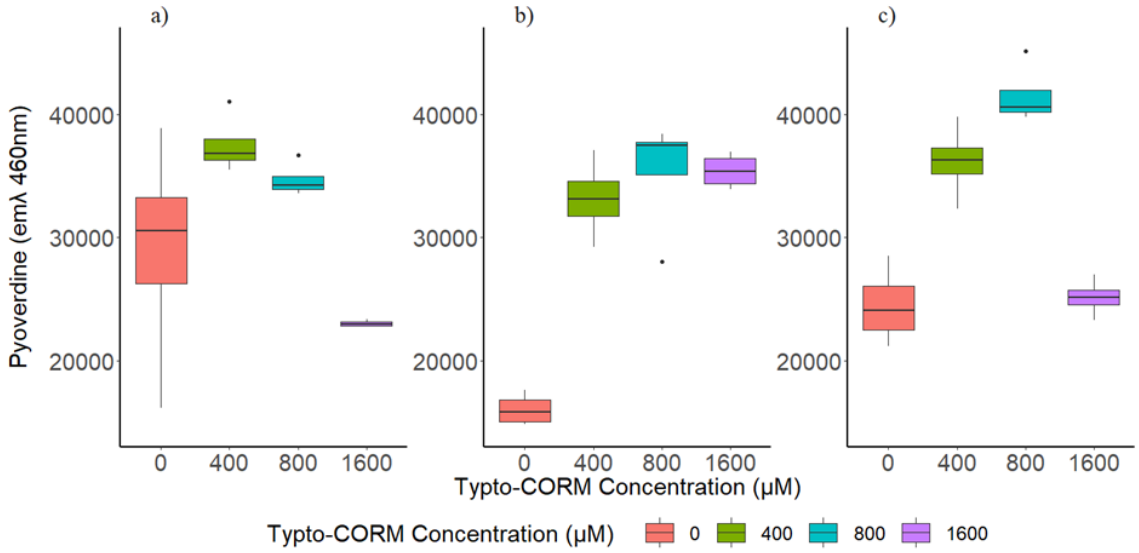

Figure 14: Effects of Trypto-CORM on the production of pyoverdine – Cultures were treated with 0 µM (red), 400 µM (green), 800 µM (blue) and 1600 µM (purple) Trypto-CORM and incubated for 24 hours at 37°C in the absence of photoirradiation a), irradiation via two-minutes-on-three-minutes-off cycled 17 times one hour post inoculation b) and five hours after incoulation c). Emission of pyoverdine in *P. aeruginosa* supernatant at 460 nm was recorded following irradiation at 400 nm. Boxes represents the range between the 25th quartile and the 75th quartile of the data with the black line in within the box representing the median. Whiskers represent the smallest and largest values within 1.5 times the interquartile range where n = 4.

Trypto-CORM treatment also significantly altered the production of pyoverdine by PAO1 (Two-way ANOVA: $F_{(3,36)}$ = 38.44, p-value < 0.005). Surprisingly, in both photoirradiation

conditions, the greatest increase in pyoverdine was observed for the 800 µM treatments. Interestingly, 1600 µM treatment that was exposed to photoirradiation five hours post-inoculation did not produce a significantly different amount of pyoverdine than the control. This is hypothesised to result from a lower level of growth for cultures exposed to this condition. Tukey *post hoc* analysis also revealed that there was no significant difference between any Trypto-CORM treatment and the control in the absence of photoirradiation (all p-values >0.05). This is presumably due to the broad range of emission values obtained for the control. A significant interaction was also observed between the concentration of Trypto-CORM treatment and the time of photoirradiation ($F_{(6,36)}$ = 10.12, p-value < 0.005). The interaction is also presumed to result from the broad range of values obtained for untreated cultures in the absence of Trypto-CORM treatment. A large variation in pyoverdine production can be seen in untreated cultures in the absence of photo irradiation (Figure 14a), however, the majority of the replicates produce more pyocyanin than cultures exposed to photoirradiation. This fits with a study conducted by Fila, Kawiak and Grinholc (2017) who found that antimicrobial blue light significantly reduced the production of various virulence factors by *P. aeruginosa.* however, photoirradiation of untreated cultures after 5 hours results in a greater production of pyoverdine than those irradiated after 1 hour for an unknown reason.

To determine if Trypto-CORM treatment increases biofilm production of PAO1 were treated with various concentrations. Cultures were exposed to photoirradiation *via* the two-minutes-on-three-minutes-off activation cycle, cycled 17 times, started either on or five hours post-inoculation. Biofilm assays were performed after 24 hours of growth. The data in Figure 15 shows the absorbance at 600 nm which was used as a proxy to measure biofilm present. Pearson's and Spearman's Ranked Correlations were used to determine if biofilm production increased with Trypto-CORM treatment.

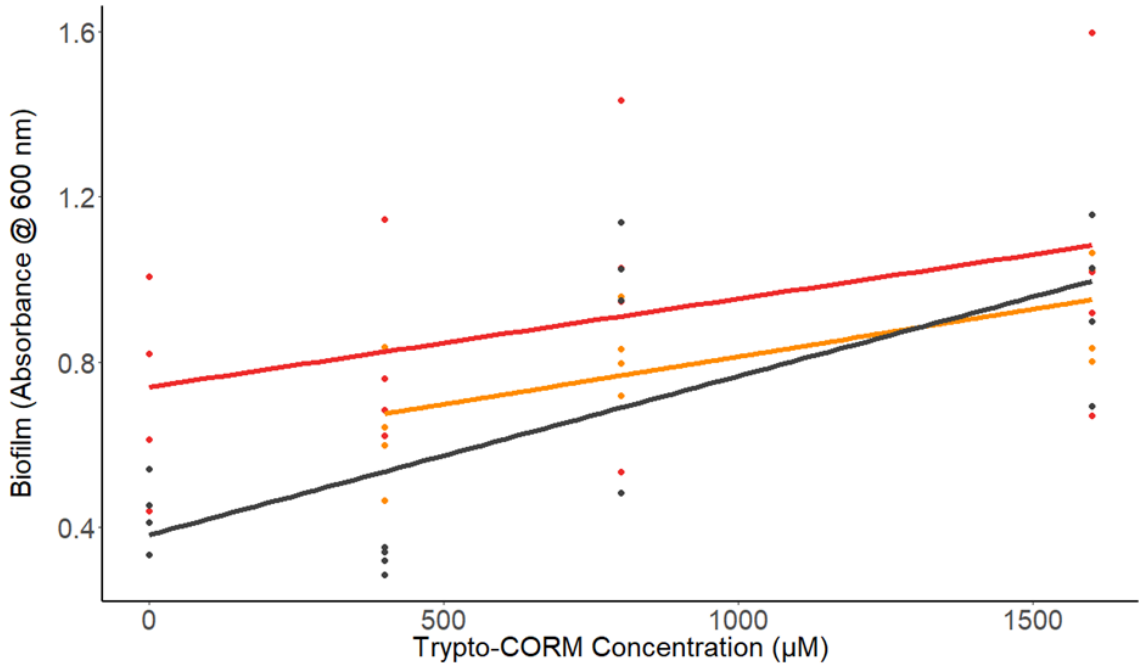

Figure 15: P. aeruginosa biofilm production following Trypto-CORM treatment – Biofilms measured using the crystal violet assay to determine the effects of Trypto-CORM concentration on biofilm production in the absence of photoirradiation (black), photoirradiation of two-minutes-on-three-minutes-off beginning 1-hour after incoulation (orange) and 5-hours after inoculation (red). Biofilm of untreated cultures exposed to photorradiation 1-hour post inccoulation not shown as data was lost.

As Trypto-CORM concentration increases there is a significant increase in biofilm production when cultures are not exposed to photoirradiation (Spearman's: r = 0.691, p-value = 0.003) or are exposed to irradiation one-hour post-inoculation (Pearson's: r = 0.689, p-value = 0.013). No significant increase in biofilm production when photoirradiation occurred five hours after inoculation (Pearson's: r = 0.413, p-value = 0.112). This result is most likely due to the large variation between replicates of the same experiment. Additionally, cultures exposed to photo-irradiation 5-hours post inoculation had more biofilm than cultures not exposed to photo-irradiation. Exposure to blue light (400nm) has been found to stimulate the production of biofilms in several *Acinetobacter* strains (Golic et al., 2013), however, the opposite effects have been noted in *P. aeruginosa* (Fila et al., 2018). It is plausible that the observed increase results from the limitations of the experimental procedure. It has been noted that slight differences in the wash steps can result in the biofilm detaching from the microplate wells (Azeredo et al., 2017). This could also explain the large variation observed between the replicates.

In general, Trypto-CORM treatment results in an increase in both biofilm and pyocyanin production. Whilst increases in pyoverdine production are observed for the intermediate concentrations of Trypto-CORM that are exposed to photoirradiation.

Virulence genes, including pyoverdine and pyocyanin, and genes controlling biofilm production are usually under the regulation of the *LuxR* quorum sensing pathway (Michael Weigert aus Straubing, 2017; Mukherjee et al., 2017; Wei and Ma, 2013). Pyocyanin is a blue secondary metabolite produced by *P. aeruginosa* that plays a key role in bacterial virulence (Price-Whelan, Dietrich and Newman, 2007; Lau et al., 2004). One role of pyocyanin in virulence is to react with reactive oxygen species produced by phagocytic host cells to protect the bacterium from oxidative damage (Vinckx et al., 2010). Pyocyanin may increase with Trypto-CORM treatment to protect the cells from oxygen species generated by the carbon monoxide released from Trypto-CORM. However, this only explains the increase in pyocyanin and not in pyoverdine and biofilms.

A study by Vinckx et al., (2010) found that the decreasing the expression of the regulator *OxyR,* which is involved with the modulation of genes in response to oxidative stress, reduces pyocyanin expression. *OxyR* has also been shown to play a crucial role in the biofilm production of *Serratia marcescens* with *OxyR* mutants being unable to generate biofilms and adhere to surfaces (Shanks et al., 2007). It is plausible the *OxyR* may also play a role in the formation of biofilms by *P. aeruginosa.*

A previous study by the Cornelis group found *OxyR* expression was required for iron uptake utilising pyoverdine but did not directly influence production (Vinckx, Matthijs and Cornelis, 2008). Although pyoverdine production does not increase through *OxyR*, Iron uptake and metabolism is directly coupled to the response to oxidative stress and pyoverdine has been shown to play a role in oxidative stress tolerance (Barrientos-Moreno et al., 2019). Therefore, pyoverdine production could also be increasing in response to oxidative stress but trough a different regulatory mechanism to *OxyR.*

3.4 Conclusions

Alteration to the activation set up of Trypto-CORM to allow for higher throughput screening of conditions has shown to drastically reduce the antimicrobial effects of

Trypto-CORM. Previous studies showed that Trypto-CORM was an effective antimicrobial that prevented the growth of S. aureus, E. coli and N, gonorrhoeae at 100 µM concentrations, however, this cannot be replicated with the current activation set up used in these experiments (Figure S9). Additionally, previous studies investigating the effects of CORM-3 on bacterial growth have shown that *P. aeruginosa* is as susceptible to CORM-3 treatment as E*. coli* (Desmard et al., 2009; Davidge et al., 2009). It is therefore hypothesised that the lack of antimicrobial activity in these experiments is the result of the activation set up. In previous experiments bacteria were cultured and treated in large volumes meaning that the pathlength of the treated cultures was significantly larger than the pathlength in these experiments. The Beer-Lambert Law states that the pathlength of a sample directly affects its absorbance. Therefore, there would be a greater absorbance of photons in the previous experiments than this experiment resulting in more CO-release from Trypto-CORM at any given time. Unfortunately, the effects of Trypto-CORM against PAO1 could not be tested in the original, larger volume, activation set up due to the unavailability of components.

For Trypto-CORM to have any antimicrobial effect on *P. aeruginosa* using this setup, concentrations of 1600 µM were required. Moreover, the antimicrobial effects exhibited in these experiments were nowhere near as strong as in previous studies. A maximum reduction of approximately 25% was observed in these experiments compared with the total inhibition noted in the previous ones. This data does not suggest the *P. aeruginosa* is insensitive to Trypto-CORM treatment and future experiments should consider testing the antimicrobial effects of Trypto-CORM against this bacterium when activated in the previous setup.

Additionally, Ward et al (2014), previously showed that Trypto-CORM has no significant effect on the viability of mammalian macrophage cells when treated with 100 µM Trypto-CORM, however, a slight decrease can be observed as Trypto-CORM concentration increases. Moreover, a study by Nobre et al. (2016) found that the CORM treatments of 500 µM or less could result in a 20% decrease in the viability of kidney epithelial cells, 90% reduction in macrophage viability and a greater than 50% reduction in hepatoma cell viability. Based on these findings it is plausible that at the

concentrations of Trypto-CORM required to exhibit antimicrobial effect on PAO1, significant damage would also be done to mammalian tissues.

Although Trypto-CORM has not shown to be an effective antimicrobial under the conditions used in these experiments this work has made some interesting discoveries and laid the groundwork for future investigations. For example, this work has highlighted the importance of treatment and activation times, as activation of Trypto-CORM during the mid-exponential phase resulted in significantly lower bacterial densities. Therefore, additional future experiments should focus on repeating previous experiments in the original set up while activating Trypto-CORM during the exponential phase of growth. Additionally, this work highlights the significance of the activation set up and how the antimicrobial effects can be lost when reducing the path length of the bacterial culture. This is an important finding that highlights that a photo-CORM that is effective *in vitro* may prove more problematic than initially though for an *in vivo* treatment. The therapeutic use of photoCORMs has been suggested to be for the treatment of dermal infections and thus can be easily irradiated. However, this too would have a short pathlength and therefore may not be effective.

4.0 Ebor-CORM

4.1 Introduction

With the ever-growing prevalence of antimicrobial resistance, resulting from misuse and overuse of antibiotics, clinicians are now resorting to the use of last resort antimicrobials to treat multi-drug resistant bacterial infections (Jansen et al., 2016). It has been suggested that the way we treat bacterial infection needs to be restructured and the use of monotherapy should be replaced with combination therapy (Tyers and Wright, 2019). The reasoning behind this is that most commonly used antimicrobials are derived from products produced by bacteria and fungi, and in natural environments, these organisms often utilise a range of antimicrobials to suppress competing microbes instead of single compounds (Challis and Hopwood, 2003).

There are three different main types of combination therapies. One of the most common type used currently is syncretic combinations. This involves the use of an antimicrobial in combination with a compound that interacts with non-essential targets and is not antimicrobial (Tyers and Wright, 2019). An example of this combination is the use of β-lactam antimicrobial with β-lactamase inhibitors to prevent the degradation of the β-lactam (Monroe and Polk, 2000). Second, congruous combinations are utilised by combining two antimicrobials that exert antimicrobial effects through different mechanisms. This method is currently employed to treat bacterial infections caused by an unknown pathogen. The Third combination therapy utilises two compounds that alone exert no antimicrobial effects but result in cell death when combined (Tyers and Wright, 2019).

As research in CORMs as potential antimicrobials has increased, several groups have explored utilising them as part of combination therapies with currently used antimicrobials. CORM-2 has shown to work effectively in combination with metronidazole, amoxicillin or clarithromycin against *H. pylori* (Tavares et al., 2013). Additionally, the same CORM boosted the antimicrobial effects of tobramycin against *P. aeruginosa* (Murray et al., 2012). Studies on a newer manganese-based Photo-CORM ([Mn(CO)3(tpa-κ3N)]Br) have shown synergistic effects with both doxycycline and colistin antibiotics (Rana et al., 2017; Betts et al., 2017).

Ebor-CORM is a manganese-based, water-triggered CORM that has been tested against both PAO1 and clinical isolates of *P. aeruginosa* from Danish cystic fibrosis patients (Figure 16) (Flanagan et al., 2018). It showed effective clearance of PAO1 but had little effect against individual clinical strains. However, when clinical strains were co-cultured or cultured all together there was a significant reduction in growth and the reason for this remains unknown (Flanagan et al., 2018).

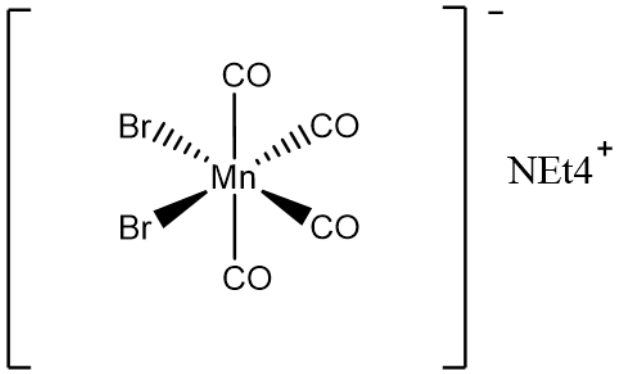

Figure 16: Structure of Ebor-CORM

4.1.1 Aims and objectives

This section aims to establish if the observed antimicrobial effects of Ebor-CORM against *P. aeruginosa* PAO1 strain can be increased by changing bacterial growth conditions and utilising Ebor-CORM as part of a combination therapy with clinical antibiotics. Additionally, this section aims to determine if Ebor-CORM is effective against antibiotic-resistant PAO1 strains. PAO1 is a model organism for *P. aeruginosa* and was selected to screen the test conditions initially to reduce the variation that has been previously noted when using clinical strains of *P. aeruginosa* (Flanagan et al., 2018).

Firstly, it was essential to establish that CO is being released for Ebor-CORM when dissolved in aqueous solution as described in previous chapter.

Secondly, because of the effects of Trypto-CORM on neighbouring cultures were observed within a microplate, through gaseous release of CO, it was important to determine if the same was true for Ebor-CORM. As a result, it was hypothesised that the growth of untreated cultures of PAO1 could be adversely affected by Ebor-CORM used to treat neighbouring cultures placed in neighbouring wells of 96-well microplates plates.

Thirdly, as with Trypto-CORM, experiments exploring the effects of Ebor-CORM in oxygen limiting conditions were conducted to test the hypothesis that Ebor-CORM would be more effective as an antimicrobial treatment under near anaerobic conditions.

Fourthly, The study previously mentioned by Betts et al. (2017) found that $[Mn(CO)_3(tpa\text{-}\kappa^3N)]Br$ showed significant synergistic antimicrobial effects with colistin. In the absence of colistin, the minimum inhibitory concentration of this photo-CORM was 1024 μg/ml, however, with the addition of 1μg/ml of colistin this value can be reduced to 32 μg/ml. This finding led to the hypothesis that the antimicrobial effect of Ebor-CORM would be greater in the presence of colistin used as a combination therapy. If this would be the case, it was also hypothesised that the synergistic effect of Ebor-CORM and colistin would be lost if tested against a colistin-resistant mutant *of P. aeruginosa*.

Finally, Like with Trypto-CORM Treatment, it is essential to ensure that virulence does not increase as a result of Ebor-CORM Treatment. Based on Trypto-CORM experiments, it was hypothesised that Ebor-CORM treatment would also result in an increase in the production of virulence factors (pyocyanin, pyoverdine and biofilm).

4.2 Methodology

4.2.1 Assessing CO Release from Ebor-CORM

Myoglobin assays were conducted as described in 2.4 to assess the release of CO from Ebor-CORM dissolved in PBS solution.

4.2.2 Assessing the effect of Ebor-CORM on neighbouring cultures.

As observed with Trypto-CORM it is possible for CO to diffuse into neighbouring wells of a microplate and affect the growth of these cultures. To determine if Ebor-CORM can affect the growth of neighbouring cultures within a microplate, cultures of PAO1 were inoculated in LB media at increasing distances from a 1000 μM Ebor-CORM solution. The optical density at 600 nm was recorded every ten minutes, for 24 hours, using a Tecan Sunrise microplate reader to assess bacterial growth.

4.2.3 Limiting Oxygen Availability

To determine if Ebor-CORM was more effective against PAO1 under aerobic or near anaerobic conditions bacterial cultures were prepared (as described 2.1). Cultures were treated with 1000, 700, 500 or 200 μM Ebor-CORM (prepared as described 2.2). Cultures not treated with Ebor-COM were inoculated with LB broth containing 2% DMSO to achieve a final working concentration of 1%, like Ebor-CORM treated cultures. To limit

gaseous exchange at the surface of the cultures a 60 µl layer of paraffin oil added to the top of the wells. Cultures were additionally prepared in the absence of paraffin oil.

4.2.4 Antimicrobial effects of Ebor-CORM in Combination with Colistin against *P. aeruginosa* PAO1

Cultures of PAO1 were prepared as described in section 2.1 and treated with either 1000, 700, 500, 200 or 0 µM Ebor-CORM in combination with 0, 1 ,2 or 4 µg/ml Colistin. Cultures not treated with Ebor-COM were inoculated into LB broth containing 2% DMSO to achieve a final working concentration of 1%, comparable to Ebor-CORM treated cultures. Cultures were incubated at 37 ^{o}C within a SpectroStar Nano microplate shaker set to shake at 200 rpm. Optical density measurements were taken every 10 minutes for 48 hours.

10 µl aliquots were removed from these cultures after 24 and 48 hours of incubation and serially diluted in phosphate-buffered saline (PBS) to determine changes in *P. aeruginosa* cell numbers as Colony Forming Units (CFU) per mL.

CFUs were determined by spotting 5 µl of diluted aliquots on LB agar and incubating at 37 ^{o}C for 8 hours. After this time, colonies within the spot were counted at 250x magnification using a light microscope. Additionally, CFUs were calculated using flow cytometry as follows. 90 µl of the diluted aliquots were stained with 90 µl of live/dead stain solution. The Live/Dead stain solution was prepared by adding 12 µl of Syto9 stain (to identify all bacteria) and 80 µl of Propidium iodide (to identify membrane compromised/dead bacteria) in 8ml of PBS. Plates were added to the Cytoflex-XL cytometer and were sampled at the medium flow setting for either a total of 10,000 bacteria events or 2 minutes (greater detail on gating and cytometry set up can be found in the appendix section A4).

4.2.5 Antimicrobial effects of Ebor-CORM in Combination with Colistin against a Colistin-Resistant Mutant of *P. aeruginosa* (Col16b)

Cultures of Col16b were obtained through the methodology outlined in appendix (section A2) by selecting a spontaneously resistant colony (after 24h growth) from LB agar plates containing 16 µg/ml colistin. For the experiments, the strain was prepared and treated with Ebor-CORM and colistin as described above in 4.2.4.

4.2.6 Assessing the effect of Ebor-CORM on Virulence

To assess the effects of Ebor-CORM on virulence (pyocyanin, pyoverdine and biofilm) cultures were prepared as described in section 4.2.4 with optical density reads being taken after 24 and 48 hours and assays were conducted after 48 hours.

4.3 Results and Discussion

4.3.1 Release of CO from Ebor-CORM

Myoglobin assays were conducted to determine if CO was released from Ebor-CORM in aqueous solution. The data in Figure 17 shows the conversion of the myoglobin to deoxymyoglobin over 2 hours when treated with 40 µM Ebor-CORM. Unlike the myoglobin spectra obtained for Trypto-CORM, there is no significant drift in the spectra when Ebor-CORM is used. Additionally, the isosbestic point at 510 nm lines up well before corrections and therefore, no corrections were made to any of the spectra obtained when assessing the release of CO from Ebor-CORM.

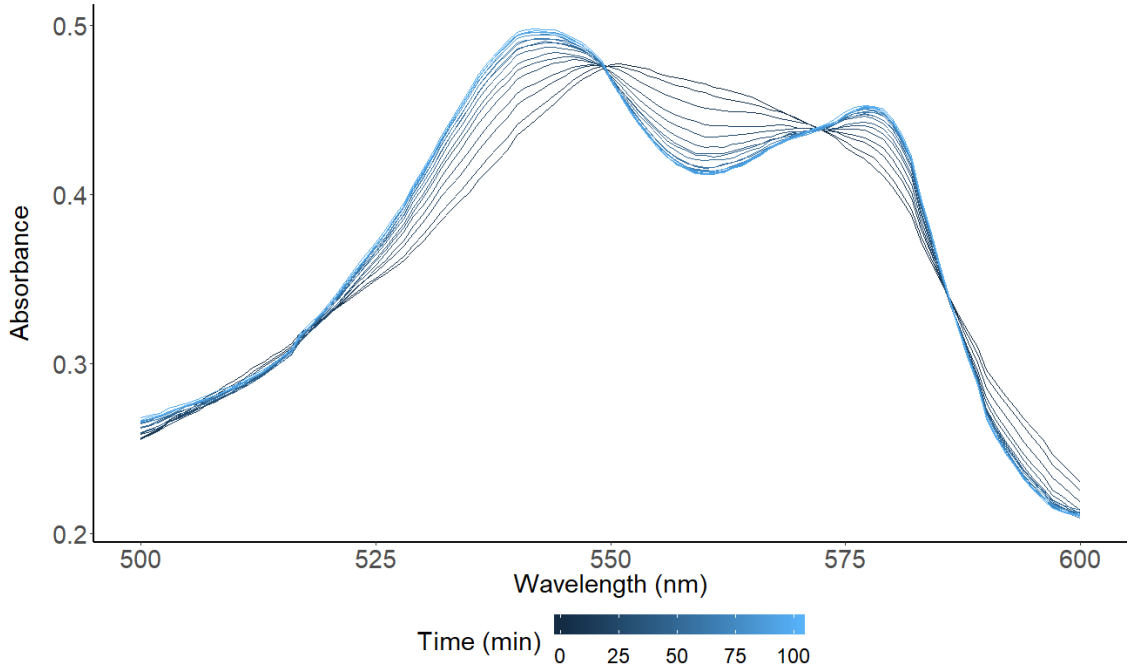

Figure 17: Conversion of deoxy-myoglobin to carboxy-myoglobin by Ebor-CORM – treatment 60 µM Ebor-CORM results in a change in absorption spectrum of the myoglobin as CO binds to it. Spectrum is the mean of six replicates.

The increase in the absorbance at 540 nm of the myoglobin spectrum is indicative of conversion of deoxy-myoglobin to carboxy-myoglobin, therefore, it can be concluded that CO is released from Ebor-CORM in aqueous solution. The increase in the

absorbance at 540 nm can be used to assess the dynamics of CO release from Ebor-CORM. Figure 18 shows the increase in absorbance at 540 nm over 102 minutes following the addition of 10, 20, 30, 40 or 60 µM Ebor-CORM to the myoglobin solution.

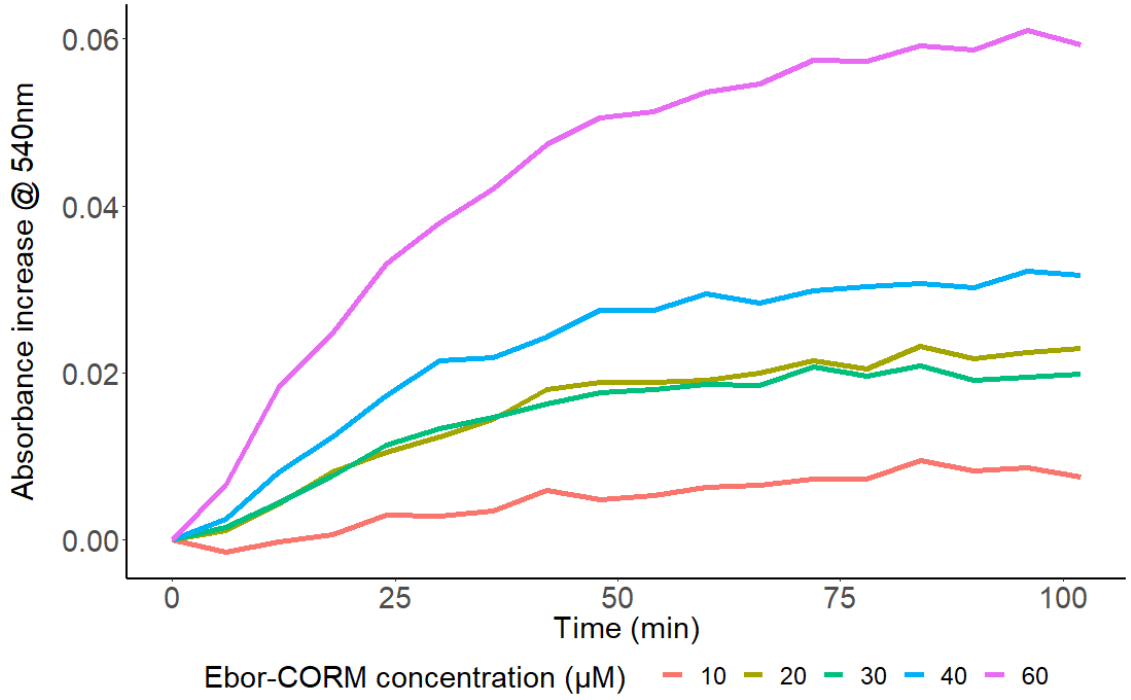

Figure 18: Carbon Monoxide release form Ebor-CORM – The increase on 540 nm indicates CO release through the conversion of deoxy-myoglobin to carboxy-myoglobin when treated with 10 (red), 20 (yellow), 30 (green), 40 (blue) or 60 µM (purple) Ebor-CORM dissolved in PBS. The data represents the mean of six replicates.

The data in Figure 18 shows that increasing Ebor-CORM concentration results in a greater increase in the absorbance at 540 nm, with the addition of 60 µM Ebor-CORM resulting in the greatest increase. Additionally, a greater rate of deoxy-myoglobin to carboxy-myoglobin conversion is observed as Ebor-CORM concentration increases (Figure 18). Both results were expected because higher concentrations of Ebor-CORM should result in the release of a greater number of CO molecules in a given time. Interestingly, there was very little difference between the increase in absorbance resulting from the addition of 20 and 30 µM Ebor-CORM. Addition of 20 µM Ebor-CORM resulted in a slightly higher final absorbance increase than the 30 µM treatment, however, statistical analysis revealed that addition of 20, 30 or 40 µM Ebor-CORM resulted in an approaching significant difference in the increase in absorbance at 540

nm after 106 minutes of incubation (Kruskal-Wallis: chi-squared = 5.9157, df = 2, p-value = 0.05193).

4.3.2 Effects of Ebor-CORM on neighbouring Cultures

With the release of CO from Ebor-CORM established, the effects of Ebor-CORM on neighbouring cultures within a microplate can be determined. Following the results obtained for Trypto-CORM, it was hypothesised that Ebor-CORM would also adversely affect the growth of cultures in neighbouring wells. This was tested by inoculating cultures of PAO1 on 96-well microplates at increasing distances (in terms of number of columns) from 1000 µM Ebor-CORM and incubating at 37°C, 200 rpm for 24 hours in a SpectroStar Nano plate reader. OD 600 nm was recorded every 10 minutes over this time course. The data in Figure 19 shows the bacterial densities of untreated cultures of PAO1 at increasing distances from Ebor-CORM.

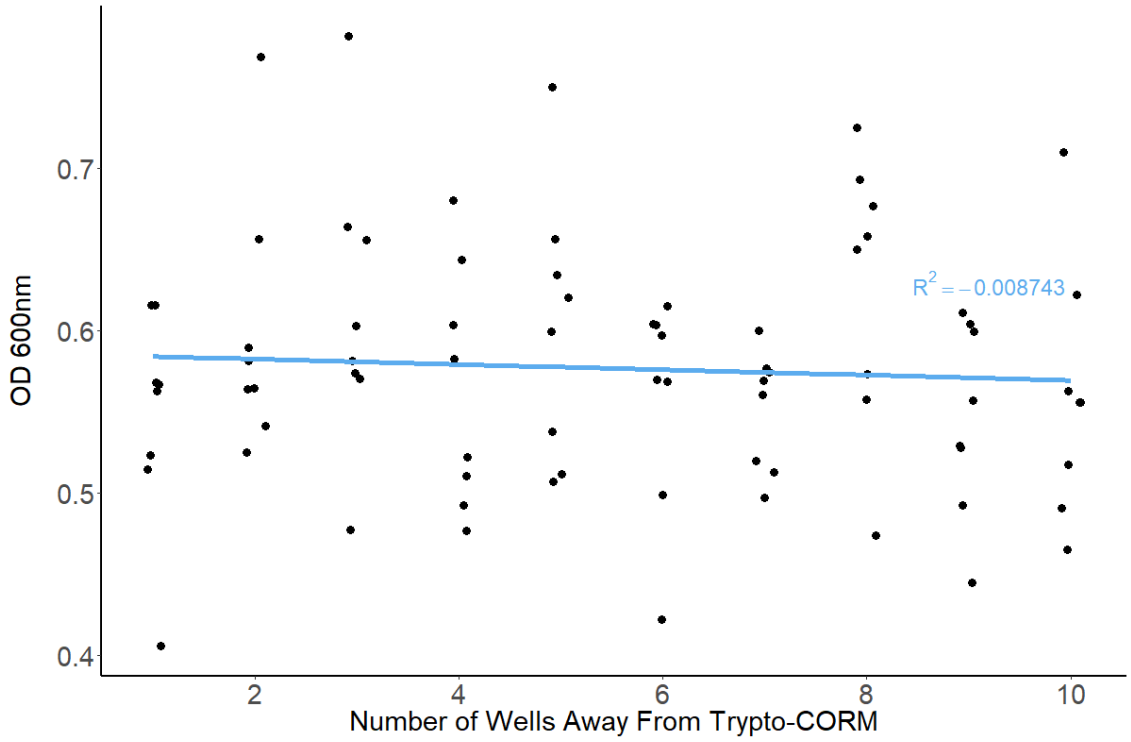

Figure 19: Effects of Ebor-CORM on the growth of neighbouring untreated cultures of *P. aeruginosa* – Densities of PAO1 cultures after 11 hours that were inculated in wells, of a 96-well microplate, at increasing distances from 1000 µM Ebor-CORM.

No significant increase or decrease in bacterial densities was observed as the distance from Ebor-CORM increased (Pearson's Correlation: r = -0.063, p-value = 0.576). The data suggest that the CO from Ebor-CORM either does not diffuse into neighbouring well or does not adversely affect the growth of cultures in neighbouring wells. The amount of CO released from Ebor-CORM is lower in a given time than Trypto-CORM based on the data shown in Figures 6 and 18. This may explain why the growth of neighbouring cultures are adversely affected by Trypto-CORM but not Ebor-CORM.

4.3.3 Effects of Ebor-CORM under Oxygen Limiting Conditions

With the knowledge that CO is released from Ebor-CORM when in solution, and that this has no significant adverse effects on the growth of neighbouring cultures, the effects of Ebor-CORM on the growth of PAO1 were further explored in oxygen-limited conditions. To test the hypothesis that the antimicrobial effects of Ebor-CORM are greater at near anaerobic conditions, half of the cultures were treated with 1000, 700, 500, 200, 0 µM Ebor-CORM and half were treated with the same concentrations of Ebor-CORM prior to being covered with paraffin oil to limit oxygen availability. Figure 20 shows the growth of PAO1 cultures treated with Ebor-CORM both a) with paraffin oil and b) without.

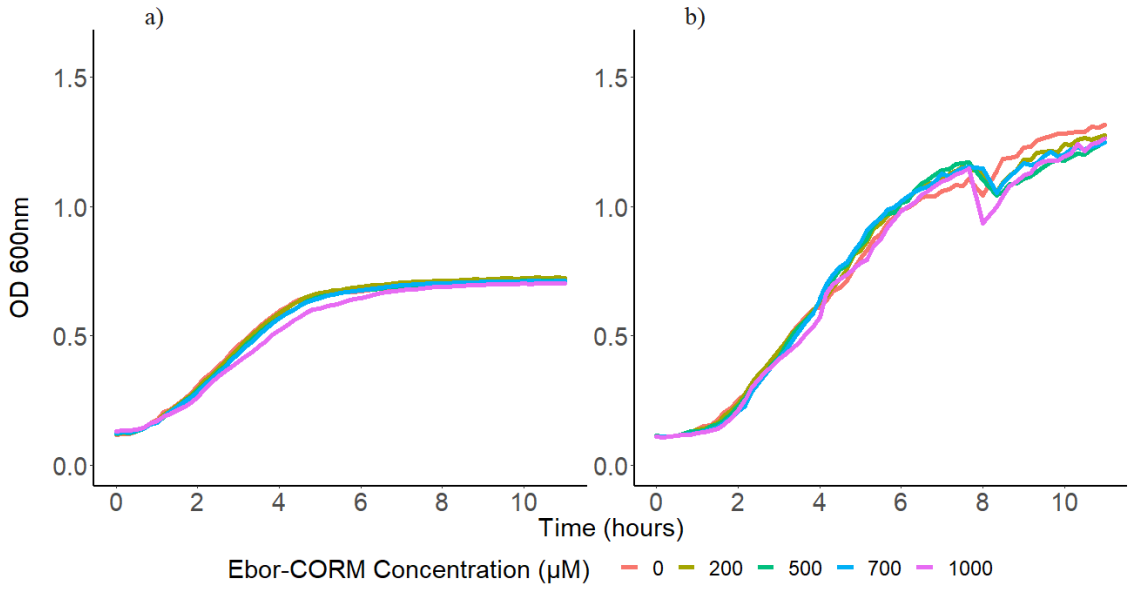

Figure 20: Growth of Ebor-CORM treated *P. aeruginosa* under oxygen limiting conditions – a) The growth of PAO1 under oxygen limiting conditions induced through the addition of a layer of paraffin oil to the top of cultures. Cultures were treated with 0 (red), 200 (yellow), 500 (green), 700 (blue) or 1000 µM

(purple) Ebor-CORM. b) the growth of Ebor-CORM treated PAO1 with freely available oxygen. All cultures were grown for 11 hours at 37 °C, 200 rpm, with OD 600 nm measurements being taken every 10 minutes. The data represents the mean of four replicates.

The growth of both treated and untreated cultures of PAO1 is similar, with little variation suggesting that Ebor-CORM has no effect on the growth of PAO1 in the presence or absence of paraffin oil. The addition of paraffin oil does, however, reduce the growth rate of PAO1 and the maximum bacterial density in general. The explanation for this effect could be the same as discussed earlier in 3.3.3. bacteria growing under oxygen limiting conditions may be expressing respiratory cytochromes that have a high affinity for oxygen resulting in lower ATP production and thus lower overall growth. The growth of untreated PAO1 under oxygen limiting conditions is significantly different to that noted previously in Figure 9. The differences in growth most likely result from the different methodologies and equipment used to test Ebor-CORM and Trypto-CORM. For example, Ebor-CORM treated cultures were placed into a Spectrostar Nano plate reader, set to a constant temperature and rotation, after inoculation with optical density measurements being recorded every ten minutes. Whereas, Trypto-CORM treated cultures were incubated in a 37°C incubator, on a rotating microplate shaker and were removed hourly to read the optical density using a Tecan Sunrise plate reader.

To test if Ebor-CORM has any significant effect on the growth of PAO1, the relative growth of treated cultures, after 11 hours of growth, compared to the controls were calculated and plotted (Figure 21). Additionally, the calculation of relative growth accounts for the differences in maximum densities in the presence and absence of paraffin oil were conducted to compare the effect of these two conditions.

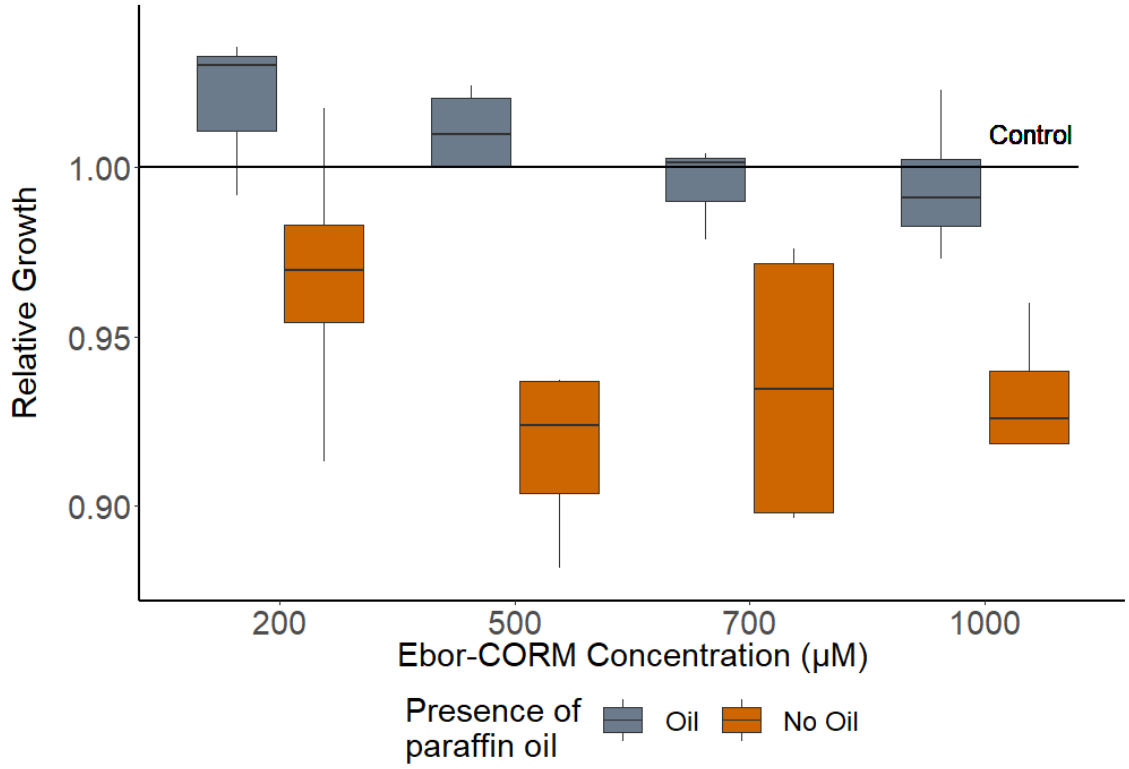

Figure 21: Densities of Ebor-CORM treated *P. aeruginosa* under oxygen limiting conditions – The relative growth of Ebor-CORM treated cultures compared to untreated cultures following 11 hours of growth at 37°C. Comparing the cultures growing under anerobic condions (orange) and under oxygen limiting cnditions induced through the addition of parrafin oil on the top of cultures (grey). Boxes represents the range between the 25th quartile and the 75th quartile of the data with the black line in within the box representing the median. Whiskers represent the smallest and largest values within 1.5 times the interquartile range where n = 4.

Ebor-CORM treated cultures growing under oxygen limiting conditions had higher relative densities than cultures that had freely available gaseous exchange (Two-way ANOVA: $F_{1,24}$ = 26.78, p-value < 0.005). This suggests that, as with Trypto-CORM, the treatment of Ebor-CORM is less affective against bacterial cultures growing under oxygen limiting conditions for the same reasons outlined in section 3.3.3. Additionally, no significant reduction in bacterial growth was observed as Ebor-CORM concentration increased ($F_{(3,24)}$ = 0.92, p-value = 0.446). Analysis via two-way ANOVA also revealed that there was no significant interaction between Ebor-CORM concentration and the presence of paraffin oil ($F_{(3,24)}$ = 0.32, p-value = 0.811). The reduction in growth observed for cultures of PAO1 growing aerobically is not as large as that which has been previously observed. Flanagan et al., (2018) found over a 50% reduction in bacterial densities of PAO1 could be achieved by 500 μM Ebor-CORM. The lack of observed reduction could

be the result of secondary metabolites in the media generating an OD reading that is higher than that of the bacteria alone. Flanagan et al, (2018) utilised flow cytometry to quantify cultures. This method could provide a more accurate understanding of the effects of Ebor-CORM and was applied with colony plating in future experiments to explore the effects of Ebor-CORM on bacterial growth.

4.3.4 Combination Treatment of Ebor-CORM and Colistin against *P. aeruginosa*

A study by Betts et al., (2017) found that $[Mn(CO)_3(tpa\text{-}\kappa^3N)]Br$, a manganese-based photo-CORM, showed synergistic effects with colistin and resulted in a greater antimicrobial affected when applied in combination. It was hypothesised that the same effect may be observed with Ebor-CORM. Minimum inhibitory concentration determination assays were conducted as described in appendix section A2.1 and a concentration of 4 µg/ml of colistin was sufficient to inhibit the growth of PAO1. Therefore, to test the hypothesis cultures of PAO1 were inoculated with either 0, 1, 2, 4 µg/ml Colistin in combination with 0, 200, 500, 700, 1000 µM Ebor-CORM. Figure 22 shows the growth of PAO1 over a 48-hour period treated with various Ebor-CORM concentrations in combination with a) 0, b) 1, c) 2or d) 4 µg/ml Colistin.

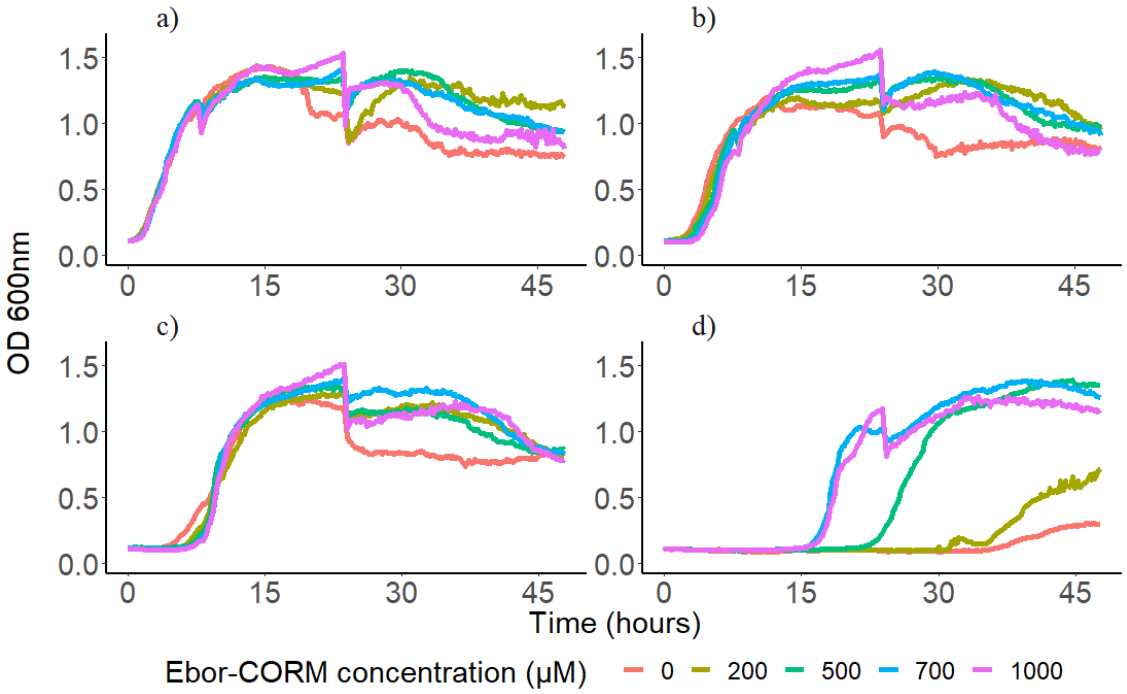

Figure 22: Effects of Ebor-CORM and Colistin combination on the growth of *P. aeruginosa* – a) The growth of PAO1 over a 48-hours following treatment with 0 (red), 200 (yellow), 500 (green), 700 (blue) or 1000 µM (purple) Ebor-CORM alone or in combination with b) 1 µg/ml colistin, c) 2 µg/ml colistin or d) 4 µg/ml

colistin incubated at 37°C, 200rpm with OD 600nm measurements every 10 minutes. The data shown is the mean of four replicates.

Slight variation in growth was observed between Ebor-CORM treated and untreated cultures exposed to 0-2 µg/ml colistin up to 24 hours, with treated cultures appearing to maintain higher bacterial densities after this time than the untreated ones. As colistin concentration increases from 0 to 2 µg/ml the lag phase of growth also increases (Figure 22a-c). Interestingly, in the presence of 4 µg/ml, which should normally inhibit the growth of PAO1, Ebor-CORM appears to stimulate growth (Figure 22d). Exponential growth for 1000 and 700 µM Ebor-CORM treatments in combination with 4 µg/ml colistin begins at approximately 15 hours. Additionally, the start of exponential growth is delayed as Ebor-CORM concentration decreases. This suggests that Ebor-CORM is providing some cytoprotective effects for cells which allows them to grow in the presence of inhibitory concentrations of colistin. The observed decrease in OD at 24 hours is presumably due to removal of liquid from cultures during the sampling. To determine if there is a significant difference in bacterial densities following treatments, the total growth of the bacteria was calculated by calculating the area under the curve of individual replicates (

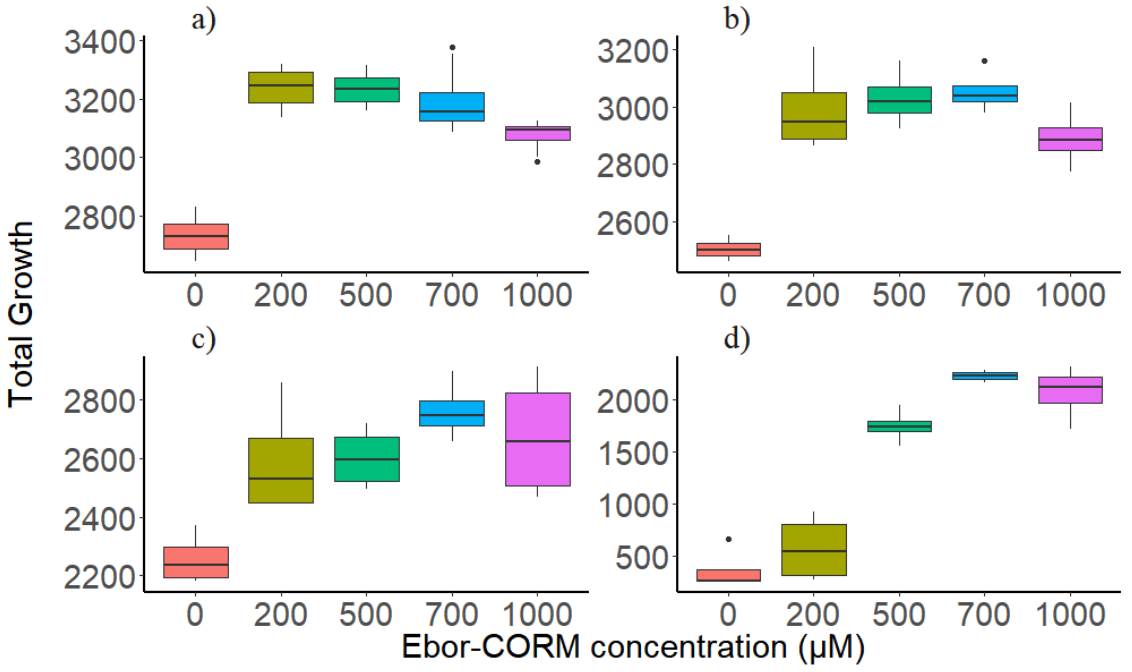

Figure 23: Effects of Ebor-CORM and Colistin combination on the total growth of P. aeruginosa over 48 hours– a) The density of PAO1 following 48 hours growth and treatment with 0 (red), 200 (yellow), 500

(green), 700 (blue) or 1000 µM (purple) Ebor-CORM alone or in combination with b) 1 µg/ml colistin, c) 2 µg/ml colistin or d) 4 µg/ml colistin. Total growth calculated by calculating the areas under the curve of individual replicates. Boxes represents the range between the 25th quartile and the 75th quartile of the data with the black line in within the box representing the median. Whiskers represent the smallest and largest values within 1.5 times the interquartile range where n = 4.

).

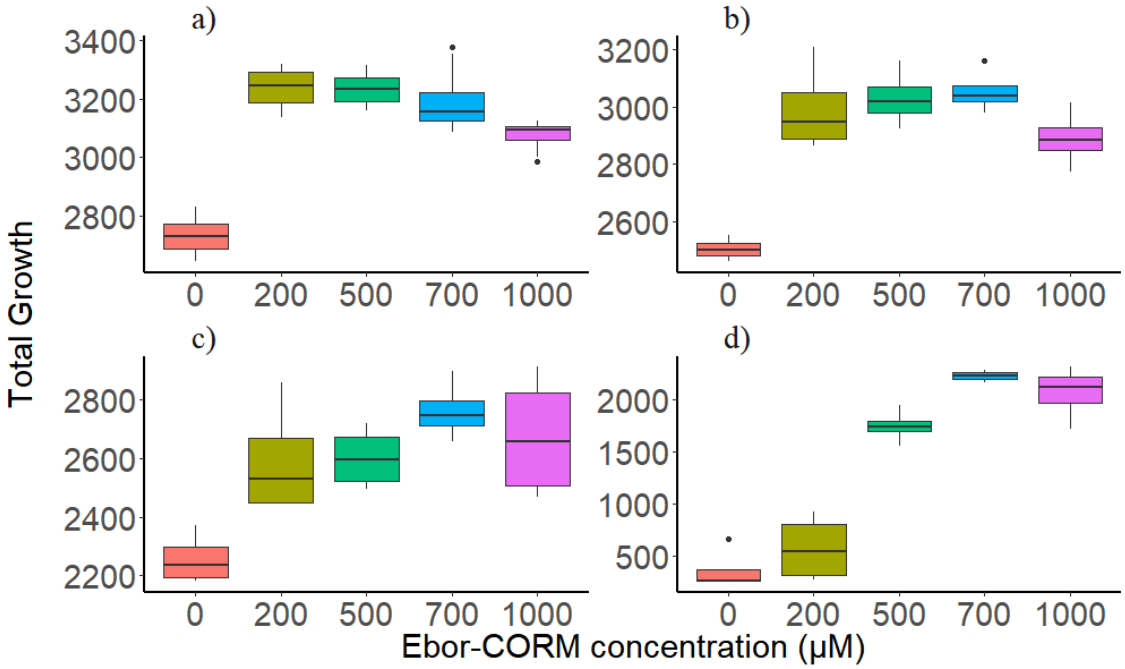

Figure 23: Effects of Ebor-CORM and Colistin combination on the total growth of *P. aeruginosa* over 48 hours– a) The density of PAO1 following 48 hours growth and treatment with 0 (red), 200 (yellow), 500 (green), 700 (blue) or 1000 µM (purple) Ebor-CORM alone or in combination with b) 1 µg/ml colistin, c) 2 µg/ml colistin or d) 4 µg/ml colistin. Total growth calculated by calculating the areas under the curve of individual replicates. Boxes represents the range between the 25th quartile and the 75th quartile of the data with the black line in within the box representing the median. Whiskers represent the smallest and largest values within 1.5 times the interquartile range where n = 4.

Analysis via two-way ANOVA revealed that Ebor-CORM treatment significantly altered the growth of PAO1 ($F_{4,80}$ = 106.96, p-value < 0.001). Interestingly, Tukey post-hoc analysis revealed that Ebor-CORM treatments >200µM resulted in significantly more growth than cultures not treated with Ebor-CORM when combined with 0 and 1 µg/ml colistin (all p-values <0.05). Additionally, in combination with 0 and 1 µg/ml colistin, all Ebor-CORM treated cultures had significantly higher growth than untreated cultures (all p-values <0.012). Colistin concentration also had a significant effect on the growth of PAO1 ($F_{(3,80)}$ = 773.73, p-value <0.001) with cultures treated with only 4 µg/ml colistin having significantly lower growth than those with 0,1 or 2 µg/ml colistin only (p-values

<0.001). A significant interaction was also observed between colistin and Ebor-CORM on the bacterial density of PAO1 cultures ($F_{(12,80)}$ = 35.78, p-value < 0.005). Levene test of homogeneity and Shapiro's normality tests were conducted on the residuals. The data was both significantly different from a homogeneous data set and normally distributed data set. However, ANOVA is a robust statistical model, and it has been argued that providing the data has a Skewness value between -2 to +2 and Kurtosis value of -8 to +8, the data is considered to be normally distributed (Joseph F. Hair Jr, 2014; Abdollahi et al., 2015). This data set had a skewness = -1.836 and a kurtosis = 5.921 and, therefore, was considered relatively normally distributed. These values have been used as references for future ANOVA analysis that do not have normally distributed residuals.

As with the previous experiment, comparison of only optical density does not account for the production of secondary metabolites. Therefore, aliquots of the cultures were taken, diluted and plated out on LB agar to determine the colony-forming units (CFU) (Figure 24), which were also later analysed using flow cytometry (Figure 25). Figure 24 shows the CFU/ml of PAO1 treated with Ebor-CORM in the presence of colistin, a) 0 µg/ml, b) 1 µg/ml, c) 2 µg/ml, d) 4 µg/ml. The same layout is used for Figure 25 which highlights the number of live bacterial events recorded per µl of sample using flow cytometry. Colonies plated from the 500 µM Ebor-CORM treatment in combination with 4 µg/ml colistin were uncountable after the 8-hour incubation as colonies had merged.

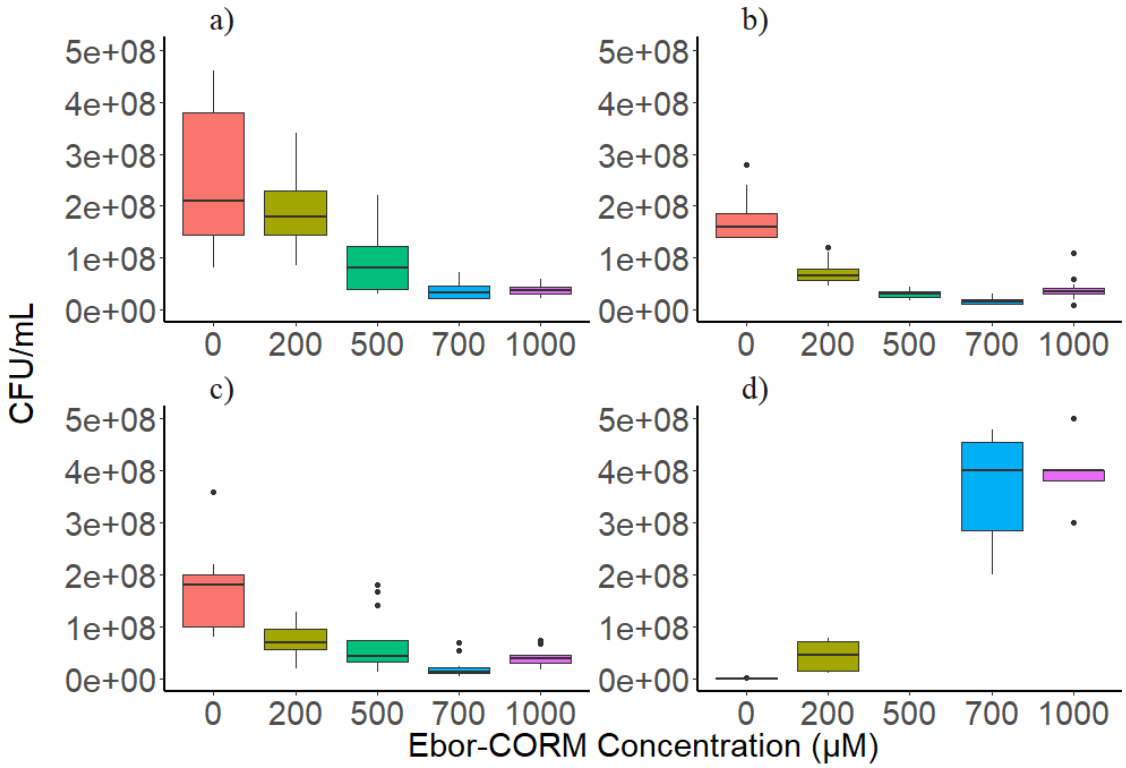

Figure 24: Effects of Ebor-CORM and colistin combination treatment on the number of colony forming units of *P. aeruginosa*– a) The CFU/ml of PAO1 after 48-hours following treatment with 0 (red), 200 (yellow), 500 (green), 700 (blue) or 1000 µM (purple) Ebor-CORM alone or in combination with b) 1 µg/ml colistin, c) 2 µg/ml colistin or d) 4 µg/ml colistin incubated at 37°C, 200rpm for 48 hours. CFU determined by plating aliqotes onto LB agar and counting colonies after 8 hours incubation at 37°C. Boxes represents the range between the 25th quartile and the 75th quartile of the data with the black line in within the box representing the median. Whiskers represent the smallest and largest values within 1.5 times the interquartile range where n = 12.

Interestingly, when plated out to determine CFU's, a decrease in CFU was observed as Ebor-CORM concentration increases in the presence of 0, 1 or 2 µg/ml colistin. However, the inverse is true in the presence of, the previously identified, inhibitory concentration of colistin (4 µg/ml). Application of Ebor-CORM results in significantly lower CFU's when cultures are treated in combination with 0, 1 or 2 µg/ml colistin and increases CFU in combination with 4 µg/ml colistin ($F_{(4,187)}$ = 19.27, p-value < 0.05). The observed decrease in CFU's with increased Ebor-CORM is most likely due to the increased amount of CO that is released in a given time. In the presence of 4 µg/ml colistin there is no difference in the CFU's for cultures treated with 200 µM Ebor-CORM and the untreated culture (p-value = 0.995) but both 700 and 1000 µM treatments result in significantly higher CFU's than the control (p-values < 0.005). A significant interaction was also noted between colistin and Ebor-CORM ($F_{(11,187)}$ = 41.46, p-value < 0.005). Additionally, Skewness and Kurtosis values were 1.700 and 5.622 respectively.

When comparing the results obtained using plating (Figure 24) and flow cytometry (Figure 25), no reduction in cell densities was observed in the absence and presence of 1 and 2 µg/ml of colistin (Figure 25a). However, the increase in bacterial densities as a result of Ebor-CORM treatment in combination with 4 µg/ml was still clearly visible (Figure 25d).

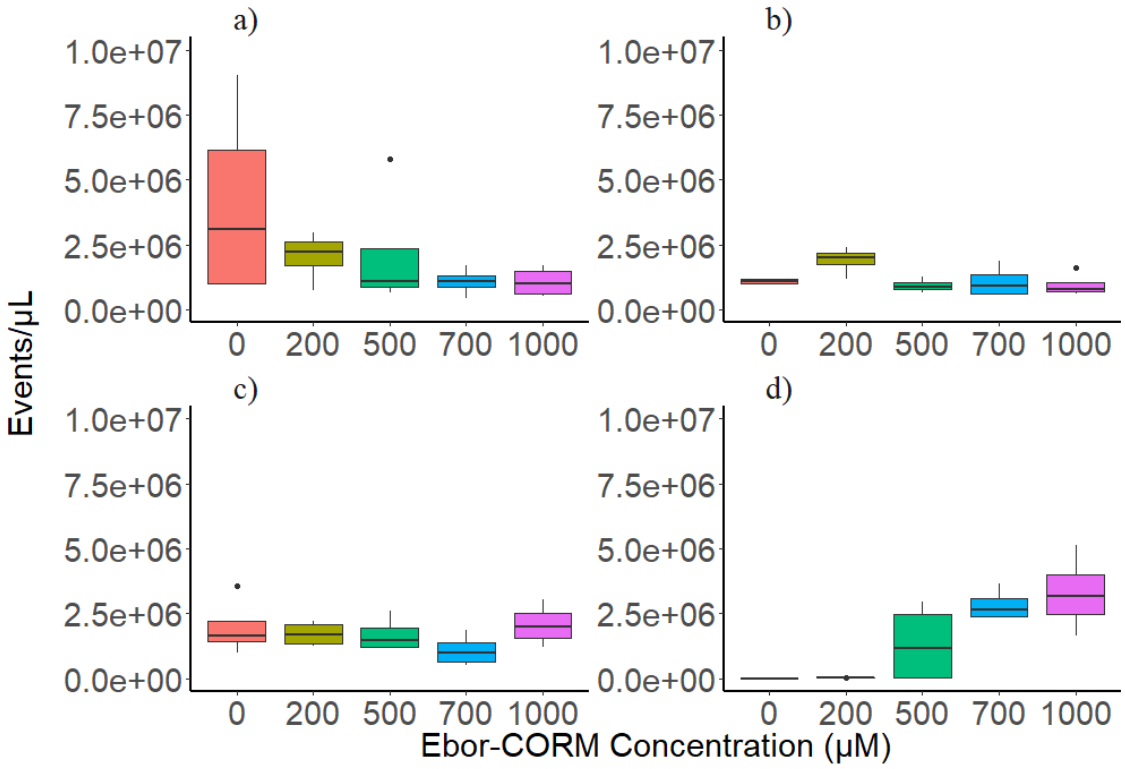

Figure 25: Effects of Ebor-CORM and colistin combination treatment on the densities of *P. aeruginosa* determined using flow cytometry – a) Densities of PAO1 following treatment with 0 (red), 200 (yellow), 500 (green), 700 (blue) or 1000 µM (purple) Ebor-CORM alone or in combination with b) 1 µg/ml colistin, c) 2 µg/ml colistin or d) 4 µg/ml colistin incubated at 37°C, 200rpm for 48 hours. The event/µL of live PAO1 cells determined using flow cytometric analysis of cultures stained with Syto-9 stain to identify bacterial cells and subtracting the value of dead cells stained with Propidium iodide. Boxes represents the range between the 25th quartile and the 75th quartile of the data with the black line in within the box representing the median. Whiskers represent the smallest and largest values within 1.5 times the interquartile range where n = 4.

No significant bacterial density reduction by Ebor-CORM was observed in general ($F_{(4,59)}$ = 0.635, p-value = 0.639870). However, in the presence of 4 µg/ml, 700 and 1000 µM Ebor-CORM does result in significantly higher densities of bacterial than in the absence of the control (p-values = 0.027 and 0.003 respectively). As with the CFU's, there was a significant interaction between colistin and Ebor-CORM on the bacterial densities determined by flow cytometry ($F_{(12,59)}$ = 3.776, p-value < 0.005).

In conclusion, treatment of PAO1 with Ebor-CORM, in the absence of colistin appears to reduce bacterial densities and thus CFU's and Events/µl. Additionally, at intermediate concentrations of colistin mixed results were obtained with Ebor-CORM treatment only sometimes reducing bacterial densities. However, this does highlight the importance of utilising methods of determining actual cellular densities rather than relying on optical densities alone as this data did not highlight these reductions. A possible explanation for the inaccuracy in the OD measurements is that although treated cultures had lower bacterial densities, there may have been greater production of secondary metabolites and pigments that absorb at 600nm, thus raising the values.

The most surprising result was that Ebor-CORM treatment facilitates the growth of PAO1 in the presence of an inhibitory concentration of colistin (4µg/ml). Cultures treated with 700 or 1000 µM Ebor-CORM grew significantly more than untreated cultures and cultures treated with 200 µM Ebor-CORM, which appeared to only produce more metabolites and products that resulted in an increase in OD.

Colistin is a positively charged polypeptide that induces bacterial cell death by disrupting the integrity of the outer membrane resulting in cell lysis (Bialvaei and Samadi Kafil, 2015). Membrane integrity is disrupted in a two-step mechanism, initially, colistin binds directly to the negatively charged outer membrane which displaces metal ions and reduced their uptake and utilisation. This is followed by interaction with lipopolysaccharide (LPS) where colistin acts like a detergent which destabilises the membrane resulting in lysis (Bialvaei and Samadi Kafil, 2015; Moffatt et al., 2010).

The most common mechanisms of colistin resistance are the modification of LPS to include a 4-amino-L-arabinose and reduction LPS biosynthesis and expression, both which disrupts the binding affinity of colistin to LPS and prevent cell lysis (Pang et al., 2019; Sabnis et al., 2020). It is possible that, in the presence of no or low Ebor-CORM concentrations, PAO1 is inducing an SOS response whereby cells do not divide and try to outlast the compound and/or develop resistance as a significantly delay in growth can be observed. It is also possible that higher concentrations of Ebor-CORM are disrupting the biosynthesis of LPS thus reducing its expression or is inducing a greater rate of mutagenesis (McKenzie et al., 2000).

P. aeruginosa also utilises a variety of adaptive mechanisms to provide resistance to a range of antibiotics such as the production of non-specific efflux pumps, which actively remove antibiotics from within the cell, and the production of biofilms which make it more difficult for antibiotics to reach their target (Pang et al., 2019; Bialvaei and Samadi Kafil, 2015). Although cultures are mainly growing planktonically, biofilms are present after 24 hours and It is possible that treatment with Ebor-CORM affects a stress response pathway causing greater production of biofilm and thus colistin cannot bind to LPS. Alternatively, the CO which is released Ebor-CORM could simply be interacting with the LPS regulation pathway resulting in reduced expression of LPS and therefore, decreasing the availability for colistin to bind to. These hypotheses remain to be tested in the future.

4.3.5 Combination Treatment of Ebor-CORM and Colistin against a Colistin Resistant Mutant of *P. aeruginosa* (Col16b)

Originally, Ebor-Corm was hypothesised to work synergistically with colistin, and that this interaction between Ebor-CORM and colistin would be disrupted when tested against a colistin-resistant strain of *P. aeruginosa*. However, as previously established, Ebor-CORM appears to offer a cytoprotective effect in the presence of inhibitory concentrations allowing cultures to grow. Therefore, to determine if the previously observed interaction was lost against a colistin-resistant mutant, cultures of Col16b were inoculated in LB media containing the same concentrations of Ebor-CORM and colistin that were previously tested. Figure 26 shows the growth of Col16b treated with 0- 1000 µM Ebor-CORM in the combination with a) 0 µg/ml, b) 1 µg/ml, c) 2 µg/ml, d) 4 µg/ml colistin. The decrease in OD at 24 hours is again presumably due to sampling, however, this appears to be having a more significant effect on cultures not treated with Ebor-CORM for an unknown reason.

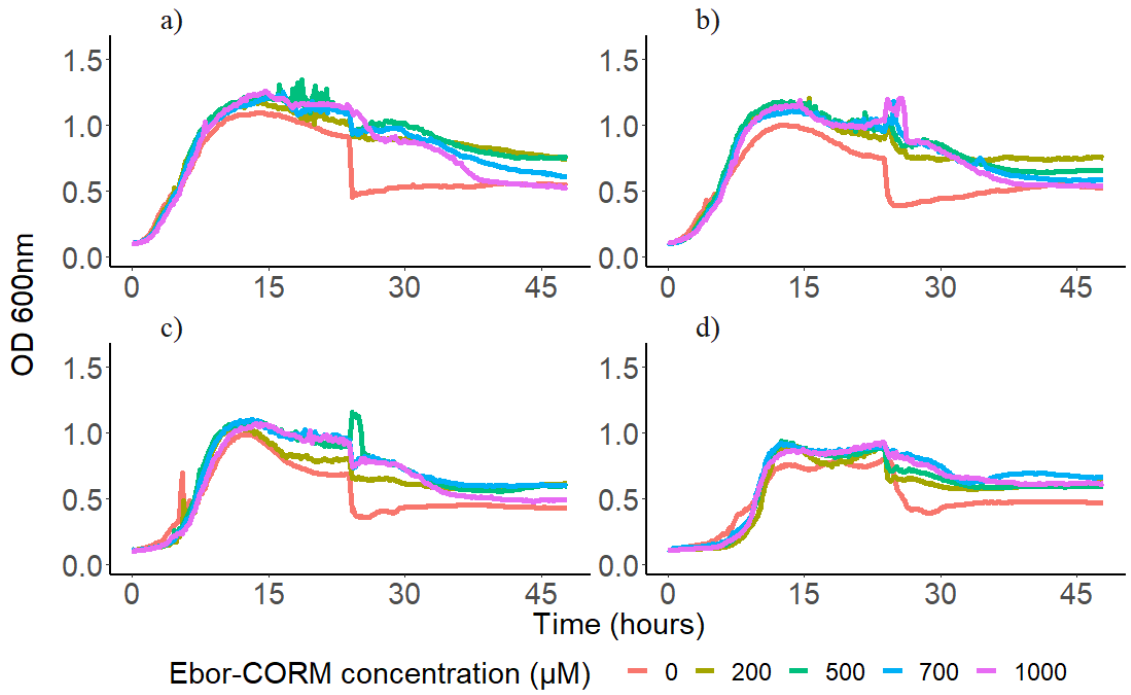

Figure 26: Effects of Ebor-CORM and Colistin combination on the growth of a colistin resistant mutant of *P. aeruginosa* Col16b – a) The growth of Col16b over a 48-hours following treatment with 0 (red), 200 (yellow), 500 (green), 700 (blue) or 1000 µM (purple) Ebor-CORM alone or in combination with b) 1 µg/ml colistin, c) 2 µg/ml colistin or d) 4 µg/ml colistin incubated at 37°C, 200rpm with OD 600nm measurements every 10 minutes. The data represents mean of four replicates.

In the absence of all treatments, the growth of Col16b is comparable to that of PAO1 and there appears to be little to no cost of resistance. Interestingly, Ebor-CORM treated cultures appear to be reaching and maintaining higher densities than untreated cultures up until 24 hours independent of colistin concentration. The most significant difference between the combination treatment of PAO1 and Col16b appeared in the presence of 4 µg/ml Colistin as hypothesised. Col16b has a colistin MIC 16 µg/ml (Figure S4), therefore, it is already capable of growing in 4 µg/ml colistin (Figure 26). Growth for Col16b in the presence of 4 µg/ml begins at approximately 8 hours in both the presence and absence of Ebor-CORM treatment. Whereas, the growth of PAO1 in the absence of Ebor-CORM treatment was very low starting after 30 hours, and in treated cultures, between 15 and 30 hours (Figure 22). The lack of a difference in the time at which growth begins between Ebor-CORM treated and untreated cultures of Col16b suggests that the cytoprotective effect of Ebor-CORM is lost when cultures are capable of growing. The previous set of experiments (section 4.3.4) highlighted the importance of measuring actual cellular densities rather than just optical densities to determine the

effects of the combination treatment. Figure 27 highlights how CFU's change with Ebor-CORM treatment in combination with colistin.

The OD 600nm of Ebor-CORM treated cultures are higher than the untreated cultures, comparison of CFU's revealed that the actual bacterial densities of Ebor-CORM treated cultures were comparable to the untreated cultures (Figure 27). This result further suggests that Ebor-CORM treatment results in the production of pigments and metabolites that absorb at 600 nm..

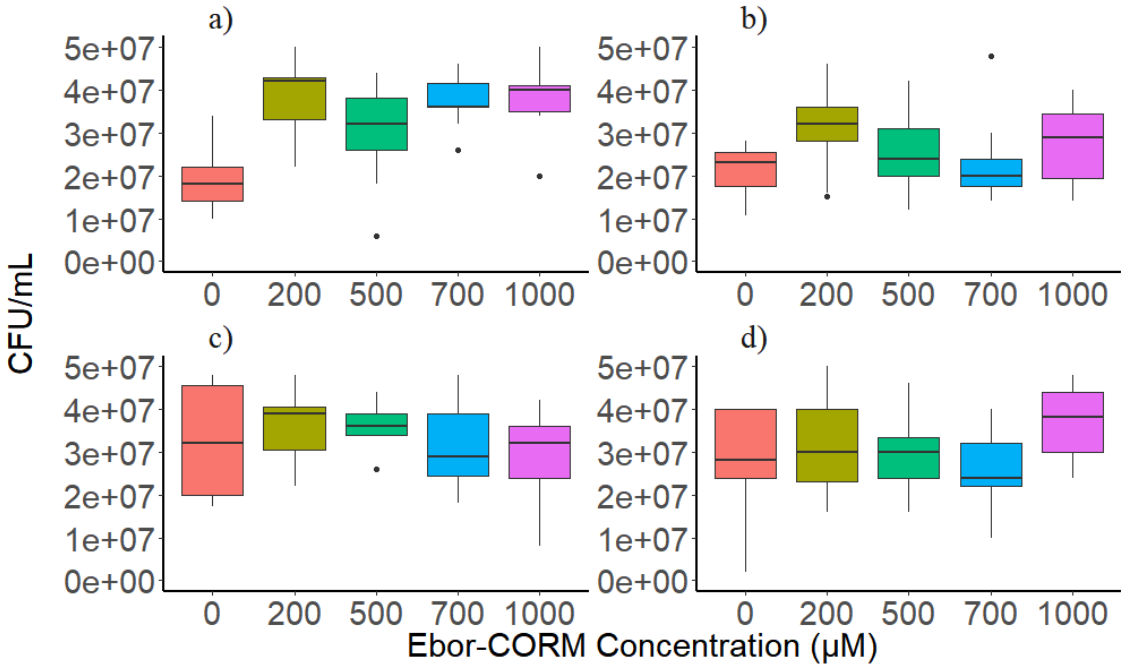

Figure 27: Effects of Ebor-CORM and colistin combination treatment on the number of colony forming units of a colistin resistant mutant of *P. aeruginosa* Col16b – a) The CFU/ml of Col16b after 24-hours following treatment with 0 (red), 200 (yellow), 500 (green), 700 (blue) or 1000 µM (purple) Ebor-CORM alone or in combination with b) 1 µg/ml colistin, c) 2 µg/ml colistin or d) 4 µg/ml colistin incubated at 37°C, 200rpm for 48 hours. CFU determined by plating aliqotes onto LB agar and counting colonies after 8 hours incubation at 37°C. Boxes represents the range between the 25th quartile and the 75th quartile of the data with the black line in within the box representing the median. Whiskers represent the smallest and largest values within 1.5 times the interquartile range where n = 12.

Two-way ANOVA was conducted to determine the significance of differences and established the presence of no interaction between Ebor-CORM and colistin ($F_{(12,152)}$ = 1.655, p-value < 0.08). Tukey analysis revealed that no significant difference in CFU's with Ebor-CORM treatment in combination colistin (all p-values <0.005). However, absence of colistin, Ebor-CORM treatments of 200 and 1000 µM significantly increased the number of viable cells (all p-values < 0.03). Additionally, as hypothesised, colistin

had no effect on the viability of Col16b independent of Ebor-corm concentration as the strain is resistant to colistin (all p-values >0.05) Again, the data failed Levene's and Shapiro's test, however, skewness = -0.113 and Kurtosis = 2.218.

Samples analysed via flow cytometry showed to be similar to those of the CFU's however no interaction between Ebor-CORM and colistin was noted (Two-way ANOVA: $F_{(12,60)}$ = 1.479, p-value = 0.157) Overall, the densities are lower than those obtained by plating for CFU's and the density of cultures treated with 2 or 4 µg/ml colistin were significantly lower than those treated with 0 or 1 µg/ml (Tukey p-values <0.005). Additionally, Ebor-CORM treatment resulted in no significant change in the number of viable cells independent of colistin concentration (all p-values >0.05).

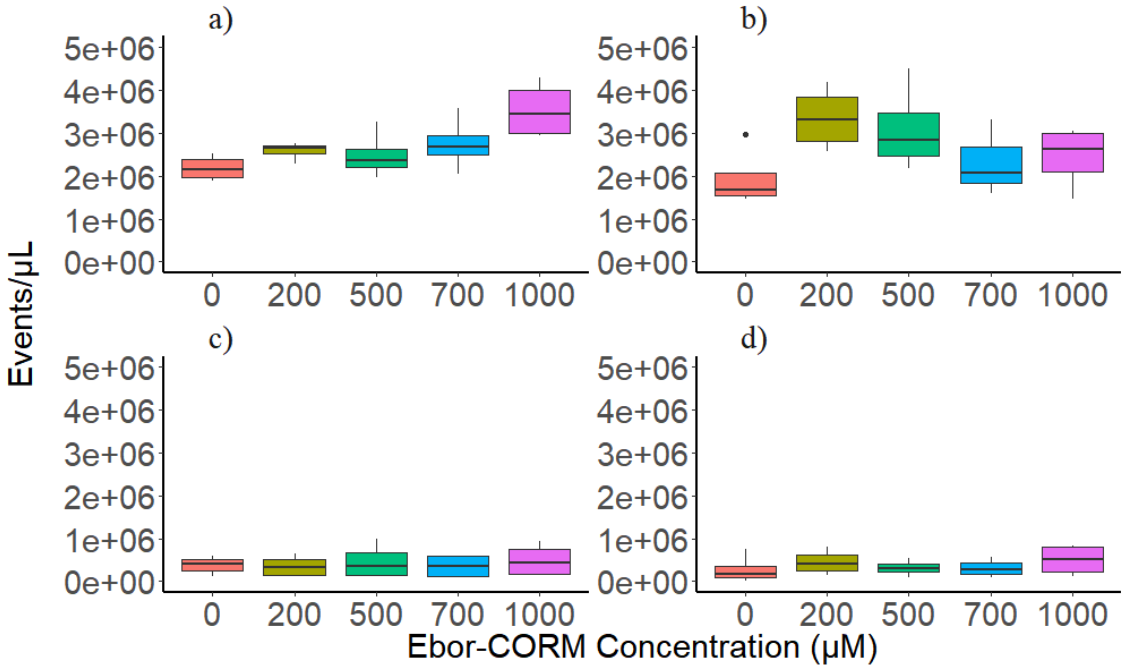

Figure 28*:* Effects of Ebor-CORM and colistin combination treatment on the densities of the colsitin resitant strain of P. aeruginosa, Col16b, determined using flow cytometry – a) Densities of Col16b following treatment with 0 (red), 200 (yellow), 500 (green), 700 (blue) or 1000 µM (purple) Ebor-CORM alone or in combination with b) 1 µg/ml colistin, c) 2 µg/ml colistin or d) 4 µg/ml colistin incubated at 37°C, 200rpm for 48 hours. The events/µL of live Col16b cells were determined using flow cytometric analysis of cultures stained with Syto-9 stain to identify bacterial cells, minus the value of dead cells identified by Propidium iodide staining. Boxes represents the range between the 25th quartile and the 75th quartile of the data with the black line in within the box representing the median. Whiskers represent the smallest and largest values within 1.5 times the interquartile range where n = 4.

To conclude, Ebor-CORM is not having an antimicrobial effect against Col16b after 24 hours growth as there is no significant reduction bacterial densities in the presence and absence of colistin. The resistance mechanism of Col16b facilitates its growth in the presence of 4 μg/ml and is presumably having the same effect that Ebor-CORM has on PAO1 when treated with inhibitory concentrations of colistin. As previously mentioned, the most likely resistance mechanism that Col16b could have would be an LPS modification or alteration in LPS expression which would prevent the binding of colistin (Moffatt et al., 2010; Bialvaei and Samadi Kafil, 2015). Alternatively, the resistance mechanism could be the result of increased biofilm production to prevent colistin binding. This is a plausible explanation because the samples analysed via cytometry after 48 hours showed that in the presence of 2 and 4 μg/ml colistin that approximately 10% of the reads were actually identified as bacteria, compared to the approximately 30% of PAO1, suggesting there was a significant amount of additional matter produced by the bacteria (Figure S8).

4.3.6 Effects of Ebor-CORM on Virulence trait production

Biofilms play a key role in bacterial virulence and tolerance to antimicrobials and may contribute to the resistance mechanism utilised by Col16b. It is also important to ensure that treating bacterial infections does not result in increased bacterial virulence and make them more tolerant of antimicrobials. Additionally, treatment with Ebor-CORM appears to increase the production of materials that alter the optical density. To test the hypothesis that Ebor-CORM treatment increases the production of pyocyanin and pyoverdine cultures of PAO1 and Col16b were inoculated with 0-1000 μM Ebor-CORM and incubated for 48 hours at 37 ^{o}C. Additionally, cultures were treated with a combination of colistin and Ebor-CORM to establish if this combination treatment results in increased production of the virulence factors. Figure 29 shows the absorbance at 691 nm that is indicative of oxidised pyocyanin. The data shows how pyocyanin levels change as a result of Ebor-CORM treatment in combination with a) 0, b) 1, c) 2 or d) 4 μg/ml colistin. This assay was combined with the assessment of pyoverdine which is laid out in the same manner in (Figure 30). Figure 30 shows the emission at 460nm following irradiation at 400 nm. This allowed for the quantification of pyoverdine and to determine how this changed as a result of the combination treatment.

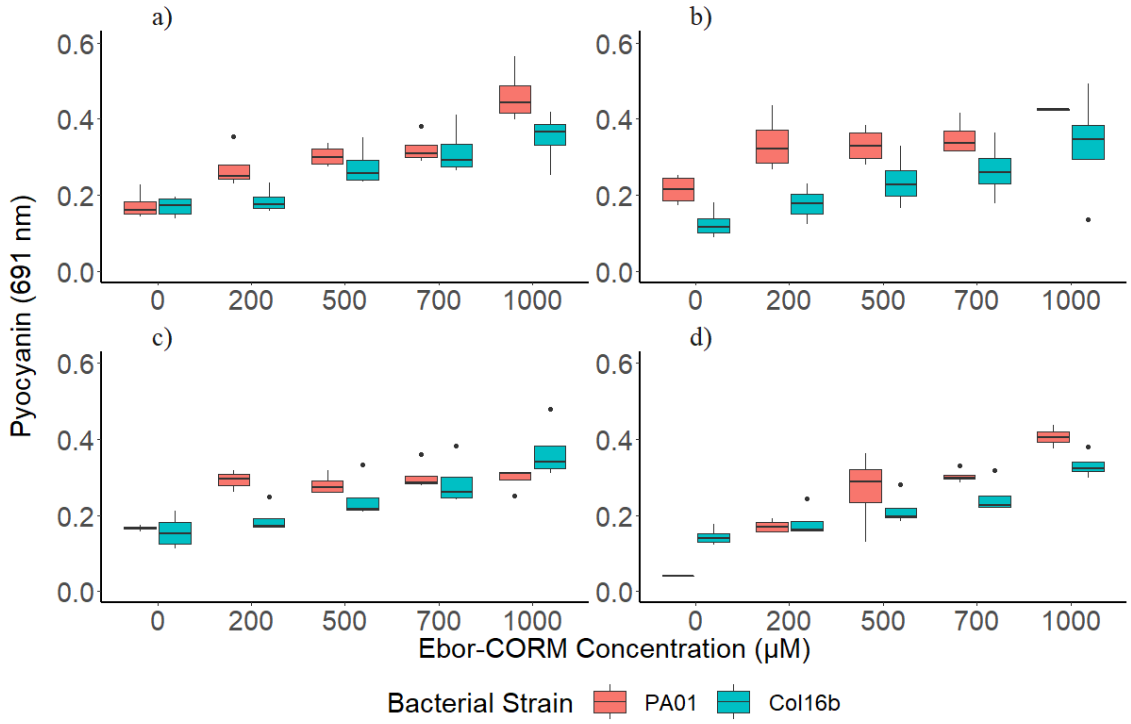

Figure 29: Pyocyanin production by *P. aeruginoasa* following Ebor-CORM and colistin combination treatments – a) Pyocyanin produced by PA01 (red) and Col16b (blue) following Ebor-CORm traetment. b) Pyocyanin produced following Ebor-CORM treatment in combination with 1 µg/ml colistin. c) Ebor-CORM treatment in combination with 2 µg/ml colistin and d) in combination with 4 µg/ml colistin. Boxes represents the range between the 25th quartile and the 75th quartile of the data with the black line in within the box representing the median. Whiskers represent the smallest and largest values within 1.5 times the interquartile range where n = 4.

An increase in pyocyanin production can be seen as Ebor-CORM concentration increases independent of colistin treatment and bacterial strain. Analysis via two-way ANOVA revealed that the observed increase in pyocyanin produced by PAO1 significantly increased as a result of Ebor-CORM concentration ($F_{(4,60)}$ = 55.61, p-value < 0.001), with Tukey post-hoc analysis revealing that 700 and 1000 µM treated cultures produced significantly more pyocyanin than untreated cultures independent of colistin (all p-values < 0.05). A significant interaction between Ebor-CORM and colistin on pyocyanin was also noted ($F_{(12,60)}$ = 3.161, p-value = 0.002).

Ebor-CORM also resulted in a significant increase in pyocyanin production by Col16b ($F_{(4,60)}$ = 25.603, p-value < 0.001). in all concentrations of colistin, only 1000µM Ebor-CORM treatments resulted in a significant increase in pyocyanin (all Tukey p-values <

0.013). No effect of colistin ($F_{(3,60)}$ = 1.541, p-value = 0.213) or interaction was noted between colistin and Ebor-CORM with Col16b as the mutant is resistant to colistin ($F_{(12,60)}$ = 0.186, p-value = 0.999).

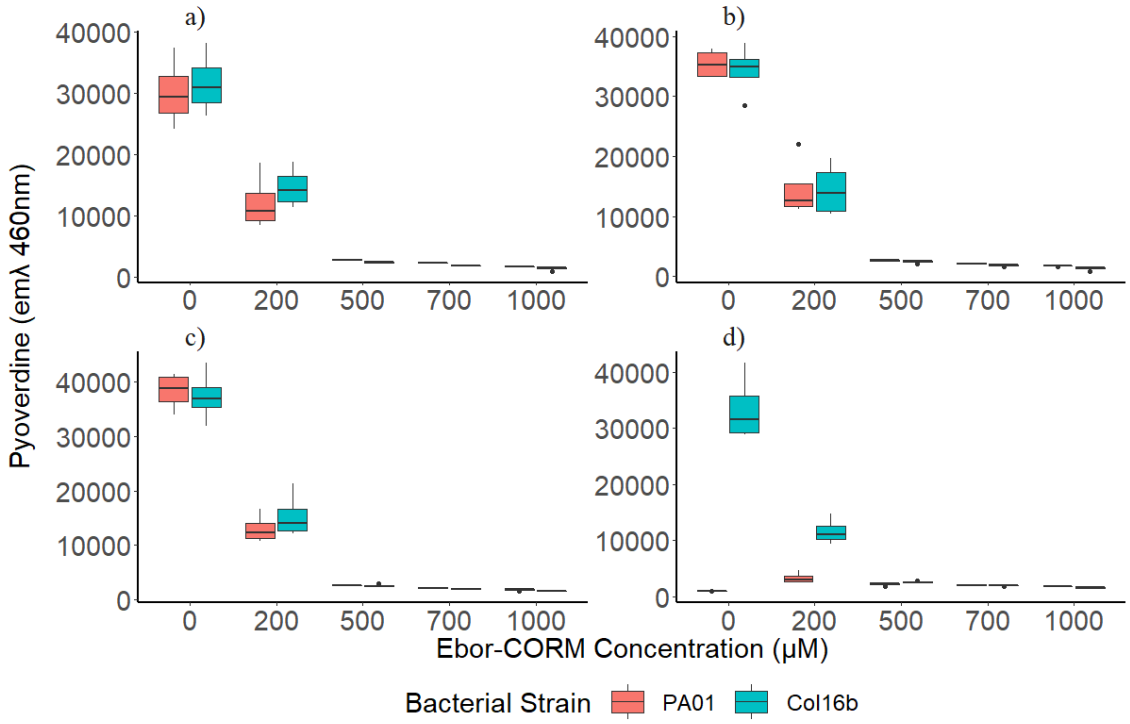

Figure 30: Pyoverdine production by *P. aeruginoasa* following Ebor-CORM and colistin combination treatments – a) Pyoverdine produced by PA01 (red) and Col16b (blue) following Ebor-CORm traetment. b) Pyoverdine produced following Ebor-CORM treatment in combination with 1 μg/ml colistin. c) Ebor-CORM treatment in combination with 2 μg/ml colistin and d) in combination with 4 μg/ml colistin. Boxes represents the range between the 25th quartile and the 75th quartile of the data with the black line in within the box representing the median. Whiskers represent the smallest and largest values within 1.5 times the interquartile range where n = 4.

Both Ebor-CORM ($F_{(4,60)}$ = 17.63, p-value < 0.001) and colistin ($F_{(3,60)}$ = 17.86, p-value < 0.001) significantly reduced PA01 pyoverdine production. Treatment of >200μM Ebor-CORM resulted in significantly lower pyoverdine in the presence of 0-2 μg/ml colistin (all Tukey p-values <0.005). Additionally, A significant interaction between Ebor-CORM and colistin occurred on the production of pyoverdine by PA01 (Two-way ANOVA: $F_{(12,60)}$ = 4.73, p-value < 0.001). The observed significant interaction and effect of colistin are presumably due to the lack of growth of PA01 in the presence of 4μg/ml colistin and lack of Ebor-CORM treatment, as cultures would not reach densities required to produce pyoverdine.

Col16b was again unaffected by colistin and is capable of growing in 4 µg/ml, increasing colistin concentration had no significant effect on pyoverdine production ($F_{(3,60)}$ = 1.264, p-value = 0.295) and no significant interaction between colistin and Ebor-CORM was observed ($F_{(3,60)}$ = 0.779, p-value = 0.669). As with PAO1 though, increasing Ebor-CORM concentration resulted in significantly lower levels of pyoverdine in cultures of Col16b ($F_{(12,60)}$ = 2.481, p-value = 0.0104) with all Ebor-CORM treatments significantly reducing pyoverdine more than untreated cultures independent of colistin concentration (all Tukey p-values <0.001).

To determine if biofilms production is altered as a result of Ebor-CORM treatment, cultures of PAO1 and Col16b were inoculated with the combination treatments of Ebor-CORM and colistin previously used and incubated for 48 hours before measuring biofilms. Figure 31 shows how the OD 600nm of crystal violet stained biofilm changes as a result of treatment with Ebor-CORM and colistin for both a) PAO1 and b) Col16b.

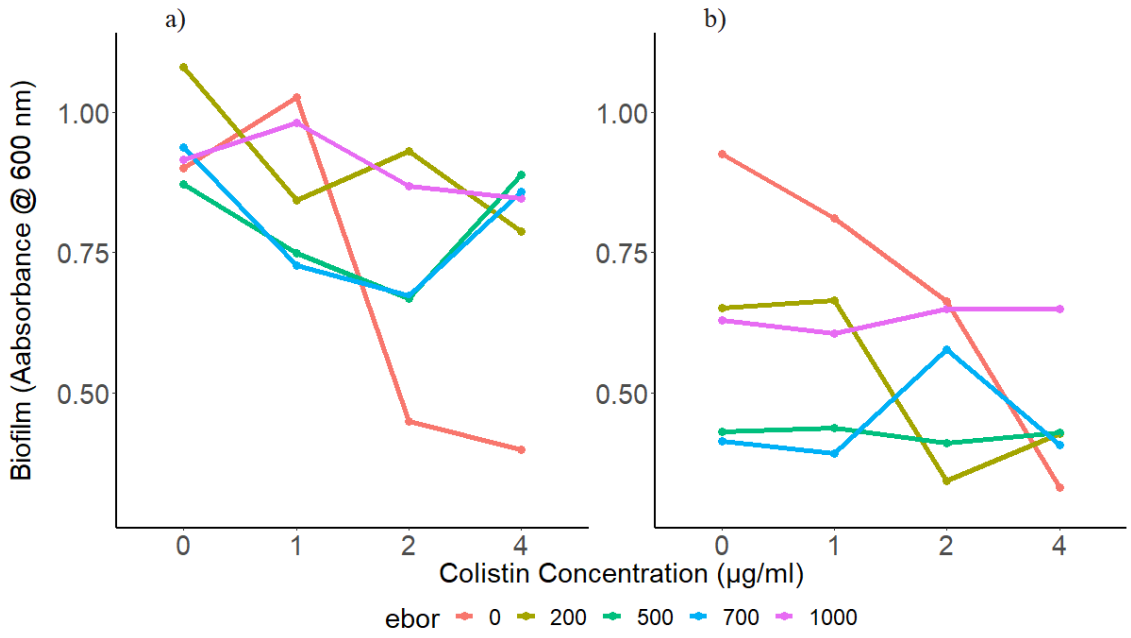

Figure 31: Effects of Ebor-CORM and colistin combination therapy on biofilm production – a) Biofim production by PAO1 following treatment of 0 (red), 200 (yellow), 500 (green), 700 (blue) or 1000 µM (purple) Ebor-CORM in combination with 0 to 4 µg/ml colistin. b) biofilm production of Col16b following ebor-CORM and colistin treatment. Data shown is the mean of 4 replicates.

No significant difference in biofilm production by PAO1 resulted from increasing Ebor-CORM treatment ($F_{(4,59)}$ = 1.930, p-value = 0.1173), however, a decrease in the amount of biofilm can be seen in the absence of Ebor-CORM and with 200 µM treatment (Figure 31a). Treatment with 4 µg/ml colistin also significantly reduced the production of biofilm in the absence of Ebor-CORM treatment ($F_{93,59)}$ = 3.074, p-value = 0.035), however, this could be the result of limited growth and cultures not reaching high enough densities. Again, no significant interaction was observed between colistin and Ebor-CORM on the production of biofilms by PAO1 (Two-way ANOVA: $F_{(12,59)}$ = 1.382, p-value = 0.2006).

Unsurprisingly, the production of biofilm by Col16b was unaffected by colistin and no interaction between Ebor-CORM and colistin was observed. However, Ebor-CORM treatment of significantly altered biofilm production ($F_{(4,52)}$ = 2.289, p-value = 0.0721) with treatment of 500 and 700 µM Ebor-CORM resulting in the lowest biofilm production in the absence of colistin.

In summary, Ebor-CORM treatment results in an increase in pyocyanin production by both PAO1 and Col16b, however, the production of biofilms and pyoverdine are both decreased. The major interaction between colistin and Ebor-CORM stems from the inability of PAO1 to grow in the presence of 4 µg/ml colistin.

It is possible that the increase in pyocyanin results from increased expression to mediate the ROS generated by the CO released from Ebor-CORM, as was described previously for Trypto-CORM in section 3.3.6. Zhu et al. (2019) has recently demonstrated that pyocyanin production increases in response to subinhibitory concentrations of antibiotics, as these can cause the accumulation of ROS, and can result in a collective antibiotic tolerance. However, this study found that pyocyanin conferred resistance to a range of antibiotic, with the exception of polymyxin B which functions in a similar manner to colistin. Although this cannot explain the increased tolerance to colistin it does highlight that combination therapy with Ebor-CORM may not be suitable against *P. aeruginosa* as may confer resistance to the other antibiotic through stimulation of pyocyanin.

It is also possible the Ebor-CORM could be interacting with *OxyR* to result in increased pyocyanin (also described in section 3.3.6). As with Trypto-CORM though these only explain increases in pyocyanin and could be potentially linked to increases in biofilm and pyoverdine production. However, in this case, both biofilm and pyoverdine levels decreased, therefore, Ebor-CORM must be interacting with additional targets to reduce the production of biofilms and pyoverdine.

A recent study by Heacock-Kang et al. (2018) found that mutations in the gene regulator PA1226 resulted in a significant reduction in biofilm production. Additionally, a second regulator (PA1413) has also been identified to be involved in biofilm formation and mutations within the gene can result in decreased biofilm formation (Heacock-Kang et al., 2017). These two regulators have been identified to act as part of a duel-regulator system that is that act in the complex regulation of biofilm formation (Heacock-Kang et al., 2018). Additionally, PA1226 is involved with the direct regulation, via activation of transcription, of the four genes that regulate pyoverdine production (PA2403-PA2406) and the gene PA3148 which plays a key role in LPS regulation (Ganne et al., 2017; Heacock-Kang et al., 2018). Therefore, reduced expression or mutations that inhibit binding of PA1226 to it targets would result in a significant decrease in both biofilm production and pyoverdine production without affecting pyocyanin as this is a separate regulatory mechanism the *LuxR* quorum sensing pathway.

As observed in 4.3.4 where cultures treated with 4 µg/ml colistin, an inhibitory concentration, were able to grow when treated with Ebor-CORM. As mentioned LPS is the binding site of colistin a reduction in LPS results in reduced sensitivity to colistin. LPS production can be regulated by PA1226 and a reduction in expression or mutation with the gene would result in significantly lower levels of LPS. It is therefore, plausible that Ebor-CORM could be interacting with PA1226 and this could explain why Ebor-CORM facilitates the growth of PAO1 in an inhibitory concentration of colistin.

In summary, Ebor-CORM could potentially be generating ROS that result in the increased the production of pyocyanin to mediate this effect. Additionally, the expression of gene regulators such as PA1226 could be reduced by Ebor-CORM preventing the activation of genes regulating pyoverdine and LPS. Alternatively, Ebor-CORM could be selecting mutations within PA1226 that prevent its binding.

4.4 Conclusions

Previous research on the antimicrobial effects of Ebor-CORM by Flanagan et al. (2018) found that 500µM Ebor-CORM reduced the viability of cultures by over 50% after 8 hours. However, in this study treatment with 1000 µM Ebor-CORM in the absence of colistin only resulted in a reduction of 35% after 48 hours when analysed by flow cytometry. The decrease in biofilm formation observed for Ebor-CORM treated cultures was also noted by Flanagan et al (2018).

Flanagan et al, (2018) additionally noted that a decrease in bacterial densities of clinical strains of *P. aeruginosa* could be observed 8 hours after Ebor-CORM treatment however, after 24 hours the reduction was no longer visible. These strains were also noted to grow slower than PAO1 and as established earlier (3.3.2) Trypto-CORM was more effective against cultures that were in the log phase of growth. This may be a contributing factor to why no long-term effect was noted, however, this does not explain the initial reduction in bacteria densities. The clinical strains of *P. aeruginosa* have likely been exposed to a range of antimicrobial treatments and have developed a range of antimicrobial resistances or broad-spectrum resistance mechanisms. The clinical strains have altered physiology which enables them to chronically infect the CF patients and is key for long-term survival (Abdulwahab et al., 2017). It is also possible that the clinicals strains used by Flanagan may be hypermutable and have mutations within proofreading proteins enabling for higher rates of mutagenesis and facilitating the development of resistance (Abdulwahab et al., 2017). Whereas the resistant strain used in this experiment was obtained through spontaneous mutagenesis rather than long-term, repeated exposure to antibiotics.

This research has also suggested that Ebor-CORM treatment is less effective when bacteria are growing under oxygen limiting conditions. However, future research should be conducted on this to confirm that actual cell densities are higher of Ebor-CORM treated cultures growing under near anaerobic conditions than cultures growing with freely available oxygen.

Additionally, this research has identified that Ebor-CORM works antagonistically with colistin and facilitates the growth of PAO1 in inhibitory concentrations of colistin. This

is thought to be the result of interaction between Ebor-CORM and the regulator PA1226 as this controls LPS production in addition to controlling pyoverdine and biofilm production, which were both significantly decreased as a result of Ebor-CORM treatment. Future research on the use of Ebor-CORM as part of a combination treatment should expand on this research and explore potential interactions with a larger range of antibiotic which, could be directly used to treat Pseudomonal infection or have low antimicrobial effects against PAO1. Additionally, the effects of CORMs on virulence gene expression should be explored further because the virulence factors produced by *P. aeruginosa* can cause significant damage to host epithelial tissues (Ballok and O'Toole, 2013).

Finally, this work has highlighted that Ebor-CORM has no effect on the bacterial densities of a colistin-resistant mutant of *P. aeruginosa* (Col16b) after 24 hours. Further research on the effects of Ebor-CORM on antibiotic-resistant bacteria could focus on strains with known antimicrobial resistances to other antimicrobials, as appose to clinical strains which could have a range of unknown resistances, in attempt to narrow the antimicrobial action of Ebor-CORM. Additional, research could also focus on exploring the use of Ebor-CORM combination therapies against a larger range of antibiotic-resistant strains in combination with a larger range of antibiotics in a checkerboard style experiment.

5.0 Discussion and Conclusions

5.1 Evaluation of the antimicrobial effects of Ebor-CORM and Trypto-CORM

This study has demonstrated that both Ebor-CORM and Trypto-CORM are capable of reducing bacterial densities of *P*. *aeruginosa* PAO1. In previous studies, Trypto-CORM has shown to be a more potent antimicrobial than Ebor-CORM, with antimicrobial effects being observed at 100 µM as opposed to 500 µM of Ebor-CORM (Ward et al., 2017; Flanagan et al., 2018). However, direct comparisons are not easily made because both CORMs were tested against different bacteria and concentration does not directly correlate to the moles of CO that are liberated from a CORM. Trypto-CORM is capable of liberating 2 moles of CO per complex and has three carbonyl groups (fig)(Ward et al., 2014). The exact moles of CO released from Ebor-CORM has not been stated, however, the compound has 4 carbonyl groups (Figure 3 and 16) Therefore, it stands to reason that a similar number of moles of CO, if not more, would be released from Ebor-CORM. As seen in Figure 6 and Figure 178 the release of CO from Ebor-CORM is significantly slower than that of Trypto-CORM which releases CO in a 'burst' when exposed to photoirradiation. This burst effect is hypothesised to cause the effects on neighbouring cultures seen in Figure 11 as more CO will be released and diffuse into neighbouring wells**.** While CO released from Ebor-CORM does not have an effect (Figure 19) and is hypothesised to be due to less CO being released in a given time and is therefore more likely to remain in solution.

In this study, Ebor-CORM has shown to be a more potent antimicrobial than Trypto-CORM against the PAO1 strain of *P. aeruginosa*. A 56% reduction in the densities of PAO1 were noted with treatment of 1000 µM compared to the maximum reduction of 25% produced by 1600 µM Trypto-CORM. However, actual densities of bacteria were not calculated for Trypto-CORM and OD 600nm was used alone to determine changes in bacterial densities. This method proved to be insufficient due to the production of secondary metabolites produced by *P. aeruginosa* that alter the optical density. Future experiments investigating the effects of Trypto-CORM on PAO1 may find greater reductions in bacterial densities if techniques such as colony plating and flow cytometry are used.

Although both CORMs have shown to reduce the bacterial densities of PAO1 in this study the concentrations required to achieve this were higher than those previously reported for the compounds (Ward et al., 2017; Flanagan et al., 2018). The photoactivation set up used in these experiments was very different from those previously used and this may the cause of the inefficiency of Trypto-CORM. Additionally, both CORMs were less effective against bacteria growing under oxygen limiting conditions. The concentrations required in these experiments are significantly higher than those that have been reported for other CORMs to be antimicrobial. CORMs -2 and -3 have been reported to result in almost complete loss of viability of *E. coli and S. aureus*, four hours after 250 µM and 400 µM treatments respectively (Nobre et al., 2007). Additionally, a newer manganese-based PhotoCORM ($[Mn(CO)_3(tpa\text{-}\kappa^3N)]^+$) has shown to significantly inhibit *E. coli* at 150 µM which is similar to that previously reported for Trypto-CORM (Tinajero-Trejo et al., 2016). The concentrations of Trypto-CORM and Ebor-CORM required to exhibit antimicrobial effects are also likely to be significantly higher than the narrow therapeutic range of CORMs and would, therefore, result in damage to host tissues (Faizan et al., 2019; Nobre et al., 2016).

Interestingly, both CORMs resulted in significant alteration of the virulence of PAO1. Ebor-CORM and Trypto-CORM result in a significantly increased production of pyocyanin. As discussed earlier, pyocyanin is a redox-active pigment that is capable of interacting with ROS to mediate the damaging effects they can have on the bacterium (Vinckx et al., 2010). Pyocyanin production is also increased as a result of treatment with sub-lethal concentration of various antibiotics and appears to be produced as part of a general stress response (Zhu et al., 2019). Therefore, this increase in pyocyanin could be the result of the mediation of ROS generated by the CORMs.

Interestingly, Trypto-CORM and Ebor-CORM had opposing effects on the production biofilms and pyoverdine, with Ebor-CORM significantly reducing the production of both these virulence factors. The effects of other CORMs on biofilm production have also been studied by other groups and they have also found CORMs can result in both increases and decreases in biofilm production. Murray et al. (2012) found that treatment of *P. aeruginosa* with sublethal concentrations of CORM-2 resulted in a significant reduction in biofilm production and maturation. However, the same CORM

has shown to both increase and decrease the production of biofilms by different strains of *E. coli* (Sahlberg Bang et al., 2016). This effect is likely due to differences between the strains *E. coli* and the stimulation and/or suppression of different pathways within the bacteria. It is possible that the differences in biofilms between Ebor-CORM and Trypto-CORM treatment cultures could be due to the interaction with different pathways as a result of different CO release rates and dynamics. For example, the release of CO from Ebor-CORM is lower than that of Trypto-CORM in a given time (Figure 6 & Figure 18). Additionally, release from Trypto-CORM is directly linked to photoirradiation and only occurs within the time that photoirradiation occurred this may result in a 'burst' effect whereas the release form Ebor-CORM could be steadier over a longer period of time. The effects of both Ebor-CORM and Trypto-CORM on bacterial virulence should be explored further. The effects of a combination treatment of Ebor-CORM and Trypto-CORM could also be explored as the CORMs have opposing effects on biofilm and pyoverdine production and may be interacting with different pathways that control virulence. Increasing bacterial virulence can result in increased resistance to other antimicrobials, in addition to causing significantly more damage to the host during an infection (Zhu et al., 2019; Ballok and O'Toole, 2013).

5.2 Antimicrobial Application of CORMs *In Vivo*

The board-spectrum effects of most CORMs have not been assessed and most compounds are tested against one species of bacteria as with Ebor-CORM. CORM-3 is the most widely studied CORM that has currently been developed however, due to interactions of the ruthenium core with bacterial functions it has not progressed as an effective antimicrobial (McLean et al., 2013). [Mn(CO)3(tqa-κ3N)]Br and Trypto-CORM are likely to be the widest studied manganese-based CORMs in terms of being tested against different bacterial species (Rana et al., 2017; Güntzel et al., 2019; Ward et al., 2017). However, these compounds have still only been tested against approximately three species of bacteria each. The broad-spectrum effects of CORMs should be evaluated to determine which bacterial species may be more susceptible to CORM treatment. Additionally, the *in vivo* efficiency and toxicity of CORMs is desperately needed to determine the therapeutic potential of CORMs as antimicrobials.

Galleria mellonella larvae, also known as wax moth larvae, have been used as the first point of call for studying the efficiency of antimicrobial clearance within a host, in addition to determining the toxicity of the antimicrobial to the host (Ignasiak and Maxwell, 2017). The use of *G. mellonella* offers a cheaper alternative to rodent studies and allows for easier high-throughput screening of compounds and concentrations (Cook and McArthur, 2013). Additionally, the immune system of *G. mellonella* is comparable to the innate immune systems in mammals and correlations have already been noted between results obtained in *G. mellonella* and mammalian models (Jander, Rahme and Ausubel, 2000; Cook and McArthur, 2013).

Despite this, there are a limited number of studies that have actually utilised this model to explore the antimicrobial effect of CORMs *in vivo.* Flanagan et al. (2018) previously studied the effects of Ebor-CORM on the survival of *G. mellonella* infected with three different strains of *P. aeruginosa.* The study found that the Ebor-CORM did not increase the survival of *P. aeruginosa* infected larvae. However, Ebor-CORM has not been studied against other species of bacteria and may have significant effects against other pathogens. Additionally, the PhotoCORM has shown to be effective against multidrug-resistant pathogenic *E. coli* (Betts et al., 2017), and more recently multidrug-resistant strains of *P. aeruginosa* and *Acinetobacter baumanniii* (Güntzel et al., 2019). Treatment *G. mellonella* had a 50% higher survival than the untreated ones after 96 hours of infection (Güntzel et al., 2019). In this study, treated *G. mellonella* were exposed to UV light to stimulate the release of CO from PhotoCORM. As *G. mellonella* larvae are only 12–20 mm in length the, UV irradiation used to activate the CORM is most likely able to penetrate into the larvae to activate the CORM (Cook and McArthur, 2013). However, UV irradiation is unable to penetrate through the dermis and reach underlying tissues (Gupta et al., 2013), therefore, for photo-CORMs to be an applicable antimicrobial they would either have to be used to treat dermal infections where photo-irradiation can be easily applied (Zobi, 2013; Kourti, Jiang and Cai, 2017). Alternatively, photo-CORMs could be applied to treat internal infections providing there is a mechanism of stimulating CO release. Advancements in the development photo-activated chemotherapeutic agents may be able to tie in here and provide a mechanism of

stimulating photo-CORMs however, this would require significantly more research (Farrer, Salassa and Sadler, 2009).

5.3 Current Applications of CORMs

CORMs were initially developed to deliver localised release of CO to tissues and organs to exploit its therapeutic potential (Nobre et al., 2007; Kourti, Jiang and Cai, 2017). It has been well documented that CO is cytotoxic to human cells and at concentrations greater than 10% haemoglobin bound to CO, negative effects begin to occur (Faizan et al., 2019; Kourti, Jiang and Cai, 2017). Despite this, there is a narrow therapeutic range in which CO can exhibit a range of therapeutic effects from reducing inflammation to protecting and preserving transplanted organs (Faizan et al., 2019).

Experiments conducted by Clark et al. (2003) explored the potential cytoprotective effects of CORMs against hypoxia in cardiac cells and heart transplantation. In the study, rat cardiac cells were treated with CORM-3 and incubated under hypoxic conditions for 24 hours before being returned to normoxic conditions for 6 hours. Treatment of 25 µM CORM-3 resulted in 100% viability of cardiac cells, whereas only 25% of untreated cells were viable following reoxygenation from hypoxia (Clark et al., 2003). Additionally, rats treated with 40 mg/kg CORM-3, 1 day prior to heart transplantation, 1 hour after transplantation and every day after transplantation resulted in a reduced rejection rate and increased survival. Untreated rats rejected transplantation and were all dead within 10 days, however, peritoneal injection of 40 mg/kg CORM-3 resulted in only a 40% rejection rate after 25 days (Clark et al., 2003). Interestingly, some of the effects exhibited by CORM-3 were also achieved with an inactive part of the complex and therefore, the ruthenium part of the complex not only exhibits part of the antimicrobial effects of CORM-3 but also the cytoprotective effects.

More recently the use of CORMs as a cancer treatment has been explored with promising results, however, their use for this application is controversial (Kourti et al., 2019; Ismailova et al., 2018). Niesel et al. (2008) showed that their manganese-based photo-CORM was capable of reducing the viability of colon cancer cells, *in vivo,* with comparable levels of reduction to the established cytotoxic agent (5-fluorouracil). The study found that the CORM was taken up *via* passive diffusion and that 100 µM

concentrations exhibited no cytotoxic effects in the absence of photo-irradiation (Niesel et al., 2008).

Additional studies have explored the use of older ruthenium-based CORMs as anticancer treatments. CORM-2 treatment has shown to significantly reduce the expression of vascular endothelial growth factor (VEGF) in breast cancer cells which plays a key role in angiogenesis and in turn, tumour development (Kourti et al., 2019). Interestingly, *In vitro* use of CORMs has also shown to increase the expression of VEGF, however, the expression was reported in non-cancerous cells and therefore, the effects of CORMs appear to be cell type-specific (Kourti et al., 2019; Li Volti et al., 2005). CORM-2 has also shown significant effects on cancer development *In vivo*. Shao et al. (2018) showed that lung tumour-bearing mice treated with 0.4 mg/kg/day of CORM-2 prevented the orthotopic development of lung tumours and prevented the decline in body weight, spleen and thymus index which was observed in untreated lung tumour-bearing mice. CORM-2 appeared to prevent tumours from developing through the suppression of inflammatory factors and inhibiting the expression of key factors involved with tumour progression (Shao et al., 2018).

5.4 Conclusion

CORMs are showing to be both a promising new therapeutic agent for the treatment of a range of medical conditions and a new class of antimicrobial agents that are effective against a range of bacterial species. However, there is still significant research to be conducted on CORMs to understand their potential applications in a real-world perspective and significantly more before CORMs reach clinical trials to be used as antimicrobials. Future research should focus how varying CORM treatment conditions can affect their antimicrobial effects, the potential combination treatments of CORMs and currently used antibiotics and the application of CORMs *in vivo* to determine how these compounds may function in real-world environments.

Appendix

A1 Photoirradiation Set-up

Figure S1: Photoirradiation setup – Consisting of the 400nm emitting LED blacklight bar supported over a Grant-bio PMS-1000i microplate shaker.

Figure S2: LED light bar – Consisting of 6x 3W LEDs housed in reflective units to provide a 120^{o} angle of light.

Figure S3: Photoirradiation control – The LED blacklight bar was connected to the Timeguard Tg77 electrical timer plug allowing for up to 20 on/off cycles to be programmed.

A2 Antibiotic Resistance Selection Methodology

A2.1 Minimum inhibitory concentrations

Minimum inhibitory concentrations of an antibiotic were first determined before deciding which concentrations would be used to select for random resistant mutants. A Stock solution 1024 µg/ml of selected antibiotic was prepared by dissolving the antibiotic in a selected solvent. 200 µl of this stock was serially diluted 1 in 2 in LB broth to 0.03125 µg/ml in a 96-well flat-bottom microplate, LB containing no antibiotic used as a negative control. Overnight bacterial cultures of PAO1 were diluted to an optical density (OD) 600 nm of 0.05 ± 0.005 using LB broth. 100 µl of diluted culture were pipetted into the antibiotic solutions in the wells of the microplate. Cultures were incubated stationary at 37^{o}C for 24 hours, after which the OD 600 nm was measured using a Tecan Sunrise microplate reader. The obtained data was plotted as a curve from low to high concentration and inhibitory concentrations were considered to be the point at which the curve plateaued.

A2.2 Resistance selection

To select for random resistant mutants within a population, 2 separate cultures of PAO1, inoculated from the same cryo-stock, were incubated for 24 hours at 37^{o}C rotating at 180 rpm in LB broth. Following incubation, cultures were centrifuged at 4^{o}C for 10

minutes at 4000 rpm to pellet the bacteria. The supernatant was removed, and the bacteria were resuspended in 1ml of LB broth, combined together and made up to a total volume of 4ml. Antibiotic plated were prepared by combining autoclaved LB agar (Formulation) at approx. 40^{o}C with antibiotic, from a stock prepared as described above, to a total volume of 40 ml to achieve the desired concentration of antibiotic. This mix was used to pour 2 Petri dish plates. 10 µl of concentrated PAO1 bacterial solution was pipetted onto each Petri dish and spread using the glass bead method. PAO1 were also plated on LB agar containing no antibiotic to ensure cells were alive. Plates were incubated at 37^{o}C until colonies were observed. After 4 days, plates with no visible were considered have no viable bacteria. 2 colonies were picked from each plate and re-streaked onto LB agar plates containing no antibiotic and incubated for 24 hours at 37^{o}C. following incubation some cultures did not grow and again were considered inviable. Single colonies were selected, regrown in LB broth overnight and cryopreserved.

In the case of Col16b, PAO1 was plated onto LB agar containing 16 µg/ml colistin and incubated at 37^{o}C as described above. The colony was selected from this plate and screened for resistance to colistin as described below.

A2.3 Determining resistance

To determine if suspected strains conferred antibiotic resistance, overnight cultures were prepared and underwent the same procedure as previously described to determine their minimum inhibitory concentration. The ancestral strain was used as a control to determine if the minimum concentration of antibiotic required to inhibit growth had increased.

A3 Colistin Resistance Mutant

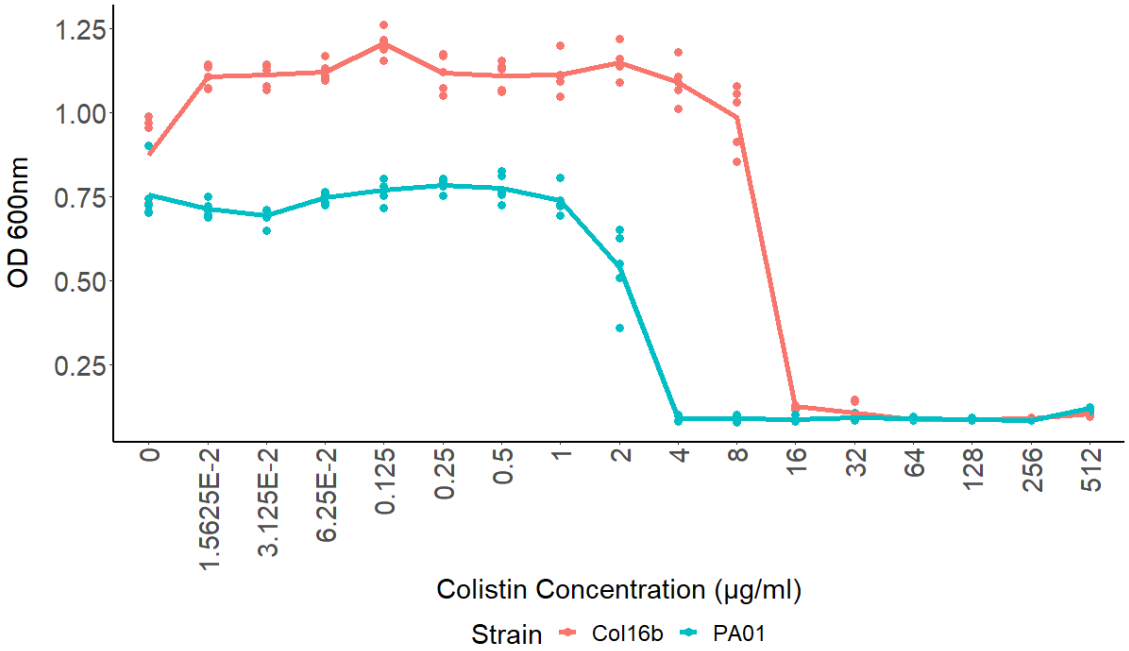

Figure S4: Inhibitory concentrations of Colistin against PAO1 and Col16b – the densities of PAO1 (blue) and Col16b (red) exposed to various concentrations of colistin to determine the MIC and if Col16b confers resistance to colistin.

A4 Flow Cytometry Gating

Initial gating used forward and side scatter to detect the bacteria based solely on size. To determine this PBS with the stain solution of Propidium iodide and Syto-9 stains was run through the flow cytometer on medium speed of 30 µl/min to obtain a background reference. As can be seen in Figure S5a, the majority of the detected events were less than 10^4 for both side scatter and forward scatter. Following this, bacterial cultures that were stained with Propidium iodide and Syto-9 stains were run through the flow

cytometer as a medium speed of 30 µl/min. Figure S5b shows the forward and side scatter obtained from a bacterial sample being run through the cytometer.

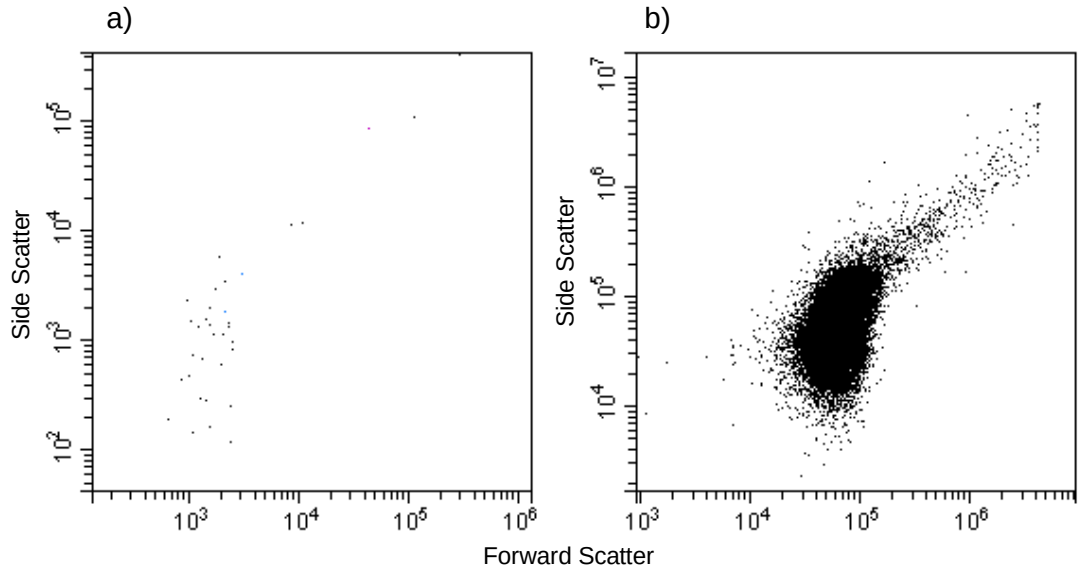

Figure S5: Scatter Gating – a) observed scatter of PBS solution containing Syto-9 and Propidium iodide stains. b) forward and side scatter of a Propidium iodide and Syto-9 stained bacterial aliquot. Both samples were analysed by a CytoflexXL cytometer with samples running on the medium setting of 30 µl/min

With it established that the bacteria can be identified within the events detected above 10^4 for forward and side scatter the actual bacteria could then be identified using the B525-FITC filter to detect all bacteria stained with Syto-9. Figure S6a shows the number of events that were recorded at different values for the B525-FITC-H filter. Syto-9 stained bacteria have higher absorbance values than unstained material using the B525-FITC filter. This plot was used to generate the Sytox 9 gate which was applied to other data to reduce the data set to only bacteria that have been Syto-9 stained (Figure S6b-c).

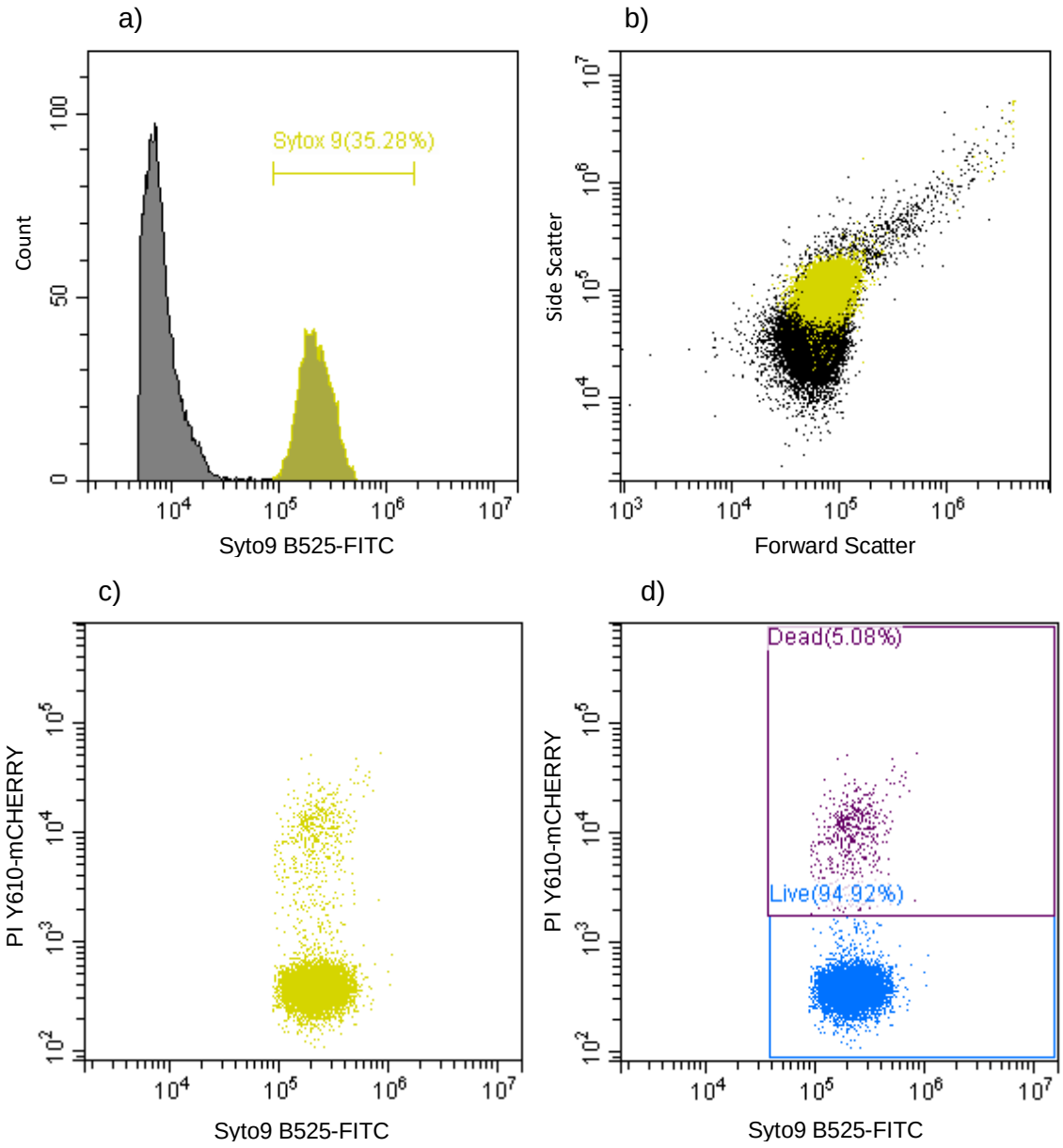

Figure S6: First Syto-9 gate and Live/dead gating – a) frequency of absorbance at 525 nm of a Syto-9 and Propidium iodide stained bacterial aliquot allowing for generation of the Sytox 9 gate. b) scatterplot of forward and side scatter values obtained of the stained bacterial aliquot all recorded events (black) Sytox 9 gated events (yellow). c) Sytox 9 gated values of the recorded absorbance of the stained bacterial aliquot at 525 vs 610 nm. d) Gates generated from the Sytox 9 gated absorbance values 525 vs 610 nm events to distinguish live bacteria (blue) from dead bacteria (purple). All samples were analysed using a CytoflexXL cytometer running at 30 µl/min.

Figure S6c shows the scatter plot of the B525-FITC filter and the Y610-mCHERRY filter. The Y610-mCHERRY filter allows for the detection of Propidium iodide stains cells.

Propidium iodide only stains membrane compromised/ dead cells and therefore, these cells have higher values for the Y610-mCHERRY filter. 2 clusters can observed within Figure S6c. These can be used to identify live and dead cells as live cells will cluster at lower Y610-mCHERRY values than dead ones live bacteria were gated at Y610 values < $2x10^3$ and the dead bacteria were gated at Y610 > $2x10^3$ (Figure S6d). The live/dead gates can be used to subset the data and calculate percentages of live and dead cells. The final gating explored further corrected the first gate using Syto-9 absorbance at 525 nm. By plotting the Syto-9 absorbance values against the size of the particles it can be clearly seen that the Sytox 9 gate (yellow) includes some events that have the correct absorbance at 525 nm but are larger than that cluster gated by S9bac+ve in Figure S7 (pink). The S9bac+ve further subsets the data to remove larger particles that be the result of extracellular material or biofilm.

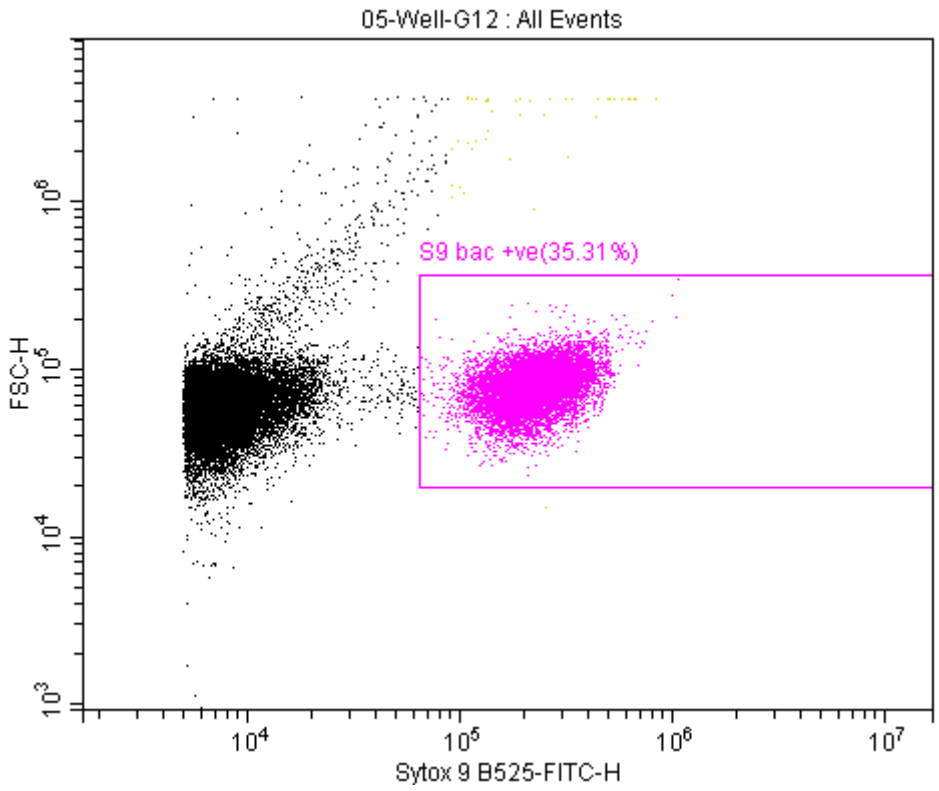

Figure S7: Second Syto-9 gating – Absorbance of events at 525 nm relative to the size of the particles represented by forward scatter. All events(black), Sytox 9 gated events (yellow) and S9 bac+ve gated events (pink).

A5 Production of Extracellular material by PAO1 and Col16

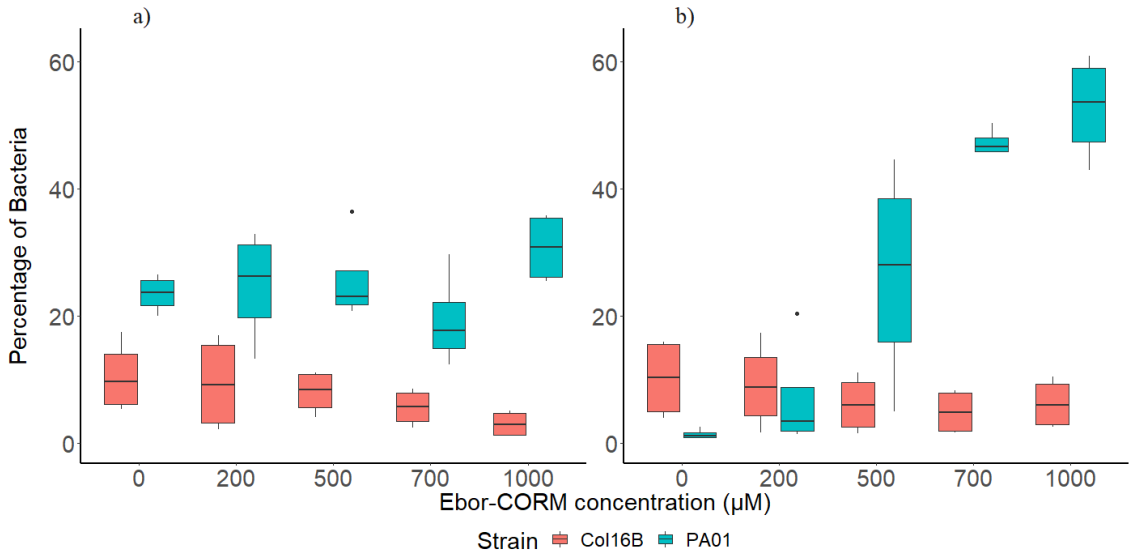

Figure S8: Production of Extracellular material by PAO1 and Col16b - percentage of PAO1 (blue) and Col16b (red) in a sample analysed by flow cytometry after 48 hours of growth and treatment with Ebor-CORM and a) 2 μg/ml and b) 4μg/ml colistin.

A6 Effect of Trypto-CORM on the growth of S. aureus

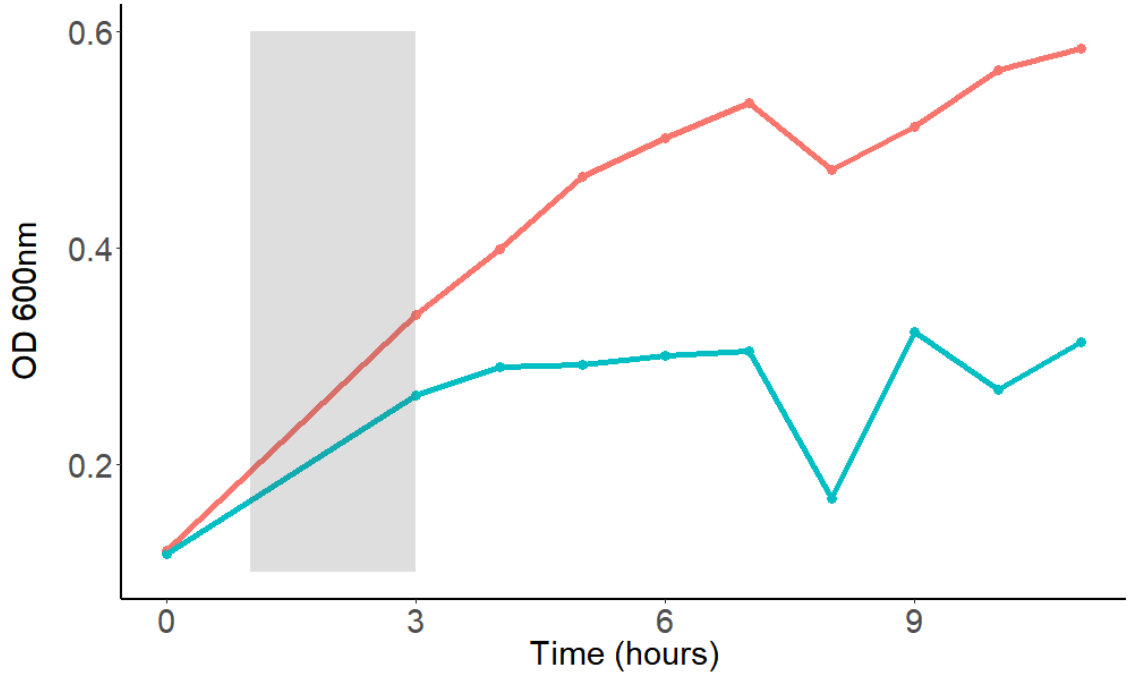

Figure S9: Effect of Trypto-CORM on the growth of S. aureus (8532) - the growth of S. aureus over 11 hours treated with 0 (red) or 100μM (blue) Trypto-CORM exposed to a 4-minute-on-1-minute-off activation cycle, cycled 17 times 1 hour post inoculation (grey box).

Abbreviations

ANOVA	-	Analysis of variance
ATP	-	Adenosine triphosphate
CF	-	Cystic Fibrosis
CFU	-	Colony forming units
CO	-	Carbon monoxide
CORM	-	Carbon monoxide-releasing molecule
DMSO	-	Dimethyl sulfoxide
DNA	-	Deoxyribonucleic acid
mg	-	Milligrams
MIC	-	Minimum inhibitory concentration
nm	-	nanometres
NO	-	Nitric oxide
O_2	-	Oxygen
OD 600nm	-	Optical density at 600 nm
PBP's	-	Penicillin binding protein
PBS	-	Phosphate buffered saline
RNA	-	Ribonucleic acid
ROS	-	Reactive oxygen species
RPM	-	Revolutions per minute
µM	-	Micromolar
µg/ml	-	Micrograms per millilitre

References

Abdollahi, A. et al. (2015). Problem-solving skills appraisal mediates hardiness and suicidal ideation among Malaysian undergraduate students. *PLoS ONE*, 10 (4), p.e0122222.

Abdulwahab, A. et al. (2017). The emergence of multidrug-resistant Pseudomonas aeruginosa in cystic fibrosis patients on inhaled antibiotics. *Lung India*, 34 (6), pp.527–531.

Agga, G. E., Schmidt, J. W. and Arthur, T. M. (2016). Effects of In-Feed Chlortetracycline Prophylaxis in Beef Cattle on Animal Health and Antimicrobial-Resistant Escherichia coli. *Applied and Environmental Microbiology*, 82 (24), pp.7197–7204.

Altoparlak, U. et al. (2004). The time-related changes of antimicrobial resistance patterns and predominant bacterial profiles of burn wounds and body flora of burned patients. *Burns*, 30 (7), pp.660–664.

Amin, R. M. et al. (2016). Antimicrobial blue light inactivation of Pseudomonas aeruginosa by photo-excitation of endogenous porphyrins: In vitro and in vivo studies. *Lasers in Surgery and Medicine*, 48 (5), pp.562–568.

Andersson, D. I. (2003). Persistence of antibiotic resistant bacteria. *Current Opinion in Microbiology*, 6 (5), pp.452–456.

Arai, H. (2011). Regulation and Function of Versatile Aerobic and Anaerobic Respiratory Metabolism in Pseudomonas aeruginosa. *Frontiers in Microbiology*, 2, p.103.

Arai, H., Jung, H. R. and Kaplan, S. (2008). Transcriptome dynamics during the transition from anaerobic photosynthesis to aerobic respiration in Rhodobacter sphaeroides 2.4.1. *Journal of Bacteriology*, 190 (1), pp.286–299.

Atkin, A. J. et al. (2011). Modification of the deoxy-myoglobin/carbonmonoxy-myoglobin UV-vis assay for reliable determination of CO-release rates from organometallic carbonyl complexes. *Dalton Transactions*, 40 (21), pp.5755–5761.

Azeredo, J. et al. (2017). Critical review on biofilm methods. *Critical Reviews in Microbiology*, 43 (3), pp.313–351.

Baharoglu, Z., Bikard, D. and Mazel, D. (2010). Conjugative DNA transfer induces the bacterial SOS response and promotes antibiotic resistance development through integron activation. *PLoS Genetics*, 6 (10), pp.1–10.

Ballok, A. E. and O'Toole, G. A. (2013). Pouring salt on a wound: Pseudomonas aeruginosa virulence factors alter Na+ and Cl- flux in the lung. *Journal of Bacteriology*, 195 (18), pp.4013–4019.

Barrientos-Moreno, L. et al. (2019). Arginine Biosynthesis Modulates Pyoverdine Production and Release in Pseudomonas putida as Part of the Mechanism of Adaptation to Oxidative Stress. *Journal of bacteriology*, 201 (22), pp.e00454-19.

Bassetti, M. et al. (2018). How to manage Pseudomonas aeruginosa infections. *Drugs in context*, 7, p.212527.

Benzing, A. et al. (1996). Effect of inhaled nitric oxide on venous admixture depends on cardiac output in patients with acute lung injury and acute respiratory distress

syndrome. *Acta anaesthesiologica Scandinavica*, 40 (4), pp.466–474.

Betts, J. et al. (2017). Antimicrobial activity of carbon monoxide-releasing molecule [Mn(CO)3(tpa-κ3N)]Br versus multidrug-resistant isolates of Avian Pathogenic Escherichia coli and its synergy with colistin. Shafer, W. M. (Ed). *PLOS ONE*, 12 (10), p.e0186359.

Bialvaei, A. Z. and Samadi Kafil, H. (2015). Colistin, mechanisms and prevalence of resistance. *Current Medical Research and Opinion*, 31 (4), pp.707–721.

Blondeau, J. M. (2004). Fluoroquinolones: Mechanism of action, classification, and development of resistance. *Survey of Ophthalmology*, 49 (2), pp.S73–S78.

Blumenthal, I. (2001). Carbon monoxide poisoning. *Journal of the Royal Society of Medicine*, 94 (6), pp.270–272.

Challis, G. L. and Hopwood, D. A. (2003). Synergy and contingency as driving forces for the evolution of multiple secondary metabolite production by Streptomyces species. *Proceedings of the National Academy of Sciences of the United States of America*, 100 (24), pp.14555–14561.

Chiorean, S. et al. (2019). Dissecting the Binding Interactions of Teixobactin with the Bacterial Cell-Wall Precursor Lipid II. *ChemBioChem*.

Cho, H., Uehara, T. and Bernhardt, T. G. (2014). Beta-Lactam Antibiotics Induce a Lethal Malfunctioning of the Bacterial Cell Wall Synthesis Machinery. *Cell*, 159 (6), pp.1300–1311.

Church, D. et al. (2006). Burn wound infections. *Clinical Microbiology Reviews*, 19 (2), American Society for Microbiology (ASM)., pp.403–434.

Clark, J. E. et al. (2003). Cardioprotective actions by a water-soluble carbon monoxide-releasing molecule. *Circulation research*, 93 (2), pp.E2–E8.

Clark, R. H. et al. (2000). Low-Dose Nitric Oxide Therapy for Persistent Pulmonary Hypertension of the Newborn. *New England Journal of Medicine*, 342 (7), pp.469–474.

Coetzee, E., Rode, H. and Kahn, D. (2013). Pseudomonas aeruginosa burn wound infection in a dedicated paediatric burns unit. *South African Journal of Surgery*, 51 (2), pp.50–53.

Comolli, J. C. and Donohue, T. J. (2004). Differences in two Pseudomonas aeruginosa cbb3 cytochrome oxidases. *Molecular Microbiology*, 51 (4), pp.1193–1203.

Cook, S. M. and McArthur, J. D. (2013). Developing Galleria mellonella as a model host for human pathogens. *Virulence*, 4 (5), pp.350–353.

Cui, L. et al. (2006). Novel mechanism of antibiotic resistance originating in vancomycin-intermediate Staphylococcus aureus. *Antimicrobial agents and chemotherapy*, 50 (2), pp.428–438.

Cunningham, L., Pitt, M. and Williams, H. D. (1997). The *cioAB* genes from *Pseudomonas aeruginosa* code for a novel cyanide-insensitive terminal oxidase related to the cytochrome *bd* quinol oxidases. *Molecular Microbiology*, 24 (3), pp.579–591.

Davidge, K. S. et al. (2009). Carbon monoxide-releasing antibacterial molecules target respiration and global transcriptional regulators. *The Journal of biological chemistry*, 284

(7), pp.4516–4524.

Dellit, T. H. et al. (2007). Infectious Diseases Society of America and the Society for Healthcare Epidemiology of America Guidelines for Developing an Institutional Program to Enhance Antimicrobial Stewardship. *Clinical Infectious Diseases*, 44 (2), pp.159–177.

Desmard, M. et al. (2009). A carbon monoxide-releasing molecule (CORM-3) exerts bactericidal activity against Pseudomonas aeruginosa and improves survival in an animal model of bacteraemia . *The FASEB Journal*, 23 (4), pp.1023–1031.

Ernst, A. and Zibrak, J. D. (1998). Carbon Monoxide Poisoning. *New England Journal of Medicine*, 339 (22), pp.1603–1608.

Faizan, M. et al. (2019). CO-releasing materials: An emphasis on therapeutic implications, as release and subsequent cytotoxicity are the part of therapy. *Materials*, 12 (10), MDPI AG., p.1643.

Farrer, N. J., Salassa, L. and Sadler, P. J. (2009). Photoactivated chemotherapy (PACT): the potential of excited-state d-block metals in medicine. *Dalton Transactions*, (48), pp.10690–10701. [Online]. Available at: doi:10.1039/b917753a [Accessed 9 December 2018].

Feklistov, A. et al. (2008). Rifamycins do not function by allosteric modulation of binding of Mg2+ to the RNA polymerase active center. *Proceedings of the National Academy of Sciences of the United States of America*, 105 (39), pp.14820–14825.

Fernández, R. O. and Pizarro, R. A. (1996). Lethal Effect Induced in Pseudomonas aeruglnosa Exposed to Ultraviolet-A Radiation. *Photochemistry and Photobiology*, 64 (2), pp.334–339.

Fila, G. et al. (2018). Antimicrobial blue light photoinactivation of *Pseudomonas aeruginosa* : Quorum sensing signaling molecules, biofilm formation and pathogenicity. *Journal of Biophotonics*, 11 (11), p.e201800079.

Fila, G., Kawiak, A. and Grinholc, M. S. (2017). Blue light treatment of pseudomonas aeruginosa: Strong bactericidal activity, synergism with antibiotics and inactivation of virulence factors. *Virulence*, 8 (6), pp.938–958.

Fishovitz, J. et al. (2014). Penicillin-binding protein 2a of methicillin-resistant Staphylococcus aureus. *IUBMB Life*, 66 (8), pp.572–577.

Flanagan, L. et al. (2018). The Antimicrobial Activity of a Carbon Monoxide Releasing Molecule (EBOR-CORM-1) Is Shaped by Intraspecific Variation within Pseudomonas aeruginosa Populations. *Frontiers in Microbiology*, 9, p.195.

Fridkin, S. et al. (2014). Vital signs: improving antibiotic use among hospitalized patients. *MMWR. Morbidity and mortality weekly report*, 63 (9), pp.194–200.

Ganne, G. et al. (2017). Iron Release from the Siderophore Pyoverdine in *Pseudomonas aeruginosa* Involves Three New Actors: FpvC, FpvG, and FpvH. *ACS Chemical Biology*, 12 (4), pp.1056–1065.

Giuffrè, A. et al. (2014). Cytochrome bd oxidase and bacterial tolerance to oxidative and nitrosative stress. *Biochimica et Biophysica Acta - Bioenergetics*, 1837 (7), pp.1178–1187.

Glowacki, R. C. et al. (2003). Antibiotic Combinations with Redundant Antimicrobial Spectra: Clinical Epidemiology and Pilot Intervention of Computer-Assisted Surveillance. *Clinical Infectious Diseases*, 37 (1), pp.59–64.

Goldman, E. (2004). Antibiotic Abuse in Animal Agriculture: Exacerbating Drug Resistance in Human Pathogens. *Human and Ecological Risk Assessment: An International Journal*, 10 (1), pp.121–134..

Golic, A. et al. (2013). Staring at the Cold Sun: Blue Light Regulation Is Distributed within the Genus Acinetobacter. *PLoS ONE*, 8 (1), p.e55059.

Gozubuyuk, A. A. et al. (2017). Epidemiology, pathophysiology, clinical evaluation, and treatment of carbon monoxide poisoning in child, infant, and fetus. *Northern clinics of Istanbul*, 4 (1), pp.100–107.

Gullberg, E. et al. (2011). Selection of Resistant Bacteria at Very Low Antibiotic Concentrations. Lipsitch, M. (Ed). *PLoS Pathogens*, 7 (7), p.e1002158.

Güntzel, P. et al. (2019). Biological activity of manganese(i) tricarbonyl complexes on multidrug-resistant Gram-negative bacteria: From functional studies to in vivo activity in Galleria mellonella. *Metallomics*, (12).

Gupta, A. et al. (2013). Ultraviolet Radiation in Wound Care: Sterilization and Stimulation. *Advances in Wound Care*, 2 (8), pp.422–437.

Händel, N. et al. (2014). Interaction between mutations and regulation of gene expression during development of de novo antibiotic resistance. *Antimicrobial agents and chemotherapy*, 58 (8), pp.4371–4379.

Händel, N. et al. (2015). Factors That Affect Transfer of the IncI1 β-Lactam Resistance Plasmid pESBL-283 between E. coli Strains. van Schaik, W. (Ed). *PLOS ONE*, 10 (4), p.e0123039.

Heacock-Kang, Y. et al. (2017). Spatial transcriptomes within the Pseudomonas aeruginosa biofilm architecture. *Molecular Microbiology*, 106 (6), pp.976–985.

Heacock-Kang, Y. et al. (2018). Novel dual regulators of Pseudomonas aeruginosa essential for productive biofilms and virulence. *Molecular Microbiology*, 109 (3), pp.401–414.

Hecker, M. T. et al. (2003). Unnecessary use of antimicrobials in hospitalized patients: current patterns of misuse with an emphasis on the antianaerobic spectrum of activity. *Archives of internal medicine*, 163 (8), pp.972–978.

Heinemann, S. H. et al. (2014). Carbon monoxide - physiology, detection and controlled release. *Chemical communications (Cambridge, England)*, 50 (28), pp.3644–3660.

Huang, C.-Y. et al. (2012). Crystal structure of Staphylococcus aureus transglycosylase in complex with a lipid II analog and elucidation of peptidoglycan synthesis mechanism. *Proceedings of the National Academy of Sciences*, 109 (17), pp.6496–6501.

Ignasiak, K. and Maxwell, A. (2017). Galleria mellonella (greater wax moth) larvae as a model for antibiotic susceptibility testing and acute toxicity trials. *BMC Research Notes*, 10 (1), p.428.

Ismailova, A. et al. (2018). An Overview of the Potential Therapeutic Applications of CO-

Releasing Molecules. *Bioinorganic Chemistry and Applications*, p.8547364.

Jander, G., Rahme, L. G. and Ausubel, F. M. (2000). Positive correlation between virulence of Pseudomonas aeruginosa mutants in mice and insects. *Journal of Bacteriology*, 182 (13), pp.3843–3845.

Jansen, G. et al. (2016). Association between clinical antibiotic resistance and susceptibility of Pseudomonas in the cystic fibrosis lung. *Evolution, Medicine and Public Health*, 2016 (1), pp.182–194.

Jesse, H. E. et al. (2013). Cytochrome bd-I in Escherichia coli is less sensitive than cytochromes bd-II or bo" to inhibition by the carbon monoxide-releasing molecule, CORM-3. *Biochimica et Biophysica Acta - Proteins and Proteomics*, 1834 (9), pp.1693–1703.

Joseph F. Hair Jr, W. C. B. B. J. B. R. E. A. (2014). *Multivariate Data Analysis, Seventh Edition*.

Kang, D. et al. (2018). Pyoverdine, a siderophore from Pseudomonas aeruginosa, translocates into C. elegans, removes iron, and activates a distinct host response. *Virulence*, 9 (1), pp.804–817.

Kang, D. et al. (2019). Pyoverdine-Dependent Virulence of Pseudomonas aeruginosa Isolates From Cystic Fibrosis Patients. *Frontiers in Microbiology*, 10, p.2048.

Kida, Y. et al. (2008). A novel secreted protease from Pseudomonas aeruginosa activates NF-KB through protease-activated receptors. *Cellular Microbiology*, 10 (7), pp.1491–1504.

Kim, H. P., Ryter, S. W. and Choi, A. M. K. (2006). CO as a Cellular Signaling Molecule. *Annual Review of Pharmacology and Toxicology*, 46 (1), pp.411–449.

Kohanski, M. A., Dwyer, D. J. and Collins, J. J. (2010). How antibiotics kill bacteria: from targets to networks. *Nature reviews. Microbiology*, 8 (6), pp.423–435.

Kourti, M. et al. (2019). Repurposing old carbon monoxide-releasing molecules towards the anti-angiogenic therapy of triple-negative breast cancer. *Oncotarget*, 10 (10), pp.1132–1148.

Kourti, M., Jiang, W. G. and Cai, J. (2017). Aspects of Carbon Monoxide in Form of CO-Releasing Molecules Used in Cancer Treatment: More Light on the Way. *Oxidative Medicine and Cellular Longevity*, 2017, p.9326454.

Krishnasamy, V., Otte, J. and Silbergeld, E. (2015). Antimicrobial use in Chinese swine and broiler poultry production. *Antimicrobial Resistance and Infection Control*, 4 (17).

Lau, G. W. et al. (2004). The role of pyocyanin in Pseudomonas aeruginosa infection. *Trends in molecular medicine*, 10 (12), pp.599–606.

Li, F., Collins, J. G. and Keene, F. R. (2015). Ruthenium complexes as antimicrobial agents. *Chemical Society Reviews*, 44 (8), pp.2529–2542.

Li Volti, G. et al. (2005). Carbon monoxide signaling in promoting angiogenesis in human microvessel endothelial cells. *Antioxidants and Redox Signaling*, 7 (5–6), pp.704–710.

Lundborg, C. S. and Tamhankar, A. J. (2017). Antibiotic residues in the environment of South East Asia. *BMJ (Clinical research ed.)*, 358, p.j2440.

Magiorakos, A.-P. et al. (2012). Multidrug-resistant, extensively drug-resistant and pandrug-resistant bacteria: an international expert proposal for interim standard definitions for acquired resistance. *Clinical Microbiology and Infection*, 18 (3), pp.268–281.

Maiques, E. et al. (2006). β-lactam antibiotics induce the SOS response and horizontal transfer of virulence factors in Staphylococcus aureus. *Journal of Bacteriology*, 188 (7), pp.2726–2729.

Mauldin, P. D. et al. (2009). Attributable hospital cost and length of stay associated with health care-associated infections caused by antibiotic-resistant gram-negative bacteria. *Antimicrobial agents and chemotherapy*, 54 (1), pp.109–115.

McKenzie, G. J. et al. (2000). The SOS response regulates adaptive mutation. *Proceedings of the National Academy of Sciences*, 97 (12), pp.6646–6651.

McKenzie, G. J. and Rosenberg, S. M. (2001). Adaptive mutations, mutator DNA polymerases and genetic change strategies of pathogens. *Current Opinion in Microbiology*, 4 (5), pp.586–594.

McLean, S. et al. (2013). Analysis of the bacterial response to Ru(CO)3Cl(Glycinate) (CORM-3) and the inactivated compound identifies the role played by the ruthenium compound and reveals sulfur-containing species as a major target of CORM-3 action. *Antioxidants & redox signaling*, 19 (17), pp.1999–2012.

Michael Weigert aus Straubing. (2017). *Pyoverdine production in the pathogen Pseudomonas aeruginosa: a study on cooperative interactions among individuals and its role for virulence*. Ludwig-Maximilians-University of Munich.

Moffatt, J. H. et al. (2010). Colistin resistance in Acinetobacter baumannii is mediated by complete loss of lipopolysaccharide production. *Antimicrobial Agents and Chemotherapy*, 54 (12), pp.4971–4977.

Mohr, F. et al. (2012). Synthesis, Structures, and CO Releasing Properties of two Tricarbonyl Manganese(I) Complexes. *Zeitschrift für anorganische und allgemeine Chemie*, 638 (3–4), pp.543–546.

Monroe, S. and Polk, R. (2000). Antimicrobial use and bacterial resistance. *Current opinion in microbiology*, 3 (5), pp.496–501.

Morris, C., Helliwell, R. and Raman, S. (2016). Framing the agricultural use of antibiotics and antimicrobial resistance in UK national newspapers and the farming press. *Journal of Rural Studies*, 45, pp.43–53..

Motterlini, R. (2007). Carbon monoxide-releasing molecules (CO-RMs): vasodilatory, anti-ischaemic and anti-inflammatory activities: Figure 1. *Biochemical Society Transactions*, 35 (5), pp.1142–1146.

Motterlini, R. and Otterbein, L. E. (2010). The Therapeutic Potential of Carbon Monoxide. *Nature Reviews Drug Discovery*, 9 (9), pp.728–743.

Muhlebach, M. S. and Noah, T. L. (2002). Endotoxin activity and inflammatory markers in the airways of young patients with cystic fibrosis. *American Journal of Respiratory and Critical Care Medicine*, 165 (7), pp.911–915.

Mukherjee, S. et al. (2017). The RhlR quorum-sensing receptor controls Pseudomonas aeruginosa pathogenesis and biofilm development independently of its canonical homoserine lactone autoinducer. *PLoS Pathogens*, 13 (7), p.e1006504.

Mulvey, M. R. and Simor, A. E. (2009). Antimicrobial resistance in hospitals: how concerned should we be? *Canadian Medical Association journal*, 180 (4), pp.408–415.

Munita, J. M. and Arias, C. A. (2016). Mechanisms of Antibiotic Resistance. *Microbiology Spectrum, American Society from Microbiology Press*, 4 (2).

Murray, T. S. et al. (2012). The carbon monoxide releasing molecule CORM-2 attenuates Pseudomonas aeruginosa biofilm formation. *PLoS ONE*, 7 (4), p.e35499.

Nagel, C. et al. (2014). Introducing [Mn(CO)3(tpa-κ3N)]+ as a novel photoactivatable CO-releasing molecule with well-defined iCORM intermediates – synthesis, spectroscopy, and antibacterial activity. *Dalton Transactions*, 43 (26), pp.9986–9997.

Nice.org.uk. (2015). *Antimicrobial stewardship: systems and processes for effective antimicrobial medicine use | Guidance and guidelines | NICE*.

Niesel, J. et al. (2008). Photoinduced CO release, cellular uptake and cytotoxicity of a tris(pyrazolyl)methane (tpm) manganese tricarbonyl complex. *Chemical Communications*, (15), pp.1798–1800.

Nobre, L. S. et al. (2007). Antimicrobial action of carbon monoxide-releasing compounds. *Antimicrobial agents and chemotherapy*, 51 (12), pp.4303–4307.

Nobre, L. S. et al. (2009). Exploring the antimicrobial action of a carbon monoxide-releasing compound through whole-genome transcription profiling of Escherichia coli. *Microbiology*, 155 (3), pp.813–824.

Nobre, L. S. et al. (2016). Examining the antimicrobial activity and toxicity to animal cells of different types of CO-releasing molecules. *Dalton Transactions*, 45 (4), pp.1455–1466.

O'Neill, J. (2014). Antimicrobial Resistance: Tackling a crisis for the health and wealth of nations. *Review on Antimicrobial Resistance*, London, pp.1–16.

Olas, B. (2015). Gasomediators (·NO, CO, and H2S) and their role in hemostasis and thrombosis. *Clinica Chimica Acta*, 445, pp.115–121.

Pang, Z. et al. (2019). Antibiotic resistance in Pseudomonas aeruginosa: mechanisms and alternative therapeutic strategies. *Biotechnology Advances*, 37 (1), Elsevier Inc., pp.177–192.

Pavlovskis', O. R. and Wretlind2, B. (1979). Assessment of Protease (Elastase) as a Pseudomonas aeruginosa Virulence Factor in Experimental Mouse Burn Infection. *INFECTION AND IMMUNITY*, 24 (1).

Price-Whelan, A., Dietrich, L. E. P. and Newman, D. K. (2007). Pyocyanin alters redox homeostasis and carbon flux through central metabolic pathways in Pseudomonas aeruginosa PA14. *Journal of Bacteriology*, 189 (17), pp.6372–6381.

Qin, T.-T. et al. (2015a). SOS response and its regulation on the fluoroquinolone resistance. *Annals of translational medicine*, 3 (22), p.358.

Qin, T. T. et al. (2015b). SOS response and its regulation on the fluoroquinolone resistance. *Annals of Translational Medicine*, 3 (22), AME Publishing Company.

Radyowijati, A. and Haak, H. (2003). Improving antibiotic use in low-income countries: an overview of evidence on determinants. *Social Science & Medicine*, 57 (4), pp.733–744.

Ramos, P. I. P. et al. (2016). The polymyxin B-induced transcriptomic response of a clinical, multidrug-resistant Klebsiella pneumoniae involves multiple regulatory elements and intracellular targets. *BMC Genomics*, 17 (Suppl 8).

Rampioni, G. et al. (2017). Effect of efflux pump inhibition on Pseudomonas aeruginosa transcriptome and virulence. *Scientific Reports*, 7, p.11392.

Rana, N. et al. (2017). A manganese photosensitive tricarbonyl molecule [Mn(CO)3(tpa-κ3 N)]Br enhances antibiotic efficacy in a multi-drug-resistant Escherichia coli. *Microbiology*, 163 (10), pp.1477–1489.

Rastogi, R. P. et al. (2010). Molecular mechanisms of ultraviolet radiation-induced DNA damage and repair. *Journal of Nucleic Acids*, p.592980.

Ryter, S. W. et al. (2002). Heme oxygenase/carbon monoxide signaling path-ways: Regulation and functional significance. *Molecular and Cellular Biochemistry*, 234, pp.249–263.

Sabnis, A. et al. (2020). Colistin kills bacteria by targeting lipopolysaccharide in the cytoplasmic membrane. *bioRxiv*, p.479618.

Sahlberg Bang, C. et al. (2016). Carbon monoxide releasing molecule-2 (CORM-2) inhibits growth of multidrug-resistant uropathogenic Escherichia coli in biofilm and following host cell colonization. *BMC Microbiology*, 16, p.64.

Santajit, S. and Indrawattana, N. (2016). Mechanisms of Antimicrobial Resistance in ESKAPE Pathogens. *BioMed research international*, 2475067.

Sato, H., Okinaga, K. and Saito, H. (1988). Role of Pili in the Pathogenesis of *Pseudomonas aeruginosa* Burn Infection. *Microbiology and Immunology*, 32 (2), pp.131–139.

Schindler, B. D. and Kaatz, G. W. (2016). Multidrug efflux pumps of Gram-positive bacteria. *Drug Resistance Updates*, 27, pp.1–13.

Shanks, R. M. Q. et al. (2007). A Serratia marcescens OxyR homolog mediates surface attachment and biofilm formation. *Journal of Bacteriology*, 189 (20), pp.7262–7272.

Shao, L. et al. (2018). The impact of exogenous CO releasing molecule CORM-2 on inflammation and signaling of orthotopic lung cancer. *Oncology Letters*, 16 (3), pp.3223–3230.

Spapen, H. et al. (2011). Renal and neurological side effects of colistin in critically ill patients. *Annals of Intensive Care*, 1 (1).

Stöhr, K. and Wegener, H. C. (2000). Animal use of antimicrobials: impact on resistance. *Drug Resistance Updates*, 3 (4), pp.207–209.

Tafani, M. et al. (2016). The Interplay of Reactive Oxygen Species, Hypoxia, Inflammation, and Sirtuins in Cancer Initiation and Progression. *Oxidative Medicine and Cellular Longevity*, 2016, pp.1–18.

Tavares, A. F. et al. (2013). The bactericidal activity of carbon monoxide-releasing

molecules against helicobacter pylori. *PLoS ONE*, 8 (12).

Tello, A., Austin, B. and Telfer, T. C. (2012). Selective pressure of antibiotic pollution on bacteria of importance to public health. *Environmental health perspectives*, 120 (8), pp.1100–1106.

Tenover, F. C. (2006). Mechanisms of antimicrobial resistance in bacteria. *American Journal of Infection Control*, 34 (5), pp.S3–S10.

Tinajero-Trejo, M. et al. (2016). Antimicrobial Activity of the Manganese Photoactivated Carbon Monoxide-Releasing Molecule [Mn(CO) $_3$ (tpa-κ ^{3} *N*)] $^+$ Against a Pathogenic *Escherichia coli* that Causes Urinary Infections. *Antioxidants & Redox Signaling*, 24 (14), pp.765–780.

Turino, G. M. (1981). Effect of carbon monoxide on the cardiorespiratory system. Carbon monoxide toxicity: physiology and biochemistry. *Circulation*, 63 (1), pp.253A-259A.

Tyers, M. and Wright, G. D. (2019). Drug combinations: a strategy to extend the life of antibiotics in the 21st century. *Nature Reviews Microbiology*, 17 (3), Nature Publishing Group., pp.141–155.

Vinckx, T. et al. (2010). The Pseudomonas aeruginosa oxidative stress regulator OxyR influences production of pyocyanin and rhamnolipids: Protective role of pyocyanin. *Microbiology*, 156 (3), pp.678–686.

Vinckx, T., Matthijs, S. and Cornelis, P. (2008). Loss of the oxidative stress regulator OxyR in *Pseudomonas aeruginosa* PAO1 impairs growth under iron-limited conditions. *FEMS Microbiology Letters*, 288 (2), pp.258–265.

Ward, J. S. et al. (2012). A therapeutically viable photo-activated manganese-based CO-releasing molecule (photo-CO-RM). *Dalton Transactions*, 41 (35), pp.10514–10517.

Ward, J. S. (2014). *Synthesis, Characterisation, and Development of Photo-activated Carbon monoxide-releasing Molecules*. University of York.

Ward, J. S. et al. (2014). Visible-light-induced CO release from a therapeutically viable tryptophan-derived manganese(I) carbonyl (TryptoCORM) exhibiting potent inhibition against E. coli. *Chemistry - A European Journal*, 20 (46), pp.15061–15068.

Ward, J. S. et al. (2017). Toxicity of tryptophan manganese (i) carbonyl (Trypto-CORM), against Neisseria gonorrhoeae. *MedChemComm*, 8 (2), pp.346–352.

Wareham, L. K. et al. (2016). Carbon Monoxide Gas Is Not Inert, but Global, in Its Consequences for Bacterial Gene Expression, Iron Acquisition, and Antibiotic Resistance. *Antioxidants & redox signaling*, 24 (17), pp.1013–1028.

Wareham, L. K. et al. (2018). The Broad-Spectrum Antimicrobial Potential of [Mn(CO) 4 (S 2 CNMe(CH 2 CO 2 H))], a Water-Soluble CO-Releasing Molecule (CORM-401): Intracellular Accumulation, Transcriptomic and Statistical Analyses, and Membrane Polarization. *ANTIOXIDANTS & REDOX SIGNALING*, 28 (14), pp.1286–1308.

Wareham, L. K., Poole, R. K. and Tinajero-Trejo, M. (2015). CO-releasing Metal Carbonyl Compounds as Antimicrobial Agents in the Post-antibiotic Era. *The Journal of biological chemistry*, 290 (31), pp.18999–19007.

Wei, Q. and Ma, L. Z. (2013). Biofilm matrix and its regulation in Pseudomonas aeruginosa. *International Journal of Molecular Sciences*, 14 (10), pp.20983–21005.

Wilke, M. S., Lovering, A. L. and Strynadka, N. C. (2005). β-Lactam antibiotic resistance: a current structural perspective. *Current Opinion in Microbiology*, 8 (5), pp.525–533.

Wilson, J. L. et al. (2015). CO-Releasing Molecules Have Nonheme Targets in Bacteria: Transcriptomic, Mathematical Modeling and Biochemical Analyses of CORM-3 [Ru(CO)3Cl(glycinate)] Actions on a Heme-Deficient Mutant of Escherichia coli. *Antioxidants & redox signaling*, 23 (2), pp.148–162.

Wu, M. et al. (2005). The Pseudomonas aeruginosa proteome during anaerobic growth. *Journal of Bacteriology*, 187 (23), pp.8185–8190.

Xu, H.-W., Qin, S.-S. and Liu, H.-M. (2014). New Synthetic Antibiotics for the Treatment of Enterococcus and Campy- lobacter Infection. *Current Topics In Medicinal Chemistry*, 14 (1), pp.21–39.

Zarb, P. and Goossens, H. (2012). Human use of antimicrobial agents. *Revue scientifique et technique (International Office of Epizootics)*, 31 (1), pp.121–133.

Zhang, W.-Q. et al. (2009). Diversity and design of metal-based carbon monoxide-releasing molecules (CO-RMs) in aqueous systems: revealing the essential trends. *Dalton Transactions*, (22), p.4351.

Zhu, K. et al. (2019). Universal antibiotic tolerance arising from antibiotic-triggered accumulation of pyocyanin in Pseudomonas aeruginosa. Balaban, N. (Ed). *PLOS Biology*, 17 (12), p.e3000573.

Zobi, F. et al. (2012). 17 e - rhenium dicarbonyl CO-releasing molecules on a cobalamin scaffold for biological application. *Dalton Transactions*, 41 (2), pp.370–378.

Zobi, F. (2013). CO and CO-releasing molecules in medicinal chemistry. *Future Medicinal Chemistry*, 5 (2), pp.175–188.